Carbon-mineral interactions and bioturbation: an earthworm invasion chronosequence in a sugar maple forest in Northern Minnesota

A THESIS
SUBMITTED TO THE FACULTY OF
UNIVERSITY OF MINNESOTA
BY

Amy Marie Lyttle

IN PARTIAL FULFILLMENT OF THE REQUIREMENTS
FOR THE DEGREE OF
MASTER OF SCIENCE

Kyungsoo Yoo

May 2013

Acknowledgments

First and foremost I would like to express my appreciation and gratitude to my advisor, Kyungsoo Yoo, for this wonderful research opportunity. He has provided valuable guidance in both research and the writing process. He has been a great mentor and without his wonderful support I would not have been able to complete this work.

This research was supported by the generous funding from the United States Department of Agriculture-NRI to Kyungsoo Yoo, Anthony Aufdenkampe, and Cindy Hale. I would like to thank all who have contributed to this project, especially Alex Blum, Kathryn Resner, Jim Barott, Rebecca D. Knowles, and Cristina Fernandez.

Thank you to my committee members – Sarah Hobbie, Brandy Toner, and Stephen Sebestyen – for providing assistance throughout my entire graduate career. Each and every committee member has been a great mentor and provided invaluable advice over the past three years. I cannot express how grateful I am to have worked with such wonderful scientists.

I would like to thank the Stroud Water Research Center for providing me with the opportunity to visit and conduct research. A special thanks to Anthony Aufdenkampe and Stephanie Dix for their exceptional assistance and guidance.

I would like to thank my lab group, office mates, and fellow graduate students who have provided an enjoyable work environment and assistance along the way.

Thanks to Jay and Joanne Bell who early on provided insight and support in my decision to enter graduate school. Finally I must thank my family and friends who have also provided tremendous support, especially throughout these past three years!

~In Memory of Pam Gengler~

1955-2013

Abstract

European earthworm species have been introduced into previously glaciated hardwood forests in North America over the past centuries. The invasive earthworms reorganize soil structure, losses of carbon and nitrogen, and the reduction in abundance and diversity of understory communities. One of the direct impacts of earthworms on soils is increased bioturbation, which has domino effects on soil properties that include decrease in litter layer and thickening and increasing bulk density of the A horizons. Such enhanced interactions between organic matter and minerals due to invasive earthworms and earthworms in general have been studied in the context of soil carbon cycle. In this study we attempt to better understand exotic earthworms' impacts on the sorption of organic matter on mineral surfaces and how this fundamental process determining the soil carbon storage and turnover is affected by bioturbation and different earthworm functional groups. Despite the reduction of total C inventory with the arrival of endogeic species, such reduction is largely derived by the loss of light density fraction C. In contrast, the C inventory in heavy density fraction – which we associate with mineral-sorbed - shows little change, which is consistent with likewise stable inventories of mineral surface areas and C-covered mineral surface areas. Mineral-sorbed C pool appears to be in dynamic equilibrium across the diverse ecological stages of earthworm invasion. Our study suggests that the direction and size of changes in soil C inventory in response to bioturbators in general and invasive earthworms specifically will be strongly dependent upon the soil depth profiles of mineralogy and texture.

Table of Contents

List of Tables

List of Figures

Chapter 1.

Coverage of soil organic carbon on mineral surface and soil carbon inventory along an earthworm invasion chronosequence in a northern hardwood forest in Minnesota

Chapter Summary

I studied the effects of invasive European earthworms on organo-mineral interactions in a northern hardwood forest. I hypothesized that increased soil mixing will lead to increased contacts between organic matter (OM) and mineral surfaces and increased carbon (C) inventory in soils. Exotic European earthworms are invading many forests in North America where native earthworms were decimated by the last glacial activities. When introduced into these ecosystems, these earthworms enhance bioturbation and thus alter physical interactions between minerals and OM. Mineral protection of OM has been recently emphasized as a prime mechanism for stabilizing C in soils. To understand how and to what degree OM sorption onto mineral surface respond to earthworm invasion in general and to different functional groups of earthworms specifically, we studied an active earthworm invasion chronosequence in a sugar maple forest in the Chippewa National Forest located in northern Minnesota. In the presence of earthworms, the A horizon expands at the expense of the litter layer and the E horizon. The A horizon's C inventory is reduced dramatically with the arrival of endogeic earthworms which actively mix the A horizon, and this decrease is largely due to the decline of organic matter in the light mineral-free faction. The C inventory in the heavy mineral-associated fractions does not change along the transect. While the depth distribution of minerals' specific surface area (SSA) in A horizons is dramatically altered by endogeic species, the mineral surface area within the actively mixed A horizon is at a dynamic equilibrium, as endogeic earthworms not only facilitate the formation of secondary iron (Fe) oxides with high SSA and thicken the A horizons, but also incorporate silt minerals with low SSA from the

underlying loess materials. In the soils inhabited by endogeic species, a smaller fraction of surface area is covered with organic matter, highlighting that organic matter sorption on mineral surface in the A horizon becomes limited by available mineral-free OM. This study reveals that the responses of soil C inventory to invasive earthworms will be highly sensitive to the pre-existing depth profiles of soil mineralogy and associated SSA and the species compositions of the earthworm population that changes along the stage of earthworm invasion.

Keywords: Earthworm invasion, soil carbon, minerals, exotic species, specific surface area.

1. Introduction

Earthworms are one of the best-known bioturbators. Not native to previously glaciated forests in North America, earthworms have been invading the areas previously devoid of them (Wagner et al., 1977; Coderre et al., 1995; Hale, 2005a and b). Over the past centuries, human activities – such as agriculture, dumping of unused fishing bait, logging, and recreation, transport of soil contaminated with earthworms and/or their cocoons – have facilitated earthworm invasion (Gates, 1982; Alban and Berry, 1994; Hale et al., 2005a; Hale, 2008a). Earthworm introduction into these previously glaciated areas results in significant modifications of soil morphology and nutrient cycling (Alban and Berry, 1994; Scheu and Parkinson, 1994a and b; Bohlen et al., 2004a and c; Frelich et al., 2006; Hale et al., 2008b). Among these ecosystems, northern hardwood forests in North America have been the subjects of intensive studies on the effects of invasive earthworms in the soil C and nitrogen cycling (Hale et al., 2005a; Frelich et al., 2006; Bohlen et al., 2004b and c; Hale et al., 2008b). Results from these studies over the past decade further showed that declines in native understory communities and dramatic changes in soil structure in the northern hardwood forests are a direct response to the invasion of European earthworms (Alban and Berry 1994; Scheu and Parkinson 1994b; Gundale 2002; Bohlen et al. 2004c; Hale 2004; Hale et al., 2005a and b; Hale et al., 2006).

In agricultural settings, it is well known that earthworms mix soil materials and break down litter materials, and thus improve both water infiltration and aeration in the soils. However, relatively few studies have examined the role of earthworms in natural

ecosystems. Lack of such studies is partly because virtually ubiquitous presence of earthworms makes it challenging to set up field comparison studies to factor out earthworms' impacts on soils. Studies on the effects of invasive earthworms on soils show that forest soils respond to earthworm activities very differently than garden and agriculture soils. Moreover, the degree by which the forest responds to earthworm invasion is a function of species and biomass present. Three main ecological groups for European earthworms affect the forest distinctly based on their feeding and dwelling habits. Epigeic earthworms inhabit the litter layer only, endogeic earthworms burrow and eat in the mineral soil actively mixing the A horizon, and anecic earthworms are deep burrowers, feeding on fresh litter. Most notably, invasive earthworms redistribute leaf litter deep into the soil, expanding the A horizon at the expense of the O horizon (Hale et al., 2005a). Nonetheless, studies have shown that despite the redistribution of soil OM into deeper soil depths, invasion of exotic earthworms often results in a net loss of C from the soils (Langmaid, 1964; Alban and Berry, 1994, Bohlen et al., 2004b)

While soils in the formerly glaciated forests are seriously altered in their morphology and physical and chemical properties by exotic earthworms, soils are also critical contributors in the global C cycle. Soils represent the largest active terrestrial C reservoir (Oades, 1988; Rumpel and Kögel-Knabner, 2011), containing three times as much C as found in the atmosphere or living plant tissue (Schmidt et al., 2011). As C is exchanged between Earth's atmosphere, fossil fuels, oceans, vegetation and soils, terrestrial ecosystems withdraw CO_2 from the atmosphere through photosynthesis and sequester much of the C within the plant litter and soils. Accordingly, because of soils'

capacity to possibly offset much of the atmospheric CO_2 or to trigger the runaway atmospheric CO_2 increase, the preservation of OM in soil has been a growing topic of research over the past decade. Though studies generally find that exotic earthworm species cause a loss of the leaf litter layer in previously earthworm-free forests, there are conflicting data on the effects of earthworms on C storage within mineral soils. In hardwood forests in northern Minnesota, Alban and Berry (1994) found an annual decrease in soil C inventory following earthworm invasion by a rate of 0.06 kg C m^{-2} yr^{-1} to a depth of 50 cm but did not see any significant changes in C inventory in soils at the 25-50 cm layer in northern Minnesota's hardwood forests, indicating most of the change happened in the upper 25 cm of soil. Burtelow (1998) found a reduction in the litter layer's C inventory, but reported trivial increases in C stored in the A horizons and an overall decrease in soil profile integrated C inventory in hardwood forests located in New York, USA. Net loss of C from litter layer and soil profile (to the depth of 12cm) in earthworm-invaded soils was also reported by Bohlen et al. (2004b) at a sugar maple dominated forest in northeastern USA. On the other hand, Bohlen et al. (2004a) show no net loss in C from the soil profile in maple-dominated forests in northeastern USA. In similar hardwood forests throughout northern Minnesota, Hale et al. (2005a) also did not find a decrease in C from mineral soil, rather C inventory in the top 12 cm of mineral soil increased with the earthworm invasion. Wironen and Moore (2006) found a decrease in litter layer but an overall increase in C inventory to a depth of 30cm in earthworm invaded soils in mountainous sugar maple dominated forest in Quebec, Canada. These conflicting reports demand a process-based understanding of how exotic earthworms

affect soil C inventory over the course of their invasion history.

The amount of C stored in soils is controlled by the balance of plant primary productivity and decomposition. Three major processes contribute to the protection of C from microbial activities: chemical recalcitrance, physical protection by minerals, and sorption of OM on mineral surface (Baldock and Skjemstad, 2000; von Lutzow et al., 2006). Organic matter may persist in soils: it is chemically recalcitrant due to highly stable chemical structures (Rumpel and Kögel-Knabner, 2011). Stable chemical structures - often found in lignin, lipids and tannins – allow the compounds to be less biodegradable and lead to accumulation in the soil (von Lutzow et al., 2006). When OM is occluded within aggregates, OM may become inaccessible to microorganisms and their enzymes (Baldock and Skjemstad, 2000; von Lutzow et al., 2006). Aggregates may also reduce oxygen flow hindering aerobic decomposition (Sollins et al., 1996; von Lutzow et al., 2006). Lastly, sorption of OM on mineral surface via ligand exchange, polyvalent cation bridges, or weak interaction makes the OM less exploitable by microorganisms (Chenu and Stotzky, 2002; von Lutzow et al., 2006). Of these three major processes that contribute to the preservation of OM in soils, recent studies converge on identifying mineral protection (aggregate occlusion and surface adsorption) as the primary mechanism for long-term accumulation and retention of OM in soils (Schmidt et al., 2011). Organic matter within the heavy clay fraction of soils is older than OM in lighter fractions (Chenu and Stotzky, 2002; Eusterhues et al., 2003; Ludwig et al., 2003; von Lutzow et al., 2006). During the formation of Hawaiian soil for example, C turnover times were found to be closely and positively coupled with the abundances of non-

crystalline minerals with high SSA (Torn et al., 1997).

It is not clear, however, how OM association with minerals is generated and altered as a function of bioturbation in soils (Schmidt et al., 2011). This is a critical gap in knowledge given that soil mixing enables OM and soil mineral particles to be redistributed within a soil profile and thus provokes their physical contacts. High inputs and concentrations of C are typically found in the topsoil, while minerals with high SSA are more abundant in illuvial subsoil horizons at deeper depths. Therefore, one may argue that soils are not likely to produce maximum OM-sorption on mineral surface because the components (OM and minerals) are physically separated. When soils are perturbed via bioturbation, however, OM in the topsoil and the clay minerals in the subsoil may be forced to physically interact and thus facilitate the sorption of OM on mineral surface.

Because of their ability to physically move soil materials and remove large quantities of leaf litter, earthworms are important ecosystem engineers that may have dramatic impacts on OM sorption on mineral surface. In this thesis, I investigated an earthworm invasion chronoseqeunce in a sugar maple forest in northern Minnesota to reveal how soil mixing affects OM sorption on mineral surface and thus soil C inventory. The study site, previously established by Hale in 1998 (Hale 2004), includes a transect that stretches approximately 200 meters. Hale (2005a and b) documented that earthworm invasion along this transect occurred through a series of invasion waves of different ecological functional groups of earthworms. Therefore, I was able to examine the impacts of specific earthworm functional groups on OM-mineral interactions. I explicitly test the following two hypotheses: (1) Burrowing earthworms (endogeic and anecic species) will

increase minerals' SSA in the A horizon by incorporating clay minerals from the underlying B horizon; (2) earthworms that actively mix the A horizon (endogeic species) will increase OM sorption on minerals' surface by accelerating soil mixing.

2. Methods

2.1. Study Site

My study site is located in a hardwood forest dominated by sugar maple (*Acer saccharum*) and basswood (*Tilia americana*) within the Chippewa National Forest in Northern Minnesota, USA (Fig. 1-1). The climate is humid, continental, and cold temperate, with mean annual temperature of 4 ˚C (Minnesota State Climatology Office 2003). The mean annual precipitation is 50-65 cm, with the growing season varying between 100 and 120 days (Adams et al., 2004). The surficial geology of the site includes Guthrie glacial till overlain by silt loam loess cap of varying depths (Adams et al., 2004). The land surface is gently rolling with seasonal wetlands.

The soils belong to the Warba series and are classified as fine-loamy, super active, frigid Haplic Glossudalfs (Soil-Survey, 1997/2006). We measured that the depth to the carbonate rich glacial till ranged from 90-160 cm. Earthworm-free soils have soil profiles featuring O horizon, thin A horizon, acidic E horizon, and clay-rich B horizon below which lies calcareous glacial till. The uniform thickness, mineralogy, texture, and pH of the E horizon indicate that the horizon is a locally reworked loess cap (Resner et al., 2011). The forest litter layer is made of leaves, twigs and roots, and is over 5cm thick in the earthworm-free areas. The A horizons, rarely exceeding 3cm thickness in earthworm-

free areas, have many fine roots. Prior to earthworm invasion, the A horizon materials have weak very fine granular structure and very fine sandy loam texture (Soil Survey, 1997/2006). The loess materials have very fine sandy loam texture and fine roots present. The loess layer has a weak thin platy structure and is grayish brown in color. Underlying the loess cap are well-developed clay rich B horizons. The depths to the calcareous C horizons are ~100 cm.

The ~200 meter long studied transect extends from a soil near a road into the forest where earthworms are absent (Fig. 1-2). The transect consists of 19 plots that are approximately 10 meters apart. Each plot has three replicates. The invasion threshold, which was previously termed as the leading edge of the earthworm invasion by Hale et al., (2005a and b), was visually determined at the location where dramatic change in leaf litter biomass occurs from patchy to no litter layer to a thick forest floor. A well-developed forest floor occurs in front of the invasion threshold (~150-190 m in 2009) where soils are lightly invaded by earthworms, and mineral soil is exposed behind the invasion threshold (~0-150 m in 2009) where soils are heavily invaded by earthworms. This threshold was found at 90 meters in 1999 (Hale, 2005a and b).

2.2. Soil Sampling

Soil pits were excavated in 2009 to the depths of soil-glacial till parent material at 0, 50,100, 150, 160, and 190 meters (Fig. 1-2). From the excavated pits, soil samples were collected in 2.5 cm increments in the A horizon, 5 cm increments in the E horizon (loess cap), and 10 cm increments in the B horizon. Bulk densities were determined for each horizon using a sliding hammer corer followed by drying and weighing of the core

samples. In 2011, soil cores with 3.175 cm diameter and 30 cm length were collected adjacent to all plots along transect B to detail the thicknesses of A and E horizons along the transect. All chemical analyses were performed on <2 mm fine fractions.

2.3. Earthworm Sampling and Identification

Earthworms were collected at 10 m intervals along transect B (Fig. 1-2) in 2009 from 0.3 m^2 subplots using liquid mustard extraction (Lawrence and Bowers, 2002; Hale et al., 2005a). We sampled earthworms during September when earthworms are sexually mature and thus it is easier to identify their species. Collected earthworms were killed in 70 % isopropyl and preserved in 10 % formalin. Earthworm taxonomy was determined following Schwert (1990), Reynolds (1977), and Hale (2007). Ash-free dry (AFD) Earthworm biomasses were calculated according to regression model developed in Hale et al., (2004).

Earthworms were classified into three functional groups based upon feeding and dwelling habits. The epigeic group consists of relatively small earthworms, typically ranging from 0.7-2 cm in length. These earthworms feed and dwell in leaf litter and do not burrow in mineral soils. Earthworms that dwell within shallow mineral soils are in endogeic functional group. These earthworms rarely feed at the surface; rather they ingest the mineral soil and digest its organic materials. The endogeic group also creates a system of connected non-permanent burrows in the mineral soil. Finally, anecic earthworms feed on surface litter and pull the litter into their deep permanent burrows in mineral soils. These earthworms are the largest in length and biomass.

Dendrobaena octaedra is a small bodied earthworm that feeds and dwells in the litter layer, thus this earthworm is part of the epigeic group. *Apporectodea* species containing *A. caliginosa, A. rosea,* and *A. trapeziodes,* and *Octolasion trytaeum* are all part of endogeic group as they dwell and feed in the mineral soil and create burrows. *Lumbricus rubellus* adults are a distinctive epigeic species that can mix into the upper horizon, and is therefore termed epi-endogeic as it presents characteristic of both epigeic and endogeic groups. On the other hand, *Lumbricus terrestris* adults are a deep burrowing species that feed on fresh litter at the surface and are strictly anecic. *Lumbricus rubellus* and *Lumbricus terrestris* are impossible to differentiate when not sexually mature, so *Lumbricus* juveniles were grouped into the epi-anecic category because they present characteristic of epigeic, endogeic, and anecic groups.

2.4. Carbon Contents Measurements

Given that the underlying glacial till contains carbonates, oven dried soil samples were treated with Hydrochloric acid to remove carbonate prior to analysis. Soil organic C contents were determined by VarioMax CN Elemental Analyzer at the USDA ARS facility in the University of Minnesota. Duplicate samples of 0.5 g were used to analyze C contents in soil and leaf litter. Standards were run every 20 samples.

2.5. Density Fractionation

Eighteen soil samples (~3 samples within the A horizon at each pit) across the invasion gradient were selected for density fractionation. Samples were initially wet sieved (2-mm), followed by dry sieving at 250 um. Soil samples <250 um were mixed

with 2.0 g cm^{-3} sodium polytungstate (Torressan, 1987; Savage, 1988) and placed on a shaker for 2-3 hours at room temperature. Based on the results from Sollins et al. (2009 and 2006), a density of 2.0 g cm^{-3} was used to ensure complete removal of organic debris and to focus on OM associated with mineral surfaces. Settled materials were retrieved and rinsed with deionized water until electrical conductivity of the solution was ≤50 μS cm^{-1} (Eusterhues et al., 2005). The samples were then oven dried at 60 °C.

2.6. Carbon and Nitrogen Stable Isotopes Analysis

Heavy and light density fractionated soils (<250 μm) were analyzed for C and nitrogen (N) contents as well as values of $\delta^{13}C$ and $\delta^{15}N$. Samples were analyzed by a coupled Element Analysis-Isotope Ratio Mass Spectrometer (EA-IRMS), at Stroud Water Research Center. Analytical error for the instrument was ± 0.47% for $\delta^{13}C$ and ± 0.08% for $\delta^{15}N$. A standard material of IU Acetanilide was run every 20 samples.

2.7. Specific Surface Area Measurements

Specific mineral surface area (SSA) was measured for fine fractions (<2 mm) of bulk soil samples. Coarse fractions explain less than 5 % of collected soil masses. SSA was measured using a TriStar 3020 Surface Area and Porosity Analyzer located in the Department of Soil, Water, and Climate at the University of Minnesota. Based on the Brunauer-Emmett-Teller (BET) theory, isotherm data were collected at 11 different pressure points at a temperature of 77 K using N_2 as adsorbent gas. Each sample weighed ~1.5 g. The samples were degassed prior to analysis to remove any excess water and

contaminants on the surfaces: samples were heated at 150 °C and purged by N_2 gas for 4-6 hours.

After initial SSA analysis of untreated soil, OM was removed from the same samples to reveal the mineral surface covered by OM. The OM-removed samples were then subject to the identical SSA analysis procedure described above. Because OM typically has low SSA (~1 m^2 g^{-1}), removal of OM is critical in estimating total mineral SSA (Chiou, 1990; de Jonge and Mittelmeijer-Hazeleger, 1996; Pennell et al., 1995). Several methods have been used for removing OM. These methods include wet heating, muffling and hypochlorite oxidation; however, these methods are known to affect the SSA of Fe oxides (Sequi and Aringhieri, 1977; Weilder and Stanjek, 1998; Mikkuta et al., 2005). Considering the tradeoffs between incomplete OM removal and mineral alterations, we followed the procedures used in Wagai et al., (2009) where OM is removed by muffling samples at 350 °C for 12 hours.

The BET theory also considers the *C (italics)*-constant, which represents the enthalpy of N_2 gas sorbed directly onto the particle surface, (Webb and Orr, 1997; Mayer, 1999). The *C*-constant is an indicator to differentiate between organic and inorganic surfaces, as N_2 gas absorbs onto organic surfaces more weakly than on polar mineral surfaces (Wagai et al., 2009). Higher *C*-constant values (or enthalpies) indicate sorption onto naked mineral surfaces and low values indicate sorption onto organically coated minerals. It has been observed that *C*-constants are high for oxides with large SSA whereas *C*-constants are low for organic materials (Mayer, 1999). Using a regression analysis described in Mayer (1999), the *C*-constants were calculated and used to assess

the OC coverage on mineral surfaces.

2.8. Iron Oxides Extractions

Because Fe oxides provide large specific surface areas (Eusterhues et al., 2005; Kaiser and Guggenberger, 2007), I measured extractable Fe chemistry on selected soil samples from heavily invaded (0 and 50 m) and minimally invaded (160 and 190 m) soils. Samples from three depths in the A horizons were analyzed. Soil samples of 0.75 g were mixed with sodium dithionite, sodium citrate, and sodium bicarbonate to remove both crystalline and non-crystalline Fe oxides in the soil (Holmgren, 1967). Extracts were then analyzed with ICP-AES at the Research Analytical Laboratory at the University of Minnesota. Non-crystalline Fe oxide pool was estimated by ammonium oxalate dark extraction (McKeague and Day, 1966; Jackson 1986; Torn et al., 1997; Masiello et al., 2004). Soil samples of 0.5 g were mixed with 50 mL of ammonium oxalate at pH 3 and placed on a shaker for four hours. Later, samples were centrifuged and an aliquot of the extract was analyzed by the ICP-AES.

2.9. Quantitative XRD

Soil samples, 1 g each, were ground with a ZnO standard. Using a Siemens D500 instrument at the United States Geological Survey, Boulder, CO, XRD spectra were collected from 5 to 65 degrees 2θ with Cu and Kα radiation. Using the RockJock program, mineral concentrations were determined according to Eberl (2003).

2.10. Calculations

2.10.1. Mass equivalent depths

When plotting soil depth profiles of elemental concentrations, we used mass equivalent depth with the unit of g cm^{-2} in the place of cm. The mass equivalent depth factors in the varying soil bulk densities (thus volumetric compaction or dilation) in comparing the depth profiles of various elemental concentrations under different influence of invasive earthworms. The mass equivalent depth is calculated as:

$$\text{Mass Equivalent Depth} = \sum_{i=1}^{N} (\Delta z_i \times BD_i) \quad (1)$$

where BD is the bulk density (g cm^{-3}), Δz is the thickness of a sampled layer (cm), i indicates the i-th layer sampled, and N is the total number of sampled layers above the depth of interest. Across the studied transect, the lower A horizon boundaries are found at the depths of 7-17 cm which have mass equivalent depths of 1.9-9.8 g cm^{-2}, and the lower boundaries of the loess cap were found at the depths of 34-56 cm which have mass equivalent depths of 34-58 g cm^{-2}.

2.10.2. Carbon Inventories

A soil C inventory was calculated for individual horizons as well for entire soil profiles. Soil C inventory for a horizon, X, is calculated as:

$$CI_X = \sum_{i=1}^{N} (c_i \times BD_i \times \Delta z_i) \,, \quad (2)$$

where CI_X is the C inventory of a soil horizon, X [kg C m^{-2}], c is the mass fraction of C in a sample [kg kg^{-1}], BD is the bulk density [kg m^{-3}], Δz is the thickness of a sampled layer, i indicates the i-th sampled layer within the horizon X, and N is the number of the

sampled layers in the horizon X. Coarse contents were not factored here because the samples had negligible coarse size contents.

2.10.3. Specific Surface Areas

I considered mineral specific surface area as:

$$SSA_{total} = SSA_{occluded} + SSA_{exposed}, \quad (3)$$

where SSA_{total} corresponds to the total specific surface areas of the mineral, $SSA_{occluded}$ is the area covered by OM, and $SSA_{exposed}$ represents the area not covered by OM. Operationally, SSA_{total} corresponds to the mineral specific surface areas determined after removing OM. $SSA_{occluded}$ is determined as a difference between the SSA of samples measured after and before removing OM. We then quantify the percent of mineral surface area covered by OM ($\%SSA_{occluded}$) (Wagai et al 2009) as:

$$\%SSA_{occluded} = [(SSA_{total} - SSA_{untreated})/SSA_{total}] \times 100, \quad (4)$$

where $SSA_{untreated}$ refers to mineral specific surface area determined before the removal of OM.

As a measure of relationship between mineral-associated OM and mineral surface area, we define OC loading [kg C m^{-2}] as:

$$\text{OC loading} = c_{mineral}/SSA_{total}, \quad (5)$$

where $c_{mineral}$ is the mass fraction of mineral associated C [kg kg^{-1}]. The $c_{mineral}$ is determined as C contents of heavy fractions (> 2.0 g cm^{-3}), which we operationally associate with mineral-sorbed C. In a hypothetical situation where the entire mineral surface is covered by a homogeneous layer of organic molecules, the OC loading is called “monolayer-equivalent”. The monolayer-equivalent is calculated to be 0.5 - 1.0

mg C m^{-2} (Keil et al., 1994; Mayer and Xing, 2001). The OC loading has been commonly calculated for different soils and sediments. In most cases, OC loadings were determined for the heavy fractions (>1.6-1.9 g cm^{-3}) of soils (Keil and Hedges, 1993; Keil, 1997; Kaiser and Guggenberger, 2000).

2.10.4. Statistical Analysis

Multiple and simple linear regressions were used to test the relationship between soil characteristics, distance from invasion, and earthworm biomass. ANOVA and paired t-test were used to test the effects of an individual earthworm ecological group on soil characteristics (SAS, 2010).

3. Results

3.1. Earthworm biomass and species composition

Epigeic Group (Dendrobaena octaedra)

D. octaedra contributed the least to total earthworm biomass because of their relatively small size (0.7-2 cm in length), but their population is among the highest, along with *L. rubellus*. *D. octaedra* are found across the entire transect (except at 160 and 180 m) (Fig. 1-3a).

Endogeic Group (Octolasion tyrtaeum, Apporectodea caliginosa, Apporectodea rosea, Apporectodea juveniles)

The endogeic group had a relatively large contribution to the earthworm biomass and population (Fig. 1-3b and c). *O. tyrtaeum's* presence is limited to soils near the

recreation road, indicating its recent arrival compared to other endogeic species (Fig. 1-3a). *Apporectodea* species is not found beyond 130 m.

Anecic Group (Lumbricus terrestris)

L. terrestris contributed to a significant fraction of the total earthworm biomass because the individuals had the largest biomass. Their numbers were significantly smaller than any other species (Fig. 1-3). The distribution of *L. terrestris* along the transect was variable, and its presence was limited to ≤ 60 m.

Epi-Endogeic (Lumbricus rubellus)

Epi-endogeic earthworm biomass was relatively small compared to other groups. However, their population was among the largest (Fig. 1-3c). Their distribution along the transect was patchy: they were found at only 5 distances up to 150 m.

Epi-Anecic (Lumbricus juveniles)

The epi-anecic group was among the largest contributors to biomass and population (Fig. 1-3b and c). *Lumbricus juveniles* (hereafter termed *L. juveniles*) were found up to 190 m.

As shown below, endogeic species – among the functional groups – had the most profound impacts on the C concentrations, their depth profiles, and OM-mineral sorption. We thus divide the excavated soil pits to two groups based on the presence or absence of endogeic species: the front group without endogeic species consists of soils at 150, 160,

and 190 m, and the rear group with endogeic species is made of soils at 0, 50, and 100 m.

3.2. Depth Profiles of C Concentration and C inventory

Soil C concentrations decreased with increasing depth at all sites along the chronosequence. Below the mass equivalent depth of 16 g cm^{-2} (~14 cm depth), C concentrations reached their minimum values and their differences between each site became insignificant. Soils in the rear group had significantly less C concentrations than the soils in the front group. In the front group, C concentrations declined to 0.1% at the mass equivalent depth of 4-6 g cm^{-2}, while C concentrations in the rear group did so at 10-16 g cm^{-2} (Fig. 1-4a and b).

Carbon inventories were calculated to the mass equivalent depths of 1.9 and 18.2 g cm^{-2} which largely agreed with the depths of lower boundaries of the A horizons and the loess cap horizons (Fig. 1-5), respectively. Initially I hypothesized that C inventories would increase due to an increase in OM-mineral sorption; however, C inventories decreased from 4.67 ± 0.22 kg C m^{-2} in the front group to 3.16 ± 0.49 kg C m^{-2} in the rear group. The decline in the C inventories was most evident across the endogeic forefront at 100 m. After the initial drop in the C inventory, the C inventories tended to rebound but did not recover the values prior to the arrival of endogeic species.

Across the entire transect, the A horizons contributed the largest fraction of the total soil C inventories that include the B horizons. The complete soil C inventories are provided for the six excavated soil pits in the appendices. The C inventories in B horizons varied from 0.68 to 3.0 kg C m^{-2}, but the C concentrations and bulk densities of B horizons did not vary along the transect. The thicknesses of B horizons, which varied

with local topography, appear to control C inventory of the B horizons. Therefore, the impacts of invasive earthworms on soil C inventory was limited to the upper O, A, and E horizons.

3.3. Density Fractions

Contribution of the heavy fraction (>2.0 g cm^{-3}) to bulk soil mass dramatically increased with greater degree of earthworm invasion (Fig. 1-6a). Heavy fraction contributed 11-18 % and 57-94 % to the bulk soil mass in the top 1.9 g cm^{-2} (6 cm) in the front group soils and rear group soils, respectively. The contributions of the heavy fractions to the bulk soil mass increased with increasing depth. When I combined this result with the C content of each fraction, I found that the heavy fraction contributed 4-30 % of total C in the front group soils. In contrast, the heavy fraction contributed 31-74 % of total C in the heavily invaded soils (0 and 50 m). The soil at 100 m showed an intermediate mass contribution of heavy fraction. Below the mass equivalent depth of ~5.0 g cm^{-2} (~13 cm), however, the differences in contributions of the two density fractions between the two groups of soils were negligible.

While invasive earthworms – particularly endogeic species – dramatically altered the contribution of heavy fraction to the total C in the shallow A horizons, the heavy fractions exhibited consistent C concentrations over the entire transect (Fig. 1-7a). The heavy fractions had 5-7 % C at the top of the A horizons and their C concentrations decreased with increasing depth (Fig. 1-7a). In contrast, the C concentrations in the light fractions ranged between 6-29 % at 1.3 g cm^{-2} (~ 2 cm) across the chronosequence and tended to be greater in the less invaded soils (Fig. 1-7b).

3.4. Stable Isotopes

The $\delta^{13}C$ values in the heavy fraction increased with increasing depth at all points of invasion (Fig. 1-8a). The front group soils were more enriched in $\delta^{13}C$ within the top 10 cm of mineral soil than the soils in the rear group. Below 10 cm, all soil samples had similar values of $\delta^{13}C$, again indicating a change only in the very top mineral soil. Within the light fraction of soil (< 2 g cm^{-3}), least invaded soils were more enriched in $\delta^{13}C$ (Fig. 1-8b).

Stable nitrogen isotope signatures ($\delta^{15}N$) in the heavy fractions ranged from 1.7-7.1 ‰. Least invaded soils were typically more enriched than the heavily invaded soils (Fig. 1-9). The light fraction soils had $\delta^{15}N$ values of 0.9-4.7 ‰ and also showed greater enrichment of $\delta^{15}N$ in the front group soils compared to the most invaded soils.

3.4. Mineral Specific Surface Areas (SSA)

Mineral SSA greatly increased with the removal of OM. Mineral SSA ranged from 0.62 to 4.2 $m^2\ g^{-1}$ before OM removal, while the values varied from 3.6 to 34 $m^2\ g^{-1}$ for the same samples when their OM was removed (Fig. 1-10).

Contrary to the hypothesis that stated SSA_{total} would increase with increasing earthworm biomasses, I found a decrease in SSA_{total} from the front group to rear group soils. SSA_{total} in the soils near the invasion front (150-190 m) ranged from 11-37 $m^2\ g^{-1}$ in the top 0.5-1.3 g cm^{-2} of the mineral soil, whereas heavily invaded soils' (0-100 m) SSA_{total} had values of 6-14 $m^2\ g^{-1}$ at the same mass equivalent depth. Below ~2.6 g cm^{-2} where a loess cap underlies the A horizons in the front group soils, the direction of the difference was reversed such that rear group soils showed slightly greater SSA_{total}. These

differences however, became negligible below the 15 g cm^{-2} (~14 cm depth). Unlike the SSA_{total}, $SSA_{untreated}$ tends to be slightly greater in the soils with greater degree of earthworm invasion. Additionally, the values of $SSA_{untreated}$ at 0 m peaked at 6.7 g cm^{-2}, which contrasted with SSA_{total} that consistently decreased with increasing depth without having peaks.

3.5. Mineral Surface Area covered by Organic Matter

With initial invasion of epigeic species (from 190 to 160 m), the OM-coated specific mineral surface area ($SSA_{occluded}$) of the soils increased. However, with the arrival of epi-endogeic (150 m) and endogeic species (~100 m), $SSA_{occluded}$ abruptly decreased, and continued to decrease with further earthworm invasion but only slightly (Fig. 1-11a). The $SSA_{occluded}$ exponentially decreased with increasing depth in the front group soils, but with greater degree of invasion, the depth trends showed more homogenous distributions (Fig. 1-11a).

When OM coated surface area was normalized to the SSA_{total} (Fig. 1-11b), almost the entire (~98 %) mineral surface area was covered by OM in the top 0.5-1.3 g cm^{-2} (~2 cm) of the front group soils. This fraction was found to decrease with greater degree of earthworm invasion. At 0 m, approximately 75 % of the mineral surface area was covered by OM in the top 0.5-1.3 g cm^{-2} (~2 cm) of mineral soil. This change – decrease in OM coated fractions of mineral SSA with the arrival of endogeic species – largely persisted through A to E horizon boundaries, and contrasts the initial prediction that endogeic species would increase OM sorption on the mineral surface.

3.6. Fe Oxides

Dithionite citrate extracted crystalline Fe oxides increased with increasing earthworm biomass (Fig. 1-12a). Crystalline Fe oxides ranged from 0.6 ± 0.1 % to 0.11 ± 0.02 % in the front to the rear groups, respectively, in the surface mineral soils. Similar trends were seen in ammonium oxalate extracted non-crystalline Fe oxides, where non-crystalline Fe oxides increased with increasing earthworm biomass: 0.22 ± 0.02 % in the front group and 0.29 ± 0.02 % in the rear group (Fig. 1-12b).

3.7. Qualitative XRD

Both illite/smectite and kaolinite were greatest in front of the invasion threshold and decreased with increasing earthworm biomass in the top of the mineral soil (Fig 1-13a and b). In the top 1.08 g cm^{-2}, the weight percent of illite/smectite and kaolinite were 16.4 ± 5.6 and 2.9 ± 2.0 %, respectively, in the front groups. In the rear groups where endogeic species are present, the weight percent decreased to 8.4 ± 0.45 % and 0.97 ± 0.48 % for illite/smectite and kaolinite, respectively. The weight percent of illite/smectite and kaolinite decreased with depth, and after 16 g cm^{-2} differences along the invasion gradient were trivial.

4. Discussion

4.1. Earthworm Species along the invasion gradient

In 2001, earthworms were not present beyond 150 m and the invasion threshold was at 110 m (Hale 2005a). As of 2009, earthworms were found at 180 m and the

threshold at 150 m. In eight years, the invasion threshold has advanced about 40 m at the averaged progression rate of ~5 m yr^{-1}. This rate is comparable to 6-10 m yr^{-1} reported between years 1999 and 2001 (Hale et al., 2004). The results show that spatial distributions of earthworms' ecological groups remain largely similar to those observed in 1999-2001 as the invasion progresses (Hale et al., 2004 and 2005b). Earthworms of the epigeic group are predictably the pioneer species, followed by endogeic and then anecic species. As observed in Hale (2005a), epigeic groups were found in front of the invasion threshold, and thus it is likely that they advance to areas with fresh litter and establish an environment suitable for endogeic and anecic species (Hendrix and Bohlen 2002; Frelich et al 2006). The epigeic *D. octaedra* biomass declined from the peak of 1.1 AFD g m^{-2} at 100 m to less than 0.73 AFD g m^{-2} at < 90 m. Closely behind *D. octaedra*, epi-anecic and epi-endogeic species, *L. juvenile* and *L. rubellus*, follow. It is likely that the *L. juvenile* species in front of the threshold are because they are similar to adult *L. rubellus*. Though both *Apporectodea* and *Octolasion* are endogeic species, *Apporectodea* showed strong presence up to 100 m, whereas *Octolasion* were found only near the recreational road and thus appeared to be a recent arrival. Lastly, anecic *L. terrestris* are present only within the distance ≤ 60 m.

The intensive coring data from 2011 (Fig. 1-14b) show that A horizon is thicker in areas highly populated with *Apporectodea* and *L. rubellus* ($P<0.005$). Like Gundale (2002), we found that species that burrow into the upper mineral soil (endogeic, epi-endogeic, and epi-anecic species) have the greatest effect on the A horizon thickness. Additionally, more vertically homogenized A horizons with higher bulk densities were

seen in endogeic-dominated positions along the transect. Hale (2005b) reported *L. terrestris* thickened the A horizon as much as *L. rubellus*. Our data, however, show that A horizon thickness and bulk density increase well before anecic earthworms are established (for bulk density data, see Appendix C).

4.2. Soil Carbon Depth Profiles

Soil C concentrations decrease with increasing depth at all sites, however, the presence of particular earthworm groups influences the soil C concentration depth profiles. There is a subsoil peak at 190 m, which we think reflects the presence of fine roots that have not yet been disturbed by endogeic earthworm activity. The increase in the C % in the top most soil from 190 m to 150 m could possibly be due to the introduction of epi-endogeic and epi-anecic earthworms (Fig. 1-3); the shallow burrowing of these species may incorporate the leaf litter into the mineral horizon or facilitate the leaching of dissolved organic C from the litter layer. Such increase in C concentration is followed by an abrupt reduction once endogeic earthworms are introduced, while epi-endogeic and epi-anecic earthworms persist. Similar observations were made by Hale et al. (2005a) where a decrease in A horizon C concentrations was associated with increasing total earthworm biomass. Homogenization of C concentrations within A horizons is evident in the soils inhabited by endogeic species. Additionally, the translocation the C into the lower A and E horizons is well shown in the soil at 0 m presumably due to the activities of *L. terrestris*.

4.3. Soil Carbon Inventory and Density Fractions

Like my data, Hale et al. (2005a) also reported a decrease in C concentrations with the arrival of endogeic species along the same transect. However, they saw a slight increase in C inventory from 0-12 cm due to changes in the A horizon thickness and bulk density, which is opposite to the finding here that C inventory to the mass equivalent depth of 18.2 g cm^{-2} decreases with the arrival of endogeic species. This difference is largely due to the fact that we report inventories for mass equivalent depth. As endogeic earthworms increase bulk density, the soil has more mass per given depth, which resulted in slight increase of C inventory despite the reduction in C concentrations in the upper 12 cm in Hale et al., (2005a).

The changes in bulk soil C concentration and C inventory along the studied transect largely arise from the changes in the light density fraction. Although the C inventory in the light fraction above the mass equivalent depth of 1.9 g cm^{-2} decreased from 3.4 ± 0.2 to 1.5 ± 0.7 kg C m^{-2} from the front to rear group's soil, the light fraction never contributes less than 58 % of the bulk C inventory in the A horizon (Fig. 1-5b). The light fraction particularly influences the front group's C inventory as it contributes 80-89 % to the bulk C inventory. On the contrary, C inventory in the heavy fraction above the mass equivalent depths of 1.9 g cm^{-2} persists from 0.6 ± 0.2 to 1.1 ± 0.4 kg C m^{-2} in the front to rear group soils, respectively. In the front group soils, heavy fraction contributes only 11-20 % to the A horizon's bulk C inventory. This contribution, however, increases to 18-79 % in the rear group.

4.4. Mechanisms Controlling Total Mineral SSA

In all soils examined, mineral SSA_{total} decreases with increasing soil depth in the A horizon, and this depth trend is particularly dramatic in the soils that are not inhabited by endogeic *Apporectodea* (>100 m). The high mineral SSA_{total} in the top of A horizons appears to be due to secondary phyllosilicate minerals such as illite/smectite and kaolinite whose abundances – determined from quantitative XRD – shows similar depth trends. (Fig. 1-13a and b). Kaolinite has SSA ranging from 10-20 $m^2\ g^{-1}$, while smectite and illite are known to have SSAs of 600-800 $m^2\ g^{-1}$ and 70-120 $m^2\ g^{-1}$, respectively, even though over 80 % of smectite's SSA is in internal layers (Essington, 2004). Such depth trends in the abundances of secondary phyllosilicate minerals appear to explain the high SSA_{total} at the top of A horizons.

While the very top A horizon loses SSA_{total}, the lower A horizon (~1.9 – 6.7 g cm^{-2}) gains SSA_{total} with the greater degree of earthworm invasion (Fig. 1-10b). The significantly more homogeneous depth profiles of SSA_{total} in the rear group soils are due to the endogeic earthworms actively mixing the A horizons. As endogeic earthworms expand A horizons at the expense of the loess cap, the silt materials must be incorporated into the A horizon as well. The loess cap between A and B horizons along the studied transect is remarkably homogeneous in its mineralogy dominated by quartz and potassium plagioclases (Resner et al., 2011) and have consistently low SSA of ~3.36 ± 0.42 $m^2\ g^{-1}$ (Fig. 1-10b). Therefore, we attempted to estimate how soil mixing via endogeic species – by incorporating the loess cap materials into A horizons – may lower the averaged SSA_{total} in the A horizons.

Projecting the detailed measurements of A horizon thicknesses along the transect (Fig 1-14b) and bulk density (see Appendix D), we estimate that invasive earthworms incorporate ~0.4 kg m^{-2} of the loess materials into the A horizon as they advance each meter. Therefore, if soil mixing by earthworms is solely driving the changes in the SSA_{total} in the A horizons, in addition to the vertical homogenization of SSA_{total} in A horizons, the averaged SSA_{total} of the thickening A horizons should show linearly decreasing trend with increasing degree of earthworm invasion (Fig. 1-14a). From the 190 m and 0 m, the simple mixing model predicts, the averaged SSA_{total} of the A horizon should decrease by 2.7 m^2 g^{-1} (Fig. 1-14a).

This prediction, however, does not agree with our observation (Fig. 1-14a). We calculated averaged SSA_{total} for the 0-1.9 g cm^{-2} mass equivalent depth (see Appendix B). Despite the large changes in the depth profiles of the mineral SSA_{total} along the transect (Fig. 1-10), the A horizon averaged SSA_{total} shows only a slight decrease from the front to rear group soils. Therefore, earthworm derived soil mixing alone cannot explain the spatial variation of mineral SSA_{total} observed along the earthworm invasion transect.

This discrepancy between observation and simple mass balance appears to arise because invasive earthworms simultaneously affect pedogenic crystalline and amorphous Fe oxides in the soil (Fig. 1-12). The step increase in the concentrations of the two oxide pools from 150 to 100 m agrees with the forefront of the endogeic *Apporectodea* found at 100 m (Fig. 1-3a). Because earthworm guts are highly anoxic (Drake et al 2006), Fe in the soil materials ingested by geophagous *Apporectodea* may be reduced and become soluble upon passage through the gut. The dissolved Fe then may later be re-oxidized and

re-precipitated as Fe oxides in the aerobic environment (Cornell and Schwertmann, 2003). For example, Oyedele et al. (2006) documented increase in Fe oxides as soil materials pass through earthworm guts. Secondary Fe oxides extractable by dithionite citrate and ammonium oxalate are known for their high SSA (Pronk, 2011). For instance, ferrydydrite is found to have SSA of 200-400 m^2 g^{-1} (Cornell and Schwermann, 2003), while Borggaard (1982) reported amorphous oxides as having SSA of 305-412 m^2 g^{-1} and crystalline Fe oxides as having SSA of 116-184 m^2 g^{-1}. Both Pronk et al. (2011) and Kaiser and Guggenberger (2000) indicated that crystalline Fe oxides are most likely the primary contributor to minerals' SSA in both agricultural and forested environments. Therefore, as soils are inhabited by endogeic earthworms, two factors are contributing to the SSA in the A horizon: (1) endogeic species incorporate the silt materials with low SSA from the underlying loess cap and (2) earthworms increase the amount of high SSA-secondary Fe oxides in the A horizon. The two factors appear to cancel out such that the averaged SSA_{total} in the A horizon remain largely constant across the transect.

4.5. Factors of OM-Mineral Surface Interactions

I initially hypothesized that greater mixing by earthworms, particularly epi-endogeic and endogeic species, would increase OM sorption on mineral surface by enhancing physical contacts between OM and mineral surfaces. Therefore, it is expected that absolute amount of surface area and the fraction of mineral surface area covered by OM would increase with earthworm invasion. My observations disprove this initial hypothesis. The soils inhabited only by epigeic earthworm species have not only the larger $SSA_{occluded}$ but also generally higher percentages of SSA_{total} covered with OM in

the top most A horizons (Fig. 1-11). Therefore, less mineral surface area is present and a lower fraction of the surface area is covered with OM with the arrival of endogeic species. Here we explore two reasons for this finding.

From the mineral side of OM-mineral interactions, the results show that soil mixing enhanced by endogeic earthworms does not make greater mineral surface area available to sorb organic matter. As discussed above, physical incorporation of the underlying silt materials and enhanced production of secondary Fe oxides contribute to maintaining the averaged SSA_{total} of the 0-1.9 cm g^{-2} mass equivalent depth regardless of invasion status. This is also true even when we consider the inventory of SSA_{total} in the thickening A horizons (Fig. 1-15).

Second, from the OM side of the OM-mineral sorption, the data illustrates that OM-sorption on mineral surface in the A horizon becomes rapidly limited by mineral-free OM with the arrival of endogeic species. In the front group soils where endogeic and anecic species are absent, weight % of the light fraction C with respect to the bulk soil is as high as ~26 %. At 100 m of the transect, which is the forefront of endogeic species, we observed that 12-18 % of the light fraction C at the top A horizon is already lost presumably due to earthworm consumption. If the overall progression rate of invasion threshold at 5 m yr^{-1} is applied to that of endogeic species, the top A horizon soil loses 0.85-1.83 % of its light fraction C per year after the arrival of endogeic species (Fig. 1-6, 1-7b and Fig. 1-3a). In the topsoil at 50 m, which has been inhabited by endogeic species for about 10 years, there is only less than 26 % of total C in the light fraction, compared to 96 % at 190 m. Once the same rate of invasion is also considered for *L. terrestris*, this

soil at 50 m has been habited by the anecic species for ~4 years.

Once these numbers are combined with the measured bulk densities, the A horizon inventory of light fraction is 3.4 ± 0.2. kg C m^{-2} in the front group soils and 1.5 ± 0.7 kg C m^{-2} in the rear group soils, contributing 85 % and 58 % of their total A horizon C inventories, respectively. In contrast, C inventories of the A horizon heavy fraction slightly increase from 0.6 ± 0.2 kg C m^{-2} in the front group to 1.1 ± 0.4 kg C m^{-2} in the rear group.

It is also notable that C concentrations of the light fraction materials tend to be lower in the soils with endogeic species, while the C concentrations of the heavy fraction materials do not show such trends (Fig. 1-7a and b). Accelerated decomposition of leaf litter resulting in the decrease of C contents has been reported in the presence of invasive earthworms (Filley, 2008; Holdsworth et al., 2008). Therefore, the earthworm invasion not only dramatically reduces the contributions of light fraction to the bulk soil, but also reduces the amount of light fraction C.

4.6. Mineral vs. Organic Control of OM-Mineral Sorption

There is a well-defined linear relationship between SSA_{total} and $SSA_{occluded}$ (Fig. 1-16a). The ranges of the values of $SSA_{occluded}$ and SSA_{total} become significantly narrower in the soils with endogeic and anecic species (0-100 m) when compared to the soils mostly with epigeic species (150-190 m). When all of the data are compiled together, however, the relationship between the two quantities closely follows a linear relationship with non-zero x-intercept of 3.14 m^2 g^{-1} (r^2 = 0.987) (line not shown Fig. 1-15a). When linear relations were sought separately for the two groups, the x-intercepts of the two

groups differ considerably. The x-intercepts of the front and rear groups are 2.7 m^2 g^{-1} and 5.1 m^2 g^{-1}, respectively, and their slopes are 1.1 and 1.5, respectively (lightly invaded r^2 = .993; heavily invaded r^2 = .930; Fig. 1-15a).

We interpret that the x-intercepts represent the portion of mineral surface area that is not capable of adsorbing organic matter. These non-reactive SSA are greater in the rear group soils. This non-reactive surface area contributes 4-35 % of the SSA_{total}, in the soils ≥150 m and 17-57 % in the soils ≤100 m. In both groups, the fraction of non-reactive mineral surface in SSA_{total} increases with decreasing SSA_{total}. The greater non-reactive mineral SSA in the rear group soils may reflect the incorporation of the wind-blown fine silt and sand quartz materials from the underlying loess cap.

We also assessed the nature of the surface area measured by N_2 absorption method by examining the *C*-constants determined for untreated soil samples (Fig. 1-17). Typical values of heavily organic-covered minerals range from 20-40, while mineral surface values have been reported from 70 to as high as 247 (Ahsan, 1992; Mayer, 1999; Wagai et al. 2009). It appears that most of the exposed surfaces of the topsoil materials in the front group are organic. These materials have not only the greatest C concentrations, but also low *C*-constants of ≤50, which is indicative of organic surfaces rather than mineral surfaces (Mayer, 1999) (Fig. 1-17). Some of the A horizon materials in the rear group, and the materials below A horizons display higher *C*-constants that indicate part of the mineral surface remains organic free, which is consistent with the greater non-reactive mineral surface area in the rear group soils.

Robust positive correlations are found between $SSA_{occluded}$ and SSA_{total} over the studied transect. This correlation suggests OM sorption on mineral surface increases with increasing size of the mineral surface area, with an implication that mineral SSA instead of available mineral-free OM limits OM-mineral sorption. However, there are strong positive correlations between total C concentrations and mineral SSA_{total} as both variables decrease with increasing soil depth (Fig. 1-16b). Moreover contribution of light density fraction to the total C has the same correlation with mineral SSA_{total} (Fig. 1-6b). Therefore, it is difficult to determine if available OM or mineral SSA is the limiting factor in producing mineral-sorbed OM in the front group soils.

Although the A horizon inventories of mineral SSA_{total} do not decrease with the arrival of endogeic species – due to the increase in bulk density and horizon thickness that compensate for reduction of mineral SSAtotal – the inventories of occluded mineral SSA decrease. The SSAoccluded, at least within the mass equivalent depth of 1.9 g cm^{-2}, slightly decrease from $0.29 \pm 0.04 \times 10^6$ m^2 m^{-2} in the front group to $0.15 \pm 0.005 \times 10^6$ m^2 m^{-2} in the rear group (Fig. 1-15a and b). These observations, when considered together with the C inventory in the light fraction decreasing with the arrival of endogeic, suggest that sorption of OM on mineral surface may become limited by available organic matter with the invasion of endogeic earthworm species.

4.7. OM-Mineral Sorption in Heavy Fraction

I further investigated mineral surface areas of the heavy fraction as heavy fraction C is presumed to be mineral-sorbed (Fig. 1-18). Unlike the bulk fractions, there is no significant change in the SSA_{total} of the heavy fractions. Likewise, no significant change

in the % of $SSA_{occluded}$ along the transect is found for the heavy fractions. However, both SSA_{total} and $SSA_{occluded}$ still decrease with increasing depth, and decreasing OC loadings with increasing depth persist along the chronosequence. Although larger $SSA_{occluded}$ is associated with greater C contents, the majority of the soils sampled within the heavy faction lie well above the monolayer equivalent (Fig. 1-18b).

A shift from light fraction to heavy fraction, thus mineral-free OM to mineral complexed OM, suggests that: (1) earthworm driven soil mixing is increasing contacts between mineral surfaces and OM, and creating new organo-mineral complexes, and/or (2) C within the light fraction is lost from the system via earthworm activity. It is likely that earthworm driven soil mixing creates new organo-mineral complexes as both $\delta^{13}C$ and $\delta^{15}N$ values in the heavy fraction become depleted in the earthworm invaded soils relative to non-invaded soils (Fig. 1-8a and 1-9a). This slight depletion suggests that less decomposed, or fresh, OM is being incorporated in the heavy fraction. An increase in $SSA_{occluded}$ would be indicative of additional complexes within the heavy fraction; however, no such changes were observed. Moreover, there is no net change in the percent of C in the heavy fraction across the earthworm invasion gradient; therefore, no net change in the heavy fraction C. Earthworms are most likely simultaneously destabilizing existing organo-mineral complexes and forming new complexes with fresh C. This result, together with the little change observed for the inventories of SSA_{total} and $SSA_{occluded}$ in A horizon soils, further provides explanatory mechanisms for the robust C inventory in the heavy fraction across the invasion chronosequence.

4.8. Implication of This Study

My initial hypothesis is that endogeic and anecic earthworms – by upwardly moving the clay rich B horizon materials into A horizons – increase mineral SSA of A horizon materials. However, even anecic earthworms do not appear to burrow below the loess cap into the clay B horizon at the study site. Had the A horizon directly overlaid clay rich B horizon with greater mineral SSA_{total}, earthworm driven soil mixing may have increased SSA_{total} in the A horizon with a potential to sorb more OM. A combination of increased bulk density and SSA_{total} would have significantly increased the heavy fraction C inventory. This scenario suggests that impacts of invasive earthworms on mineral-associated C pool may well depend on the initial soil depth profiles of key properties such as mineralogy and texture. If the initial depth of the A horizon is greater than 20 cm depth, it is not likely that any of the underlying materials will be mixed upward, as we did not observe any mixing activity below this depth. In this case there would only be the addition of Fe oxides produced by the earthworms, and an overall increase in SSA_{total}. On the other hand, if the lower boundary of the A horizon is less than 20 cm deep, incorporation of the underlying material would be incorporated into the A horizon in addition to the formation of Fe oxides. If the underlying material is clay or silty/clay with relatively high SSA, earthworms would incorporate minerals with high SSA into the A horizon; however if the underlying material is coarser and sandier, minerals with low SSA would be mixed into the A horizon. This study shows a case where invasive earthworms burrow in the subsoil where minerals with low SSA_{total} are present.

5. Conclusion

The initial hypotheses that (1) endogeic and anecic species will increase mineral SSA in the A horizon by incorporating clay minerals in the underlying clay right B horizon and (2) endogeic earthworms will increase OM sorption on minerals' surface by accelerating soil mixing were rejected at the study site. Instead mineral SSA and OM sorption on the minerals' surface remain in dynamic equilibrium: while invasive earthworms maintain the net amounts of mineral SSA and OM-mineral sorption, earthworms are constantly altering the source of SSA. The rejection of the first hypothesis has to do with the presence of loess cap between A and B horizons; the loess cap has low SSA therefore the incorporation of the loess material, instead of B horizon clays, into the A horizon did not increase the overall SSA of the A horizon. Furthermore, we reject the first hypothesis due to the finding that endogeic and anecic species rarely venture down below the loess cap at the study site. Regarding the second hypothesis, I found that the availability of mineral-free OM becomes the limiting factor with the endogeic consumption of mineral-free OM. Successful rejection of these hypotheses demonstrate that the hypotheses and the underlying concept are broadly applicable to other soil systems under the influence of bioturbators.

Despite the large and systematic variation in the depth profiles of mineral SSA along the earthworm invasion transect, the inventories of SSA_{total} and $SSA_{occluded}$ in A horizon soils remain largely stable. My methods allowed us to find that this stability is the result of many contributing factors including incorporation of silt materials from the underlying loess materials, the increased abundance of secondary Fe oxides, and

thickening and increased bulk density of the A horizons. The incorporation of silt and quartz materials from the underlying loess cap decreased SSA_{total} inventory, which was counter balanced by the greater abundance of secondary Fe oxides, thickness of the A horizon, and bulk density. All of these changes were driven by the arrival of endogeic earthworm species. In spite of the stable abundances of mineral SSA, it appears that the generation of mineral-sorbed OM is beginning to be limited by available mineral-free OM which rapidly decreases with the arrival of endogeic species. This result further shows that earthworm invasion may have dramatically different impacts on the mineral SSA and OM sorption on mineral surface depending on the initial mineralogy, texture, and their vertical distributions in the soils, together with species composition of the invading earthworms.

6. References

Adams MB, Loughry LH, Plaugher LP. 2004. Experimental Forests and Ranges of the USDA Forest Service. U.S. Department of Agriculture. Newtown Square PA, USA.

Ahsan T. 1992. The surface properties of pure and modified precipitated calcium carbonate by adsorption of nitrogen and water vapor. Colloids and Surfaces 64:167-176.

Alban DH, Berry EC. 1994. Effects of earthworm invasion on morphology, carbon and nitrogen of a forest soil. Applied Soil Ecology 1:243-249.

Baldock JA, Skjemstad JO. 2000. Role of the soil matrix and minerals in protecting natural organic materials against biological attack. Organic Geochemsitry 31(7): 697-710.

Blair JM, Crossley DA, Jr. 1988. Litter decomposition, nitrogen dynamics and litter microarthropods in a southern Appalachian hardwood forest 8 years following clearcutting. Journal of Applied Ecology. 25: 683-698.

Bohlen PJ, Pelletier D, Groffman PM, Fahey TJ, Fist MC. 2004a. Ecosystem consequences of exotic earthworm invasion of north temperate forests. Ecosystems 7:1-12.

Bohlen PJ, Pelletier DM, Groffman PM, Fahey, TJ, Fisk MC. 2004b. Influence of earthworm invasion on redistribution and retention of soil carbon and nitrogen in northern temperate forests. Ecosystems 7:13-27.

Bohlen PJ, Scheu S, Hale CM, McLean MA, Migge S, Groffman PM, Parkinson D. 2004c. Non-native invasive earthworms as agents of change in northern temperate forests. Frontiers in Ecology and the Environment 2(8):427-435.

Borggaard OK. 1982. The influence of iron oxides on the surface area of soil. Journal of Soil Science 33: 443-449.

Burtelow AE, Bohlen PJ, Groffman PM. 1998. Influence of exotic earthworm invasion on soil organic matter, microbial biomass and denitrification potential in forest soils of the northeastern United States. Applied Soil Ecology 9:197-202.

Chenu S, Stotzky G. 2002. Intereactions between microorganisms and soil particles. An overview. Huang PM, Bollag JM, Senesi N, editors. Interactions between soil particles and microorganisms. Weinheim Wiley-VCH-Verlag p3-39.

Chiou CT. 1990. The surface area of soil organic matter. Environmental Science Technology 24:1164-1166

Coderre D, Mauffette Y, Gagnon D, Tousignant S, Besette G. 1995. Earthworm populations in healthy and declining sugar maple forests. Pedobiologia 39:86-96.

Cornell, RM, Schwertmann U. 2003. The iron oxides: structure, properties, reactions, occurrences and uses. Weinheim (DE): Wiley-VCH. p.664.

de Jonge H, Mittelmeijer-Hazeleger MC. 1996. Adsorption of CO_2 and N_2 on soil organic matter: nature of porosity, surface area, and diffusion mechanism. Environmental Science Technology 30:408-413.

Drake HL, Schramm, Horn MA. 2006. Earthworm gut microbial biomes: their importance to soil microorganisms, denitrification, and the terrestrial production of the greenhouse gas N_2O. Soil Biology 6:65-87.

Eberl, DD. 2003. User's guide to Rockjock – a program for determining quantitative mineralogy from powder X-ray diffraction data. U.S. Geological Survey Open-File Report: 03-78. p. 46.

Essington ME. 2004. Soil and water chemistry: an integrative approach. Boca Raton (FL): CRC Press LLC. p.534.

Eusterhues K, Rumpel C, Kleber M, Kögel-Knabner I. 2003. Stabilisation of soil organic matter by interactions with minerals as revealed by mineral dissolution and oxidative degradation. Organic Geochemistry 34:1591-1600.

Eusterhues K, Rumpel C, Kögel-Knabner I. 2005. Organo-mineral associations in sandy acid forest soils: importance of specific surface area, iron oxides and micropores. European Journal of Soil Science 56:753-763.

Filley TR, McCormick MK, Crow ME, Szlavecz K, Whigham DF, Johnston CT, van den Huevel RN. 2008. Comparison of the chemical alteration trajectory of *Liriodendron tulipifera L.* leaf litter among forests with different earthworm abundance. Journal of Geophysical Research (2005=2012) 113:G1.

Frelich LE, Hale CM, Scheu S, Holdsworth AR, Henegham L, Bohlen PJ, Reich PB. 2006. Earthworm invasion into previously earthworm-free temperate and boreal forests. Biological Invasions 8:1235-1245.

Gates GE. 1982. Farewell to North American megadriles. Megadrilogica 4:12-77.

Gundale MJ. 2002. The influence of exotic earthworms on soil organic horizon and the rare fern *Botrychium mormo*. Conservation Biology 16:1555-73.

Hale CM. 2004. Ecological consequences of exotic invaders: interactions involving European earthworms on native plan communities in hardwood forests. Ph.D. Dissertation, University of Minnesota, Department of Forest Resources, St. Paul, Minnesota.

Hale CM, Frelich LE, Reich PB. 2004. Allometric equations for estimation of ash-free dry mass from length measurements for selected European earthworm species (Lumbricidae) in the western Great Lakes region. American Midland Naturalist Journal 151(1): 179-185.

Hale CM, Frelich LE, Reich PB, Pastor J. 2005a. Effects of European earthworm invasion on soil characteristics in northern hardwood forests of Minnesota, USA. Ecosystems 8:911-927.

Hale CM, Frelich LE, Reich, PB. 2005b. Exotic European earthworm invasion dynamics in northern hardwood forests of Minnesota, USA. Ecological Applications 15: 848-860.

Hale CM, Frelich LE, Reich PB. 2006. Changes in cold-temperate hardwood forest understory plan communities in response to invasion by European earthworms. Ecology 87:1637-1649.

Hale CM. 2007. Earthworms of the Great Lakes. Duluth (MN): Kollath and Stensaas Publishing. p.36.

Hale CM. 2008a. Evidence for human-mediated dispersal of exotic earthworms: support for exploring strategies to limit further spread. Molecular Ecology 17:1165-1169.

Hale CM, Frelich LE, Reich PB, Pastor J. 2008b. Exotic earthworm effects on hardwood forest floor, nutrient availability and native plants: a mesocosm study. Oecologia 155:509-518.

Hendrix PF, Bohlen PJ. 2002. Exotic earthworm invasions in North American: ecological and policy implications. BioScience 52(9): 801-811.

Holdsworth AR, Frelich LE, Reich PB. 2008. Litter decomposition in earthworm-invaded northern hardwood forests: role of invasion degree and litter chemistry. Ecoscience 15(4):536-544.

Holmgren GGS. 1967. A rapid citrate-dithionate extractable iron procedure. Soil Science Society of America Proceedings 31: 210–211

Jackson ML, Lim CH, Zelazny LW. 1986. Oxides, hydroxides, and aluminosilicates. Klute A, editor. Methods of soil analysis, Part I. Physical and mineralogical methods. Madison: Soil Science Society of America. p.101-150.

Kaiser K, Guggenberger G. 2000. The role of DOM sorption to mineral surfaces in the preservation of organic matter in soils. Organic Geochemistry 31:711-725.

Kaiser K, Guggenberger G. 2003. Mineral surfaces and soil organic matter. European Journal of Soil Science 54:219-236.

Kaiser K, Guggenberger G. 2007. Sorptive stabilization of organic matter by microporous goethite: sorption into small pores vs. surface complexation. European Journal of Soil Science 58:45-59.

Keil RG, Hedges JI. 1993. Sorption of organic matter to mineral surfaces and the preservation of organic matter in coastal marine sediments. Chemical Geology 107:385-388.

Keil RG, Montlucon DB, Prahl FG, Hedges JI. 1994. Sorptive preservation of labile organic matter in marine sediments. Nature 370:549-552.

Keil RG, Mayer LM, Quay PD, Richey JE, Hedges JI. 1997. Loss of organic matter from riverine particles in deltas. Geochimica et Cosmochimica Acta 61:1507-1511.

Kleber M, Sollins P, Sutton R. 2007. A conceptual model of organo-mineral interactions in soils: self-assembly of organic molecular fragments into zonal structures on mineral surfaces. Biogeochemsitry 85: 9-24.

Langmaid KK. 1964. Some effects of earthworm invasion in virgin podzols. Canadian Journal of Soil Science 44:34-7

Lawrence AP, Bowers MA. 2002. A test of the 'hot' mustard extraction method of sampling earthworms. Soil Biology and Biochemistry 34:549-52

Ludwig B, John B, Ellerbrock R, Kaiser M, Flessa H. 2003. Stabilization of carbon from maize in a sandy soil in a long-term experiment. European Journal of Soil Science 54: 117-126.

Masiello CA, Chadwich OA, Southon J, Torn MS, Harden JW. 2004. Weathering controls on mechanisms of carbon storage in grassland soils. Global Biogeochemical Cycles 18(4): GB4023

Mayer LM. 1999. Extent of coverage of interal surfaces by organic matter in marine sediments. Geochimica et Cosmochimica Acta 63(2): 207-215.

Mayer LM, Xing B. 2001. Organic matter-surface area relationships in acid soils. Soil Science Society of America Journal 65: 250-258.

Mikutta R, Kleber M, Kaiser K, Jahn R. 2005. Review: organic matter removal from soils using hydrogen peroxide, sodium hypochlorite, and disodium peroxodisulfate. Soil Science Society of America Journal 69:120-135.

McKeague JA, Day JH. 1966. Dithionite and oxalate-extractable Fe and Al as aids in differentiating various classes of soils. Canadian Journal of Soil Science 46:13-22.

Minnesota State Climatology Office. 2003. Minnesota climatology working group website http://climate.umn.edu, Minnesota Department of Natural Resources and the University of Minnesota, Department of Soil, Water and Climate, St. Paul , MN 55108.

Oades JM. 1988. The retention of organic matter in soils. Biogeochemistry 5:35-70.

Oyedele DJ, Schjønning P, Amunsan AA. 2006. Physiochemical properties of earthworm casts and uningested parent soil from selected sites in southwestern Nigeria. Ecological Engineering 28:106-113.

Pennell KD, Boyd SA, Abriola LM. 1995. Surface area of soil organic matter reexamined. Soil Science Society of America Journal 59:1012-1018.

Pronk GJ, Heister K, Kögel-Knabner I. 2011. Iron oxides as major available interface component in loamy arable topsoils. Soil Science Society of America Journal 75:2158-2168.

Ransom B, Kim D, Kastner M, Wainwright S. 1998. Organic matter preservation on continental slopes: importance of mineralogy and surface area. Geochimica et Cosmochimica Acta 62:1329-1345.

Resner KE, Yoo K, Hale C, Aufdenkampe A, Blum A, Sebestyen S. 2011. Elemental and mineralogical changes in soil due to bioturbation along an earthworm invasion chronosequence in northern Minnesota. Applied Geochemistry 26: S127-S131.

Reynolds JW. 1977. The earthworms (Lumbricidae and Sparganophilidae) of Ontario. Royal Ontario Museum Miscellaneous Publication, Toronto, Ontario.

Rumpel C, Kögel-Knabner I. 2011. Deep soil organic matter – a key but poorly understood component of terrestrial C cycle. Plant Soil 338:143-158.

SAS Institute Inc. 2010. JMP, version 9.0.2. SAS Institute Inc. 100 SAS Campus Drive, Cary NC 27513-2414 USA.

Savage NM. 1988. The use of sodium polytungstate for conodont separations. Journal of Micropalaeontology 7(1):39-40.

Scheu S, Parkinson D. 1994a. Effects of earthworms on nutrient dynamics, carbon turnover and microorganisms in soil from cool temperate forests of the Canadian Rocky Mountains – laboratory studies. Applied Soil Ecology 1:113-25.

Scheu S, Parkinson D. 1994b. Effects of invasion of an aspen forest (Canada) by *Dendrobaena octaedra* (Lumbricidae) on plant growth. Ecology 75:2348-2361.

Schmidt MWI, Torn MS, Abiven S, Dittmar T, Guggenberger G, Janssesn IA, Kleber M, Kögel-Knabner I, Lehmann J, Manning DAC, Nannipieri P, Rasse DP, Weiner S, Trumbore SE. 2011. Persistence of soil organic matter as an ecosystem property. Nature 478: 49-56.

Schwert, DP. 1990. Oligochaeta: Lumbricidae. Dindal DL, editor. Soil biology guide. New York: John Wiley and Sons. p.341-356.

Sequi P, Aringhieri R. 1977. Destruction of organic matter by hydrogen peroxide in the presence of pyrophosphate and its effect on soil specific surface area. Soil Science Society of America Journal 41(2): 340-342

Six J, Conant RT, Paul EA, Paustian K. 2002. Stabilization mechanisms of soil organic matter: implications for saturation of soils. Plant and Soil 241:155-176.

Soil-Survey. 1997/2006. Soil survey of Cass County, Minnesota, United States Department of Agriculture, p.300.

Sollins P, Homann P, Caldwell BA. 1996. Stabilization and destabilization of soil organic matter: mechanisms and controls. Geoderma 74(1):65-105.

Sollins P, Swantston C, Kleber M, Filley T, Kramer M, Crow S, Caldwell B, Lajtha K, Bowden R. 2006. Organic C and N stabilization in a forest soil: evidence from sequential density fractionation. Soil Biology and Biochemistry 38: 3313-3324.

Sollins P, Kramer M, Swantson C, Lajtha K, Filley T, Aufdenkampe A, Wagai R, Bowden R. 2009. Sequential density fractionation across soils of contrasting mineralogy: evidence for both microbial- and mineral-controlled soil organic matter stabilization. Biogeochemistry 96:209-231

Sørensen LH. 1975. The influence of clay on the rate of decay of amino acid metabolites synthesized in soils during decomposition of cellulose. Soil Biology and Biochemistry 7:171-177.

Torn MS, Trumbore SE, Chadwich OA, Vitousek PM, Hendricks MD. 1997. Mineral control of soil organic carbon storage and turnover. Nature 389:170-173.

Torresan M. 1987. The use of sodium polytungstate in heavy mineral separations. U.S. Geological Survey Open-File Report. p.87-590.

von Lutzow M, Kögel-Knabner I, Ekschmitt K, Matzner E, Guggenberger G, Marschner B, Flessa H. 2006. Stabilization of organic matter in temperate soils: mechanisms and their relevance under different soil conditions – a review. European Journal of Soil Science 57:426-445.

von Lutzow M, Kögel-Knabner I, Ludwig B, Matzner E, Flessa H, Ekschmitt K, Guggenberger G, Marschner B, Kalbitz K. 2008. Stabilization mechanisms of organic matter in four temperate soils: development and application of a conceptual model. Journal of Plant Nutrition and Soil Science 171: 111-124.

Wagai R, Mayer LM, Kitayama K. 2009. Extent and nature of organic coverage of soil mineral surfaces assessed by a gas sorption approach. Geoderma 149:152-160.

Wagner TL, Mattson WJ, Witter JA. 1977. A survey of soil invertebrates in two Aspen forests in northern Minnesota. St. Paul (MN): North Central Forest Experiment Station, Forest Service, General Technical Report NC-40:1-23.

Webb PA, Orr C. 1997. Analytical methods in fine particle technology. Norcross (GA): Micromeritics Instrument Corp. p301.

Weilder PG, Stanjek H. 1998. The effect of dry heating of synthetic 2-line and 6-line ferrihydrite: II. surface area, porosity and fractal dimension. Clay Mineralogy 33:277-384.

Wironen M, Moore TR. 2006. Exotic earthworm invasion increases soil carbon and nitrogen in an old-growth forest in southern Quebec. Canadian Journal of Forest Research 36: 845-854.

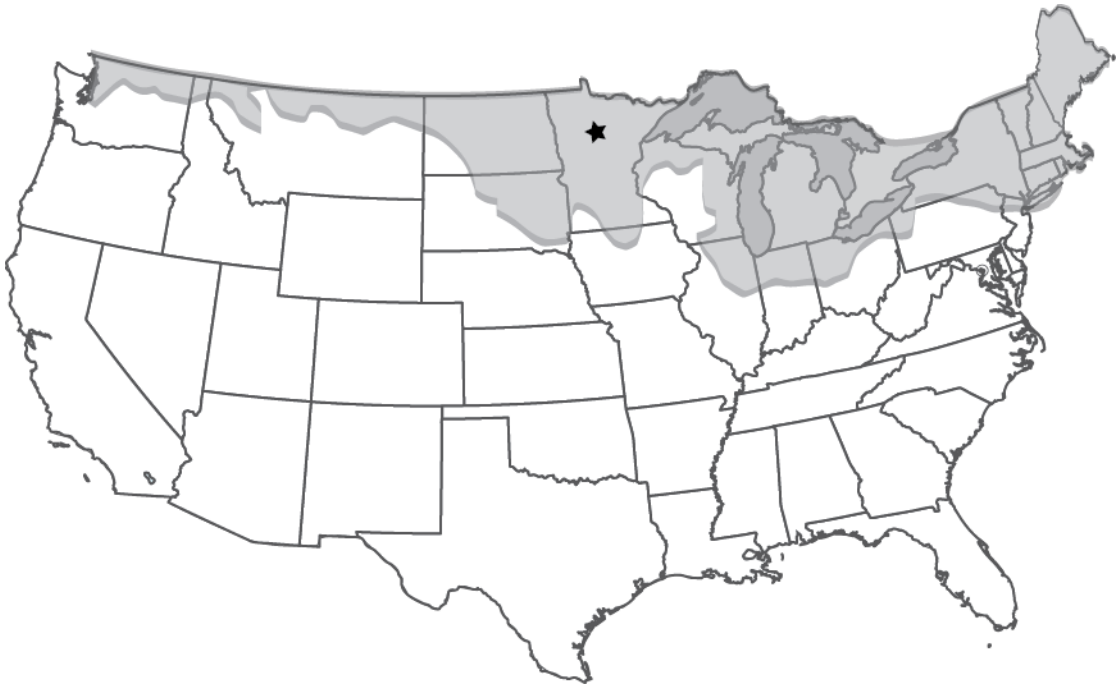

Fig. 1-1. Recently glaciated part of the N. America (highlighted) evolved without native earthworms until the recent arrival of exotic European earthworm species. The star indicates the location of my study site in northern Minnesota.

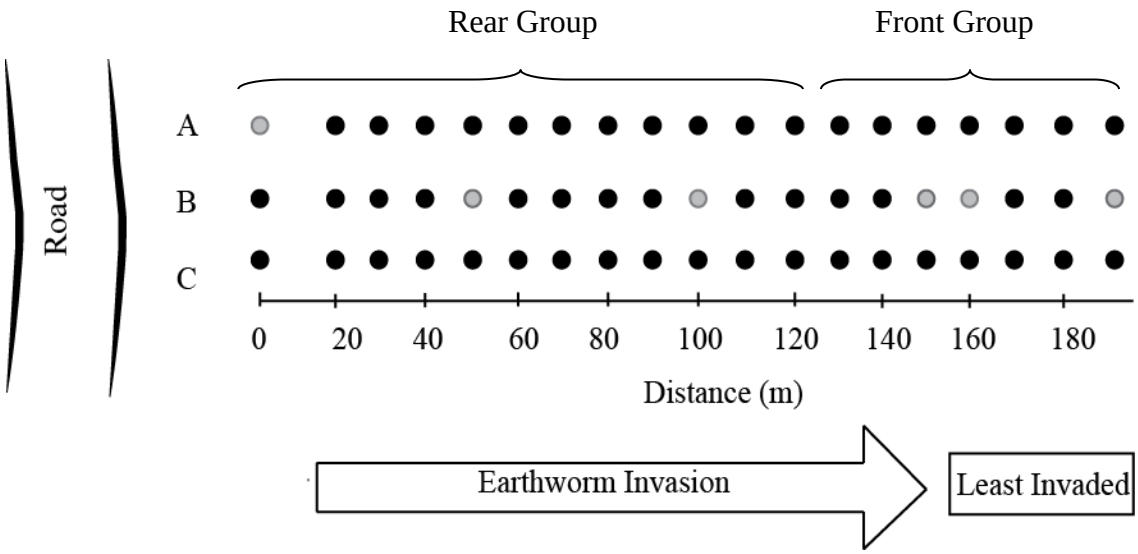

Fig. 1-2. Grey circles represent the soil pits that were excavated in 2009. Soils samples collected from these soil pits were analyzed for various measurements. Nineteen locations along the transect B were used for sampling earthworms in 2009 (Fig. 1-3) and were probed in 2011 to determine the thickness of A horizons (Fig. 1-11b). In the subsequent years of 2010 and 2011, earthworms were sampled at 10 meter intervals along the all three transects (Chapter 2 and Data in Appendix C).

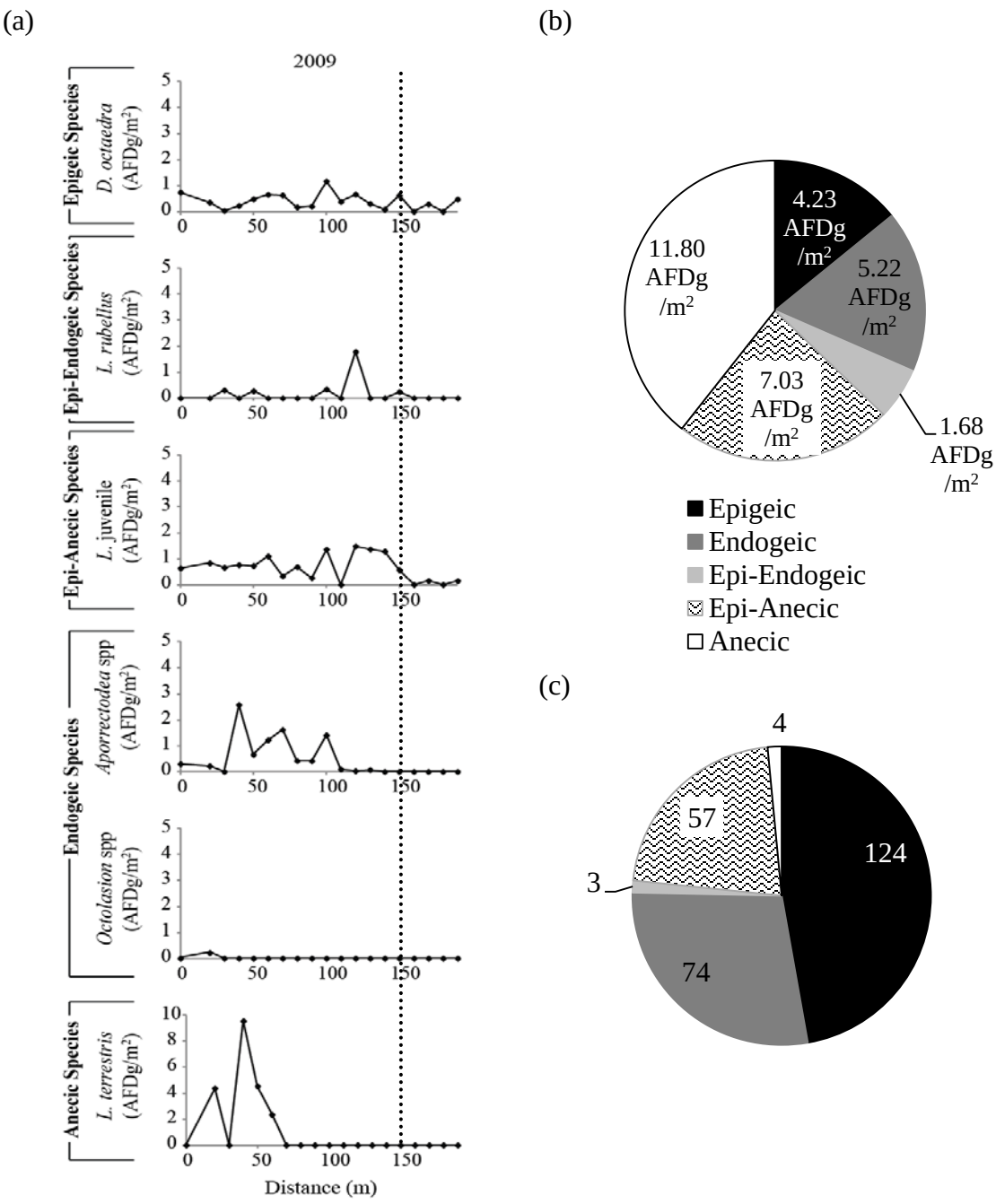

Fig. 1-3. (a) Species-specific and functional group-specific earthworm biomasses along the invasion chronosequence as sampled in 2009. Dotted line indicates the invasion threshold. In 2009, the invasion threshold was not documented. Therefore we used the long-term trend based on Hale et al (2001) and the recent observations of the threshold in 2010 and 2011 in estimating the most likely location of threshold in 2009. Individual functional groups' contributions to (b) the total earthworm biomass per area sampled (c) total number of collected individual earthworms.

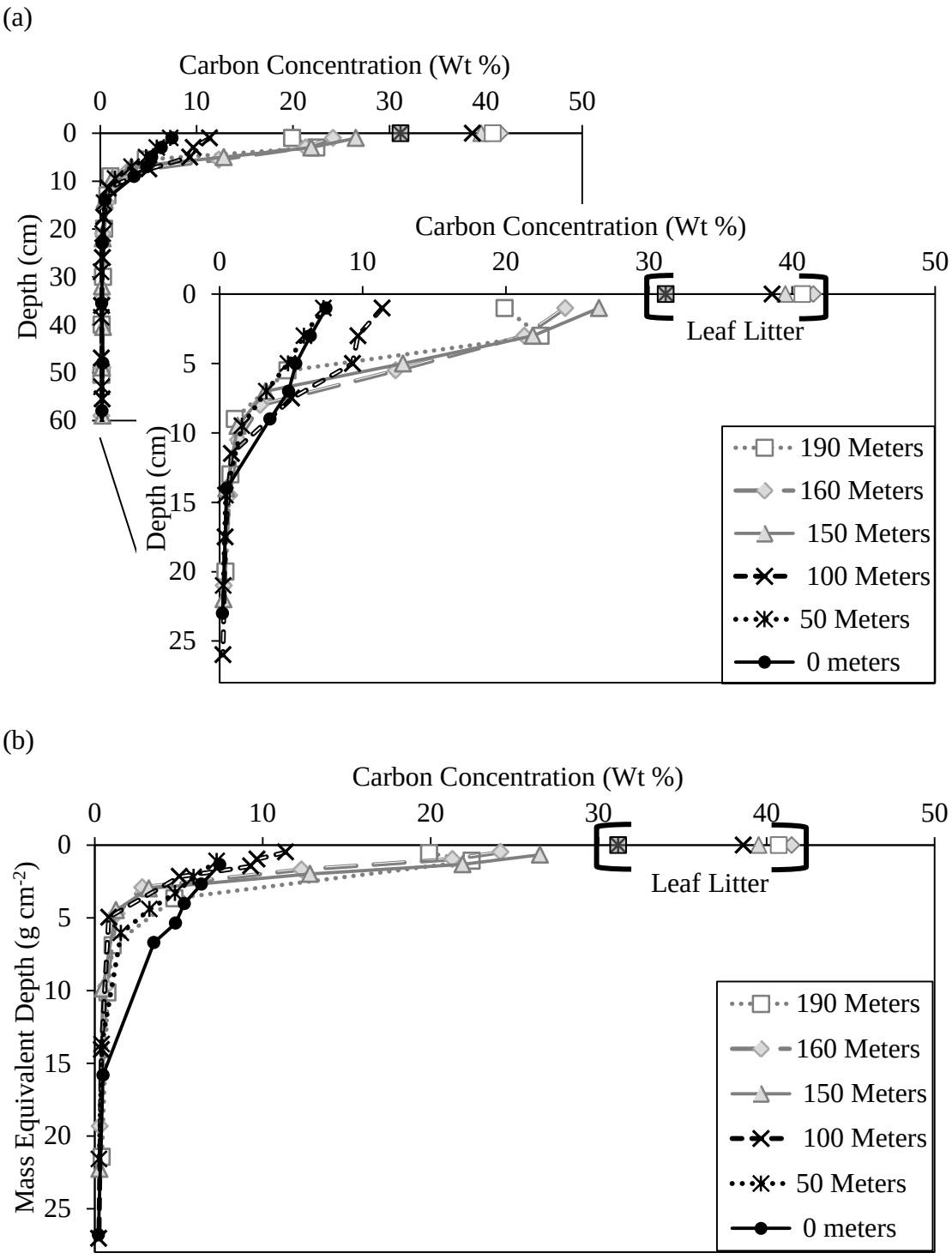

Fig. 1-4. (a) Depth profiles of organic carbon concentrations and (b) Mass equivalent depth profiles of organic carbon concentrations. By integrating the carbon concentrations by the mass equivalent depth, we obtain C inventory.

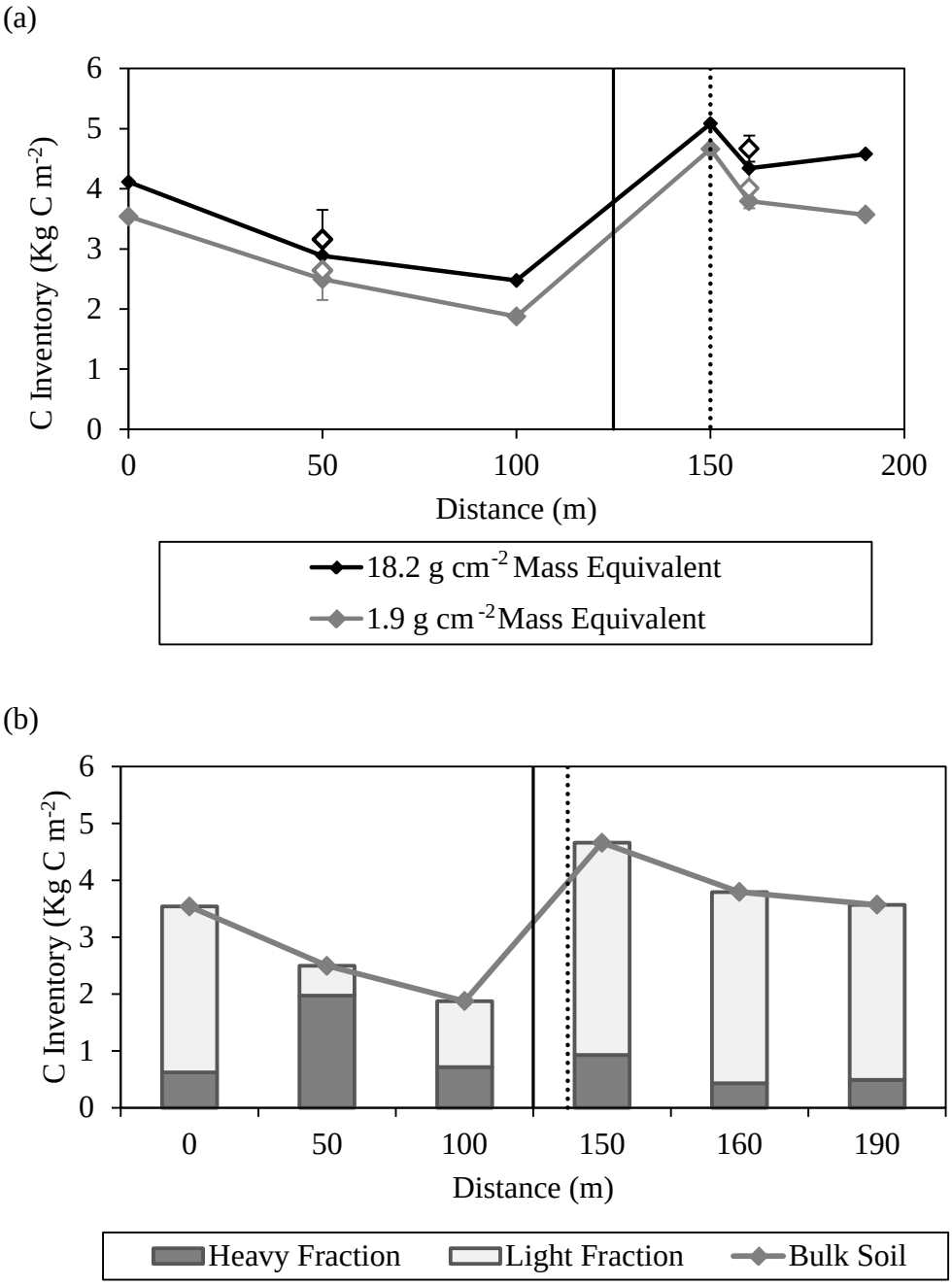

Fig. 1-5. (a) Soil C Inventory to the mass equivalent depths of 1.9 g cm^{-2} (~ A horizon) and 18.2 g cm^{-2} (A+ E horizons: ~30-35 cm). Average values and their standard errors are also plotted for the C inventories of front and rear group soils. (b) Soil C inventory in the light (< 2.0 g cm^{-3}) and the heavy (> 2.0 g cm^{-3}) fractions to the mass equivalent depths of 1.9 g cm^{-2}. The solid vertical line represents the forefront of endogeic species that divides the studied transect into the front and rear groups, and the dotted line represents the earthworm invasion threshold.

(a)

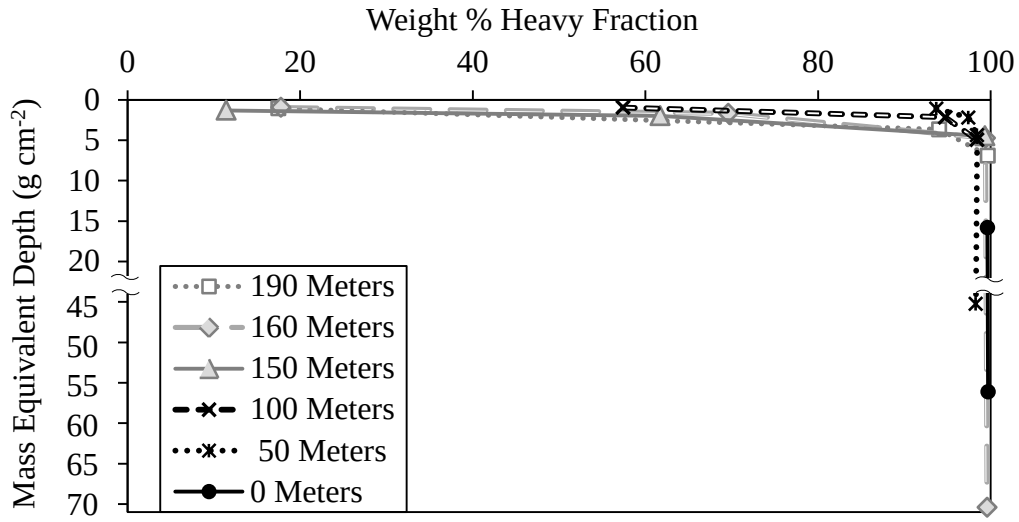

(b)

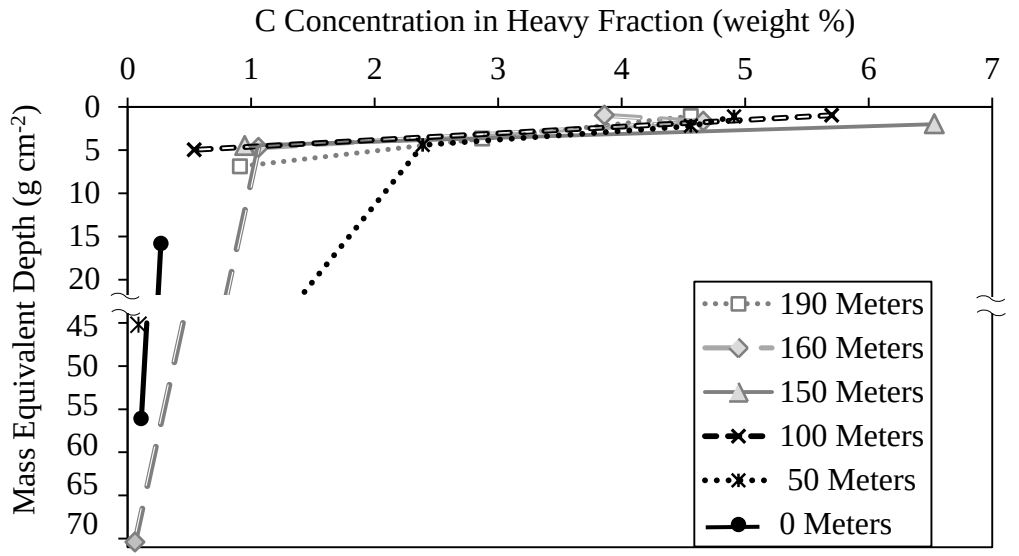

Fig. 1-6. Relationship between mass equivalent depth and (a) mass percentage of heavy fraction (> 2.0 g m^{-3}) with respect to bulk soil materials, (b) C concentrations in the heavy fraction of soil materials, (c) mass percentage of light fraction (< 2.0 g m^{-3}) with respect to the bulk soil materials, and (d) C concentrations in the light fraction of soil materials.

(c)

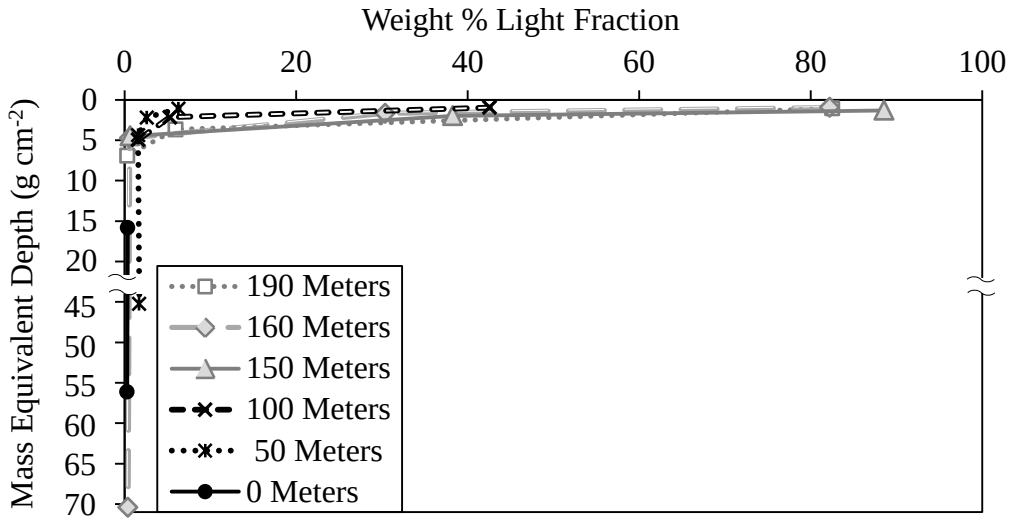

(d)

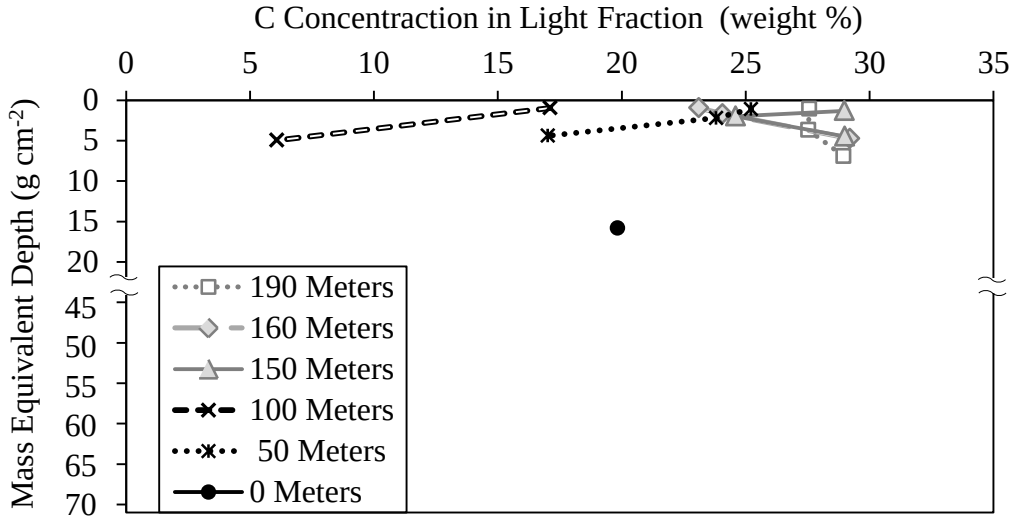

Fig. 1-6. Continued: Relationship between mass equivalent depth and (a) mass percentage of heavy fraction (> 2.0 g m^{-3}) with respect to bulk soil materials, (b) C concentrations in the heavy fraction of soil materials, (c) mass percentage of light fraction (< 2.0 g m^{-3}) with respect to the bulk soil materials, and (d) C concentrations in the light fraction of soil materials.

(a)

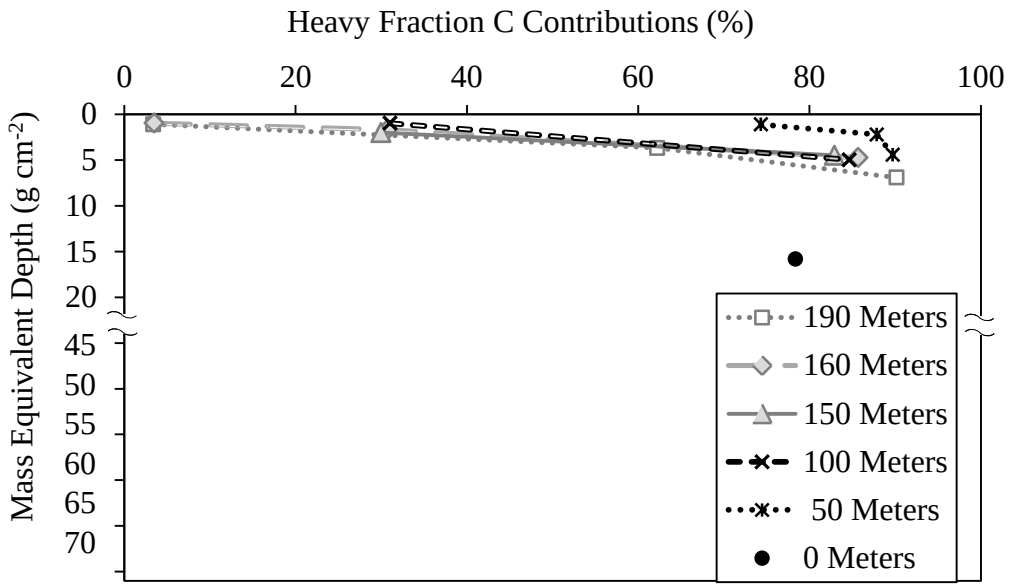

(b)

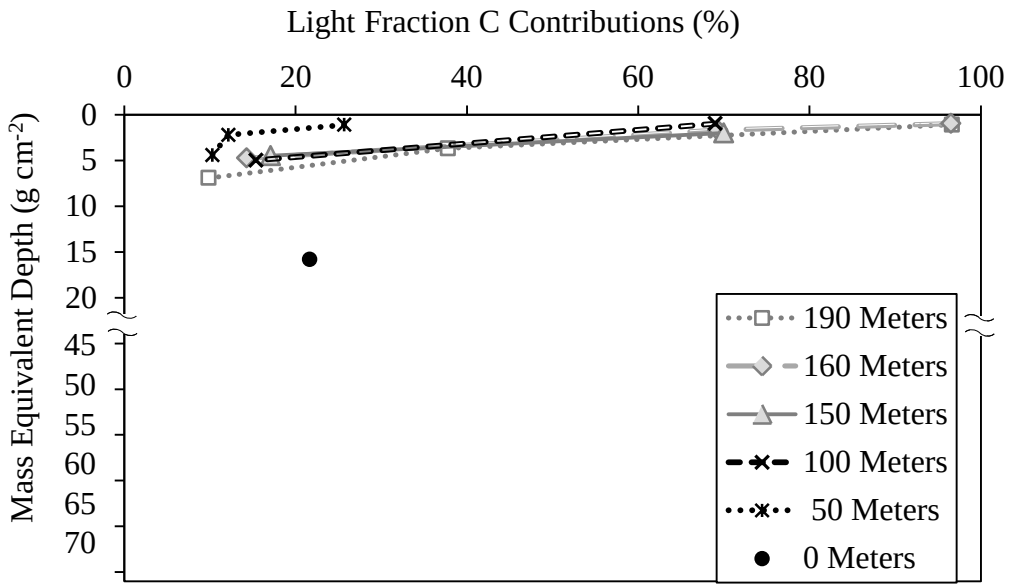

Fig. 1-7. Mass equivalent depth profiles of (a) heavy and (b) light fractions' contributions to total carbon.

(a)

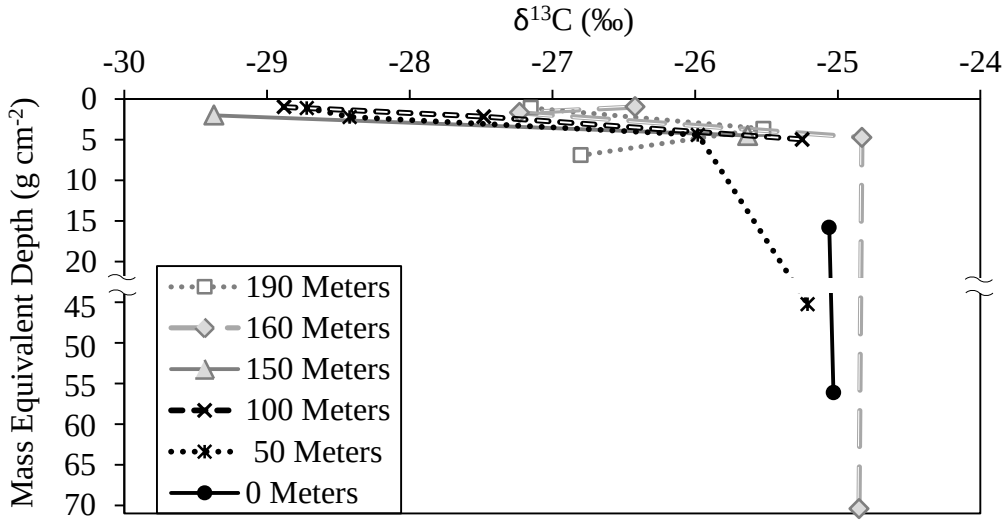

(b)

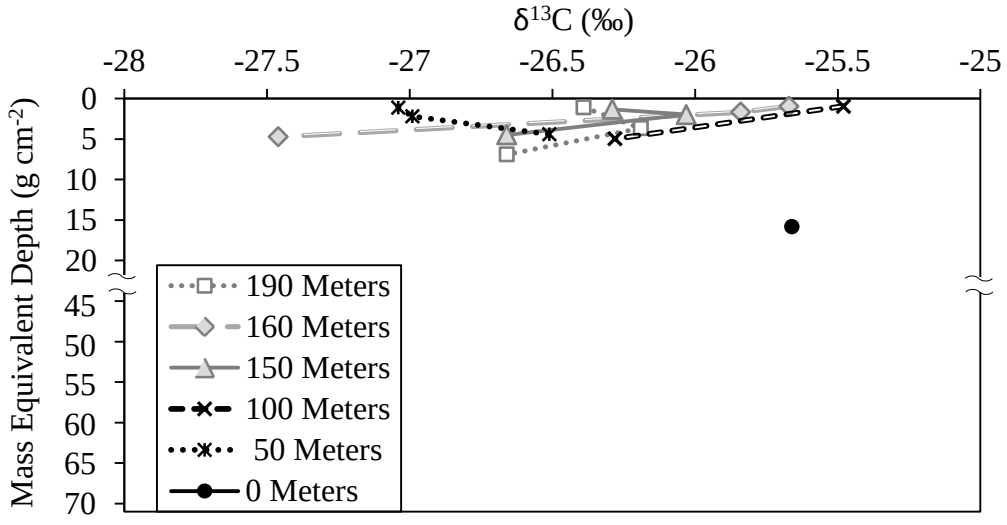

Fig. 1-8. Depth profiles of $\delta^{13}C$ values of the (a) heavy fractions (>2.0 g cm^{-3}) and (b) light fractions (<2.0 g cm^{-3}).

(a)

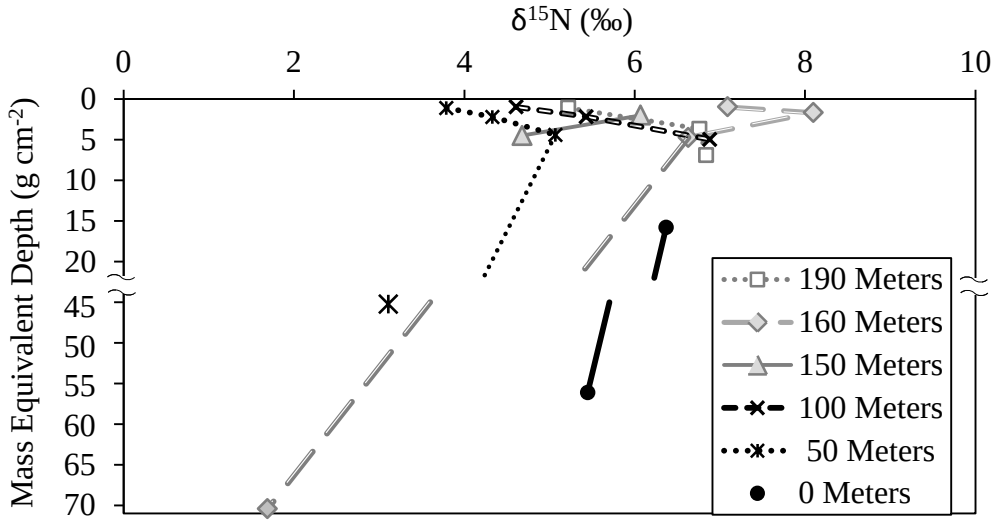

(b)

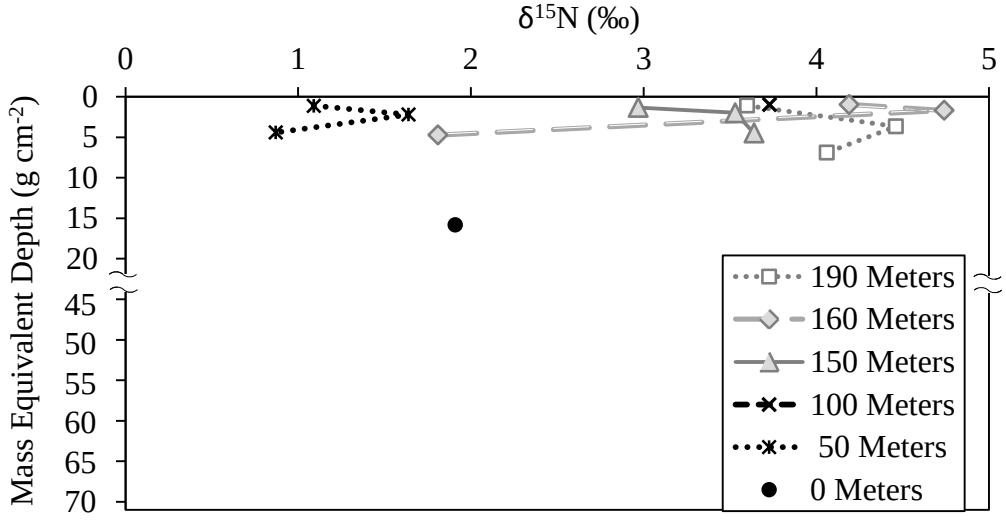

Fig. 1-9. Relationship between mass equivalent depth and values of $\delta^{15}N$ for the (a) heavy (> 2.0 g cm^{-3}) and (b) light (< 2.0 g cm^{-3}) fractions.

(a)

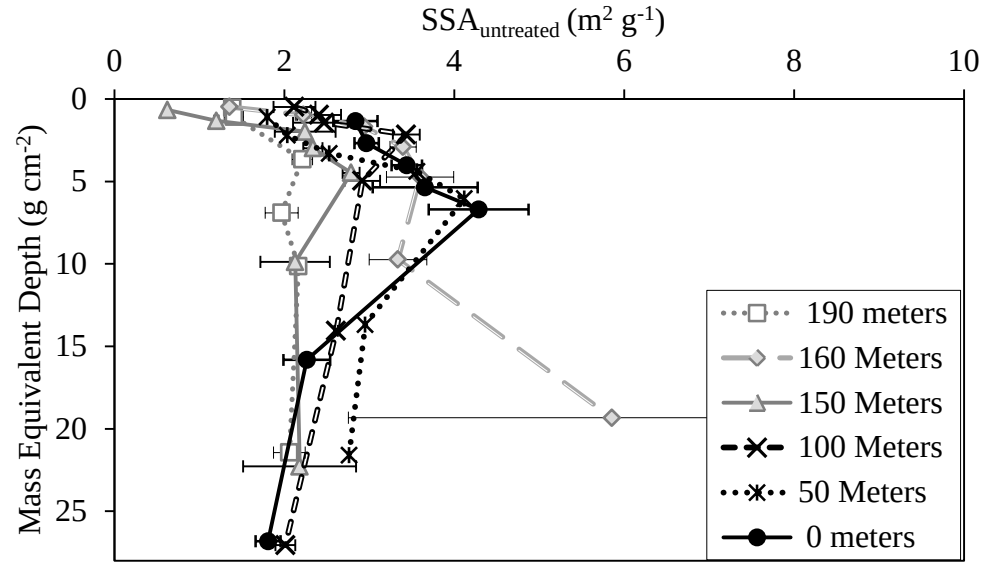

(b)

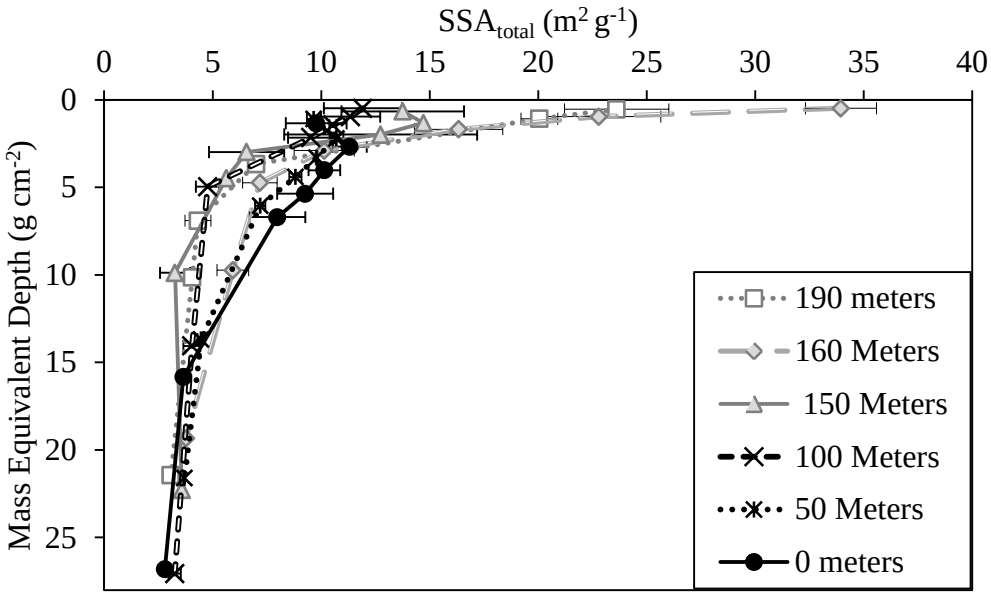

Fig. 1-10. Mass equivalent depth profiles of (a) $SSA_{untreated}$ (before removing organic matter) and (b) SSA_{total} (after the removal of organic matter).

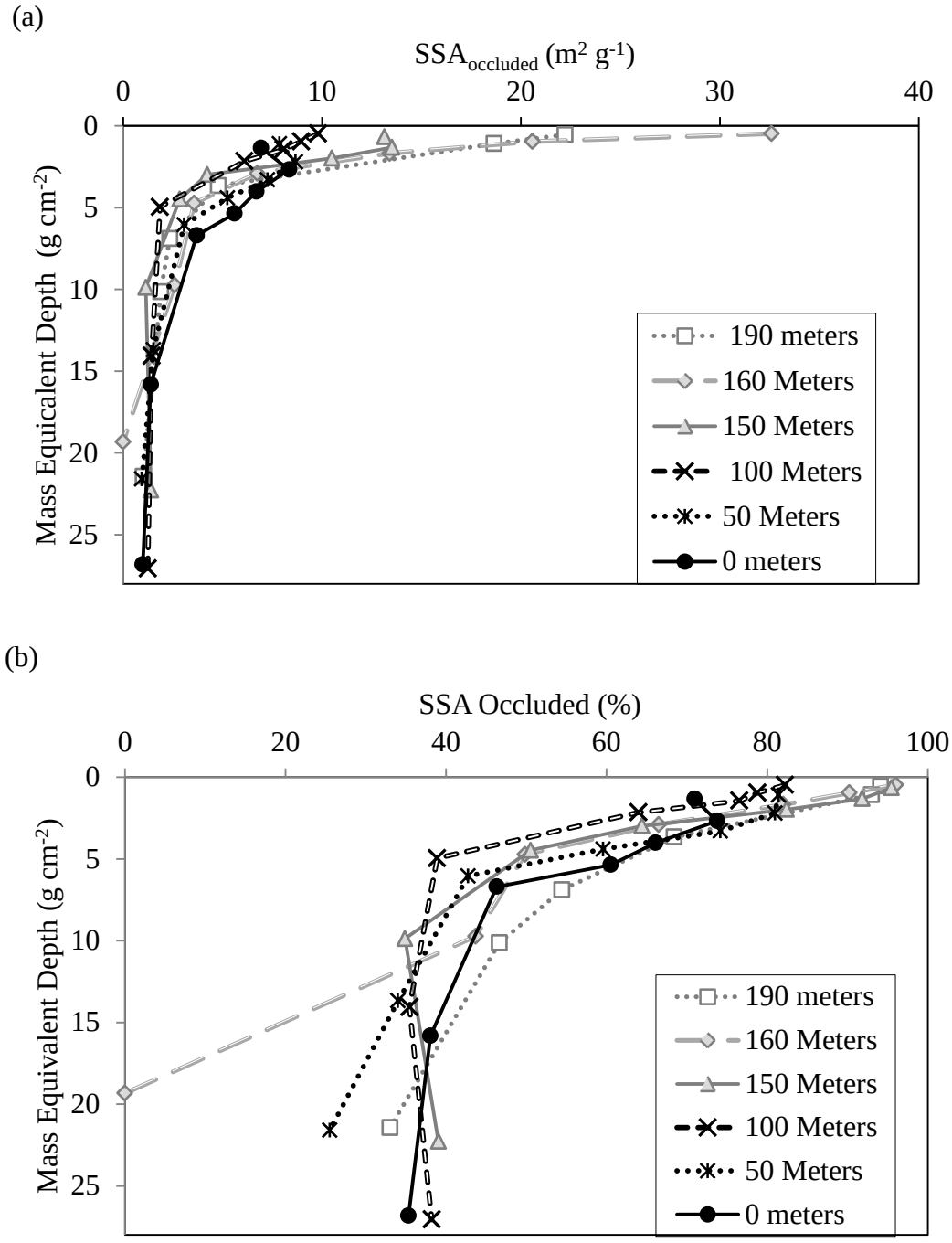

Fig. 1-11. Mass equivalent depth profiles of (a) $SSA_{occluded}$ and (b) the percent fraction of $SSA_{occluded}$ relative to the SSA_{total}.

(a)

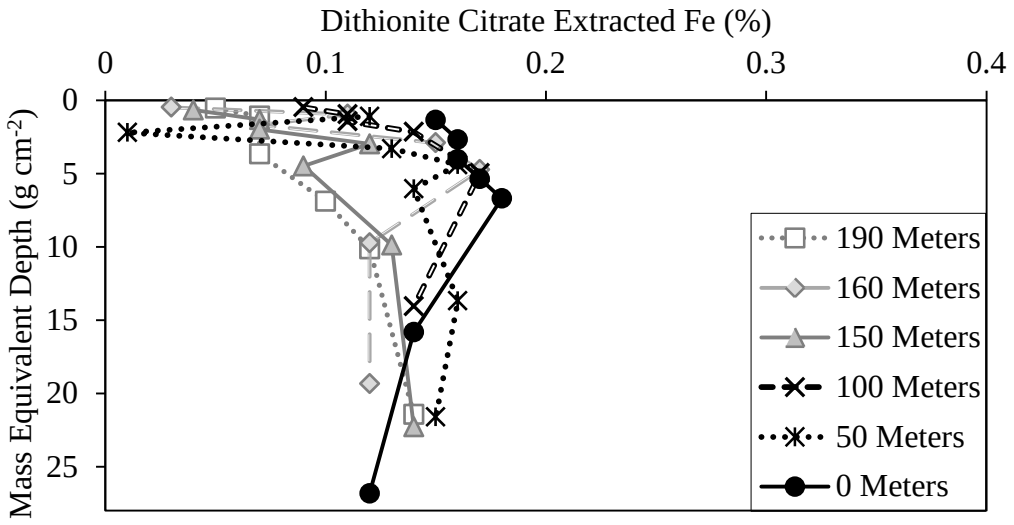

(b)

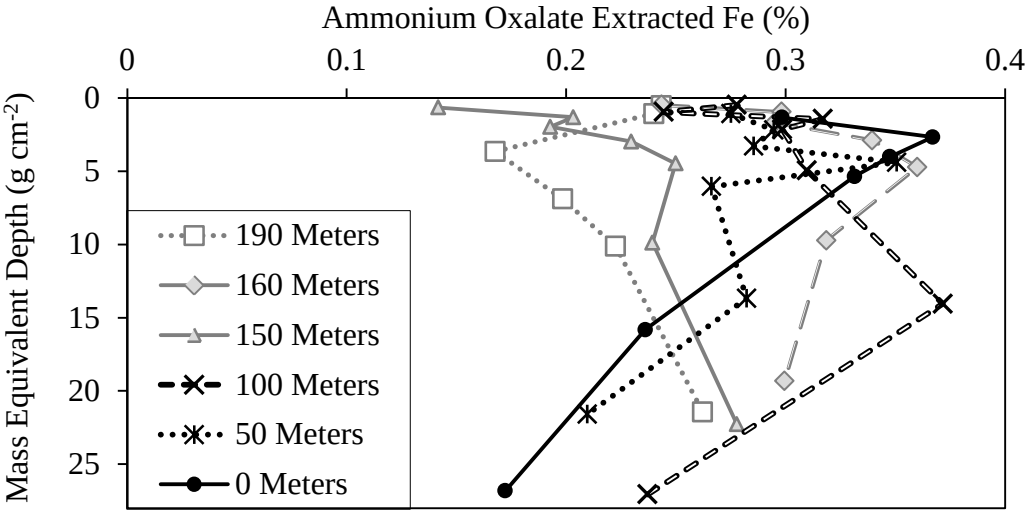

Fig. 1-12. Mass equivalent depth profiles of (a) pedogenic crystalline iron oxides as determined as citrate-bicarbonate-dithionite extractable Fe and (b) amorphous iron oxides as determined as ammonium oxalate extractable Fe.

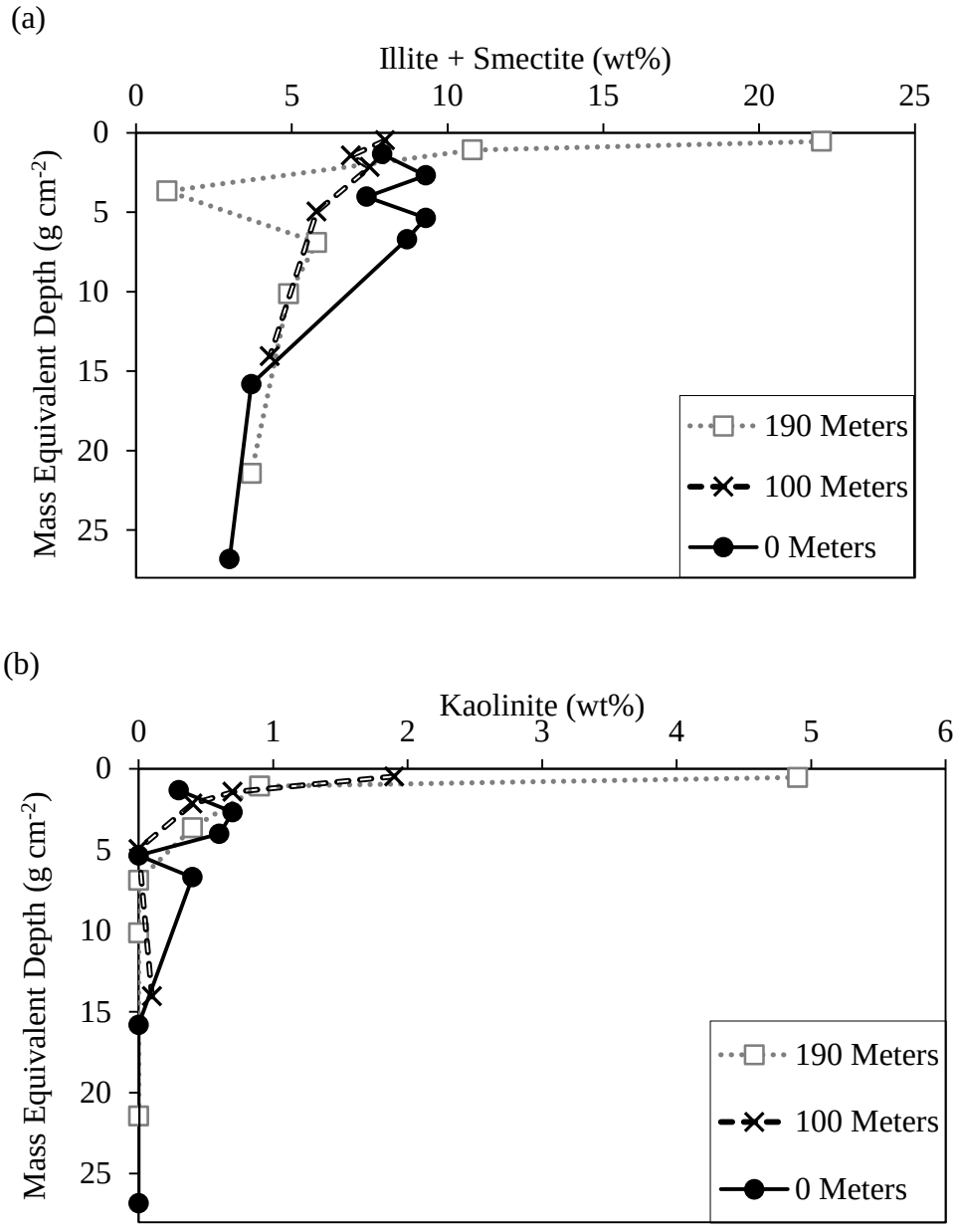

Fig. 1-13. Mass equivalent depth profiles of the concentrations of (a) illite/smectite and (b) kaolinite along the invasion chronosequence. The mineralogical composition was determined with quantitative XRD technique.

(a)

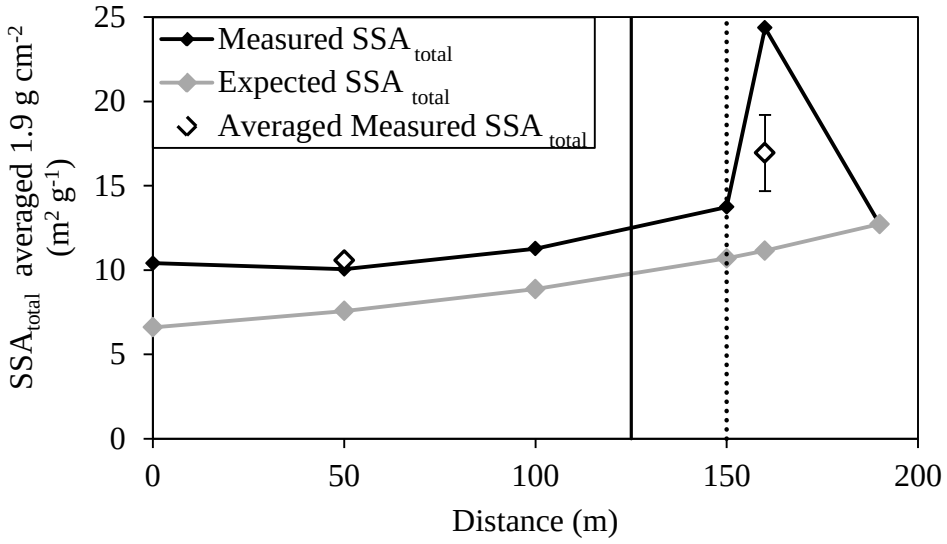

(b)

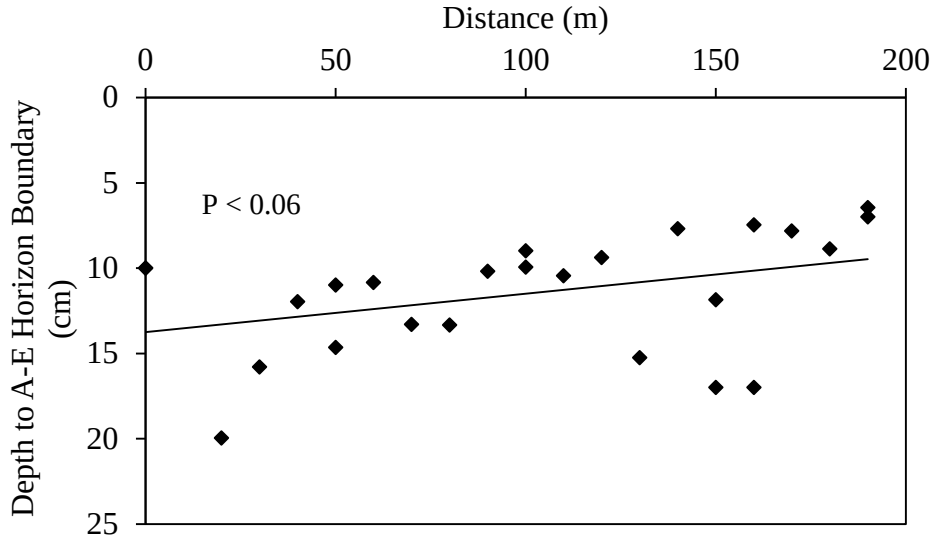

Fig. 1-14. (a) The grey colored line represents the expected trend of averaged SSA_{total} in A horizons (1.9 g cm^{-2}) if the changes in the mineral SSA_{total} in the A horizon is solely due to the mixing-driven inclusion of low SSA loess cap materials into the A horizons. The dark solid line represents actual SSA_{total} found along the transect. The solid vertical line divides the front and rear groups, and the dotted line represents the invasion threshold. (b) The changing depth to the A-E horizon boundary across the invasion chronosequence ($P < .06$).

(a)

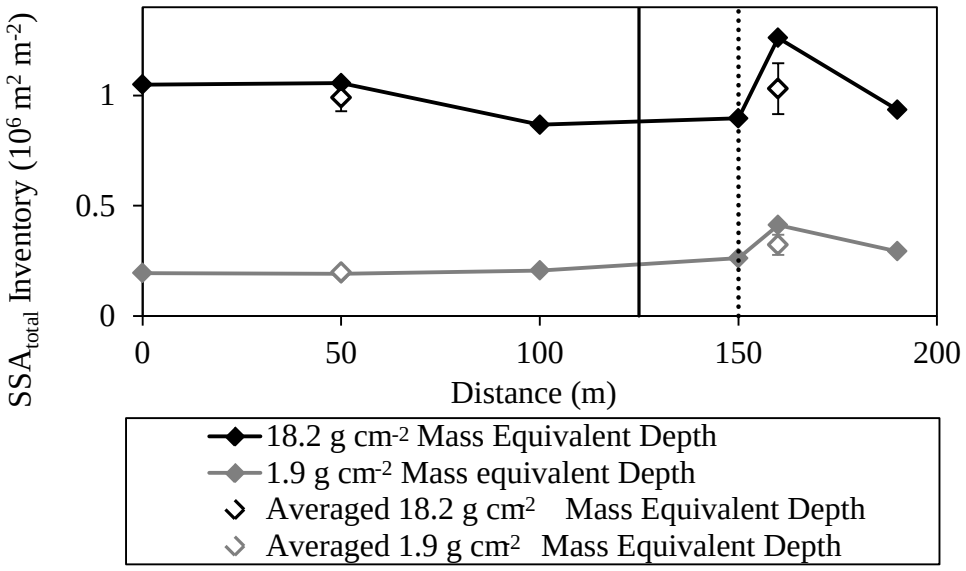

(b)

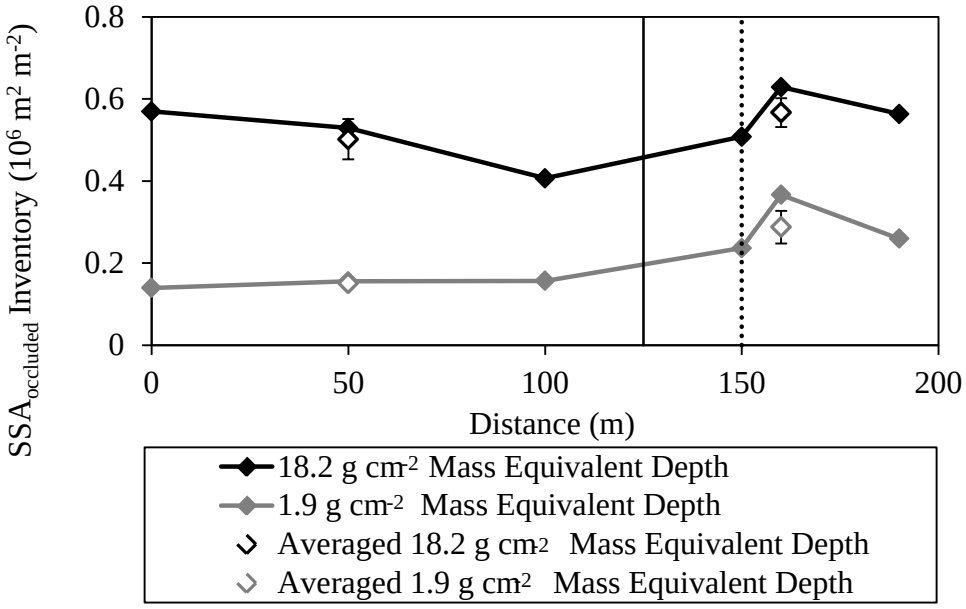

Fig. 1-15. A horizon inventories of (a) SSA_{total} and (b) $SSA_{occluded}$. Calculation of these inventories took into consideration the changes in soil bulk densities and A horizon thicknesses. Solid line separates the front and rear groups, and dotted line represents the earthworm invasion threshold.

(a)

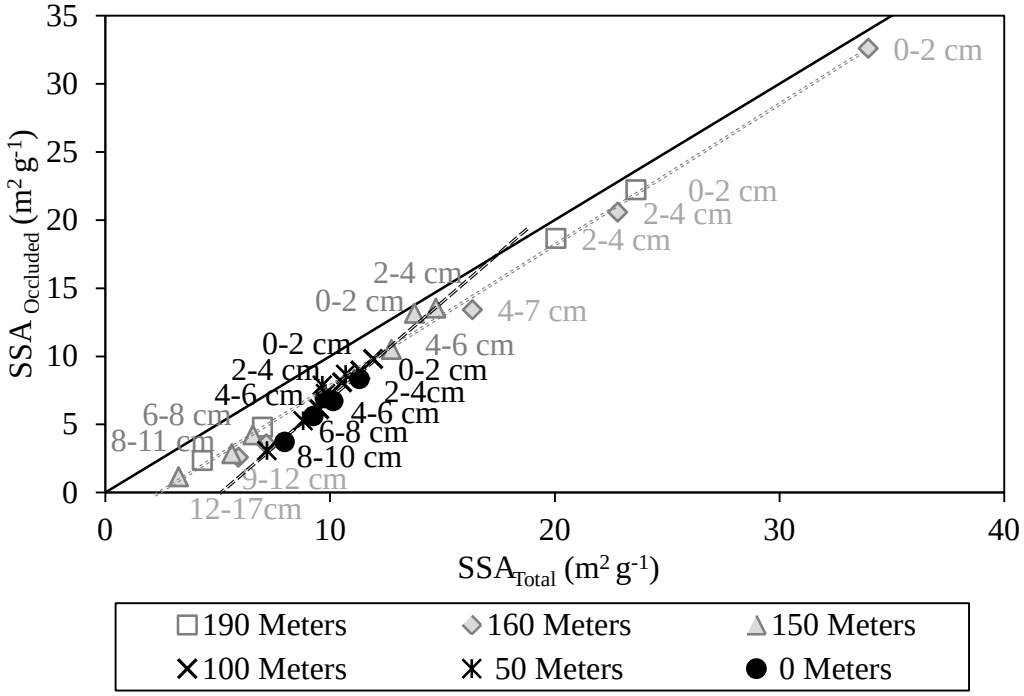

(b)

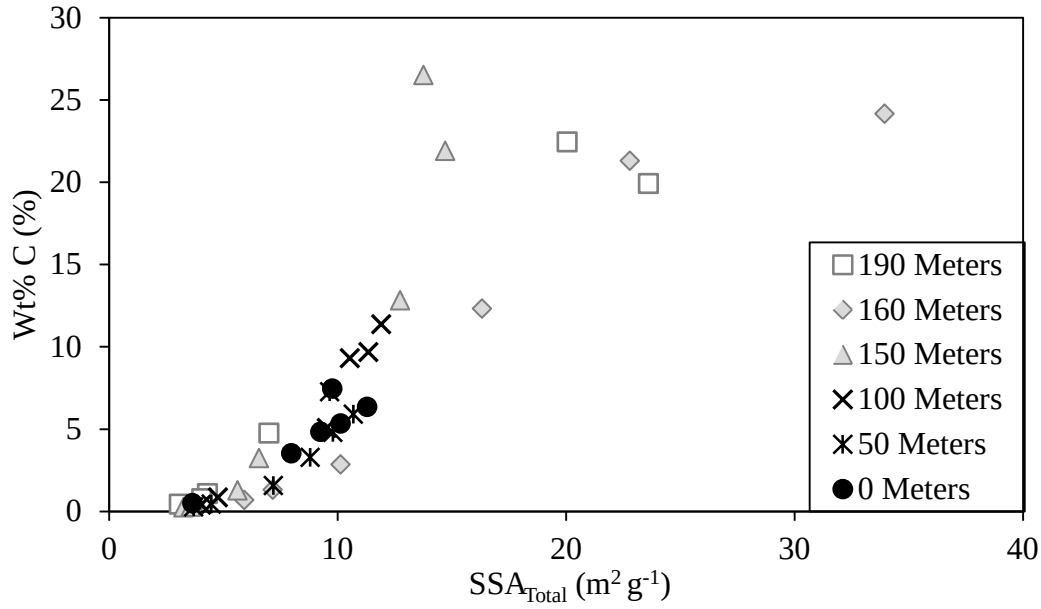

Fig. 1-16. Relationships between (a) $SSA_{occluded}$ (b) Weight % C and (c) % $SSA_{occluded}$ with respect to SSA_{total} along the earthworm invasion gradient.

(c)

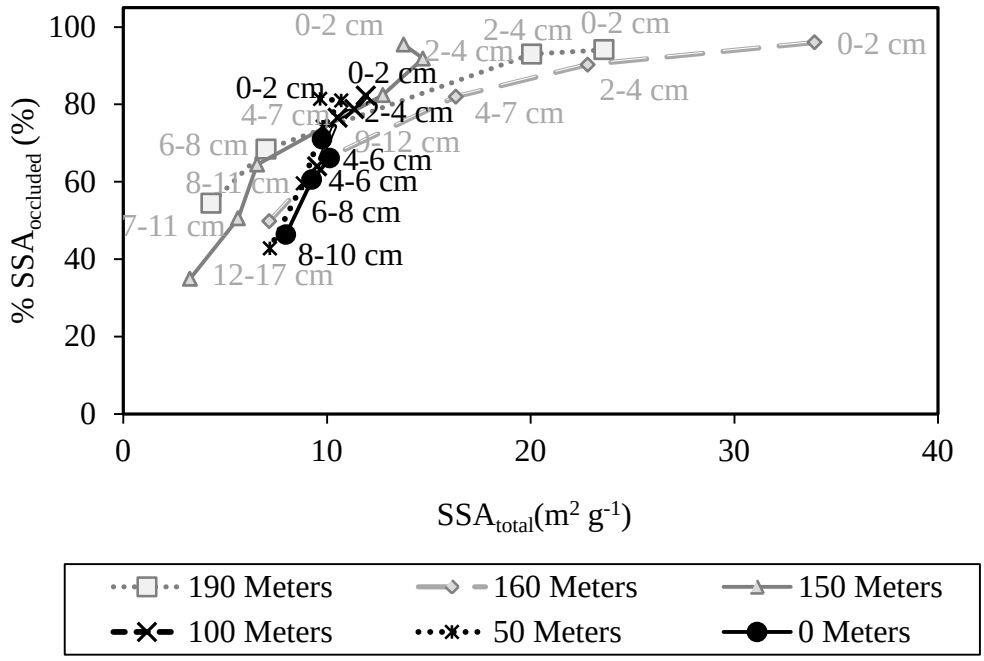

Fig. 1-16. Continued: Relationships between (a) $SSA_{occluded}$ (b) Weight % C and (c) % $SSA_{occluded}$ with respect to SSA_{total} along the earthworm invasion gradient.

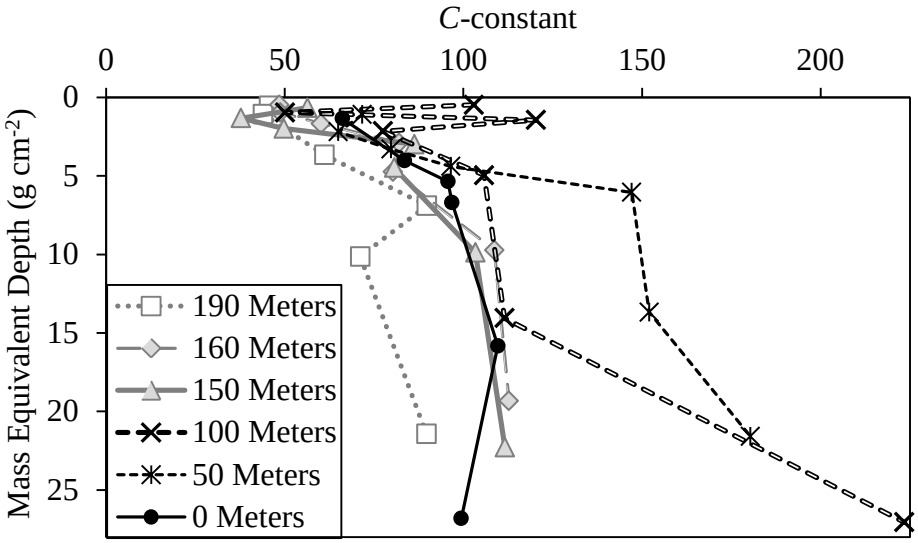

Fig. 1-17. Mass equivalent depth profiles of calculated *C*-constants across the invasion chronosequence.

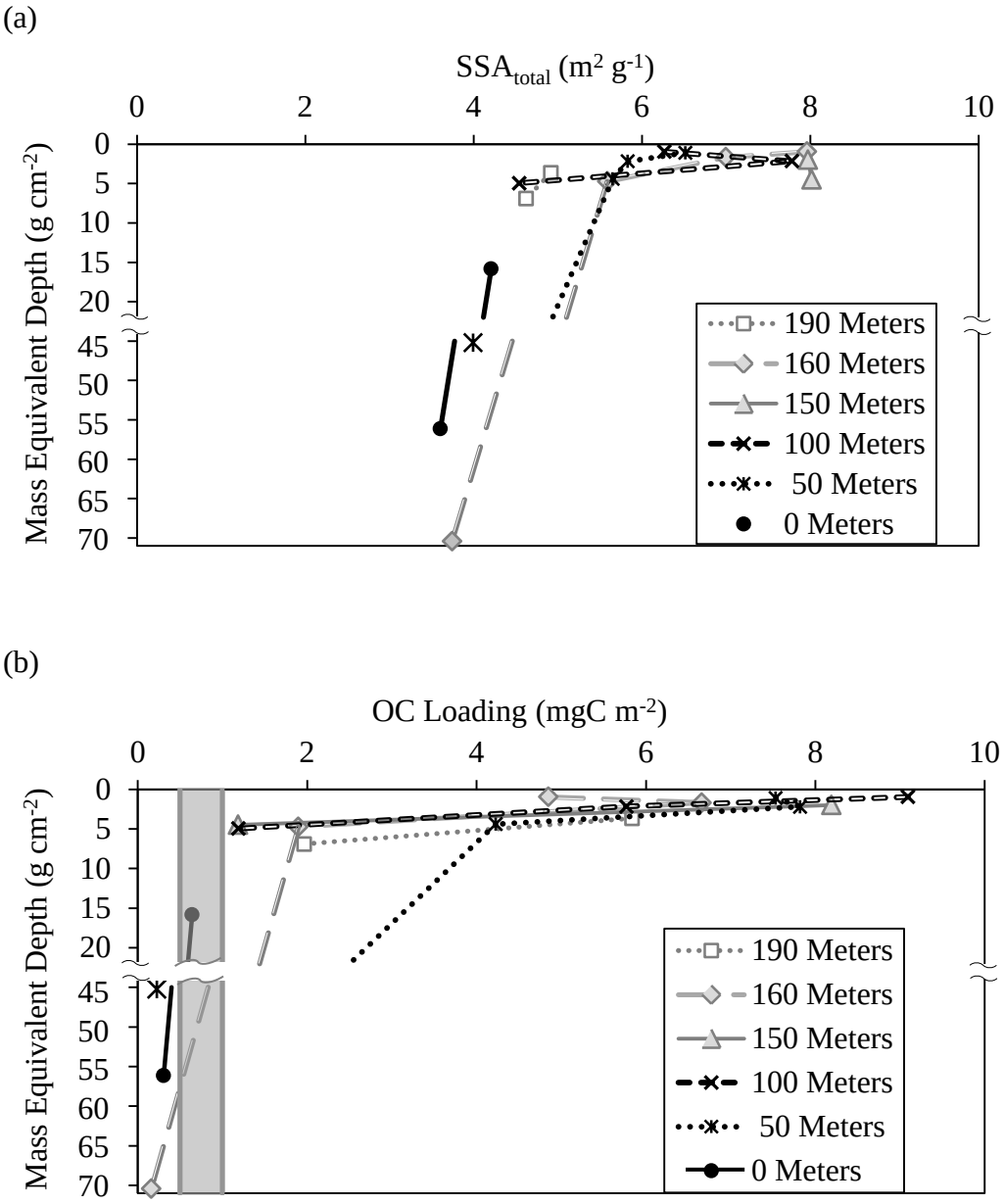

Fig. 1-18. Mineral surface area and its OM coverage in the heavy fractions. (a) Mass equivalent depth profiles of total mineral surface area, (b) Mass equivalent depth profiles of OC loading with a range indicating mono-layer equivalent, (c) Relationship between SSA_{total} and $\%SSA_{occluded}$, and (d) C contents of heavy fraction vs. measured SSA_{total} of the heavy fraction materials. Solid lines represent the monolayer equivalent.

(c)

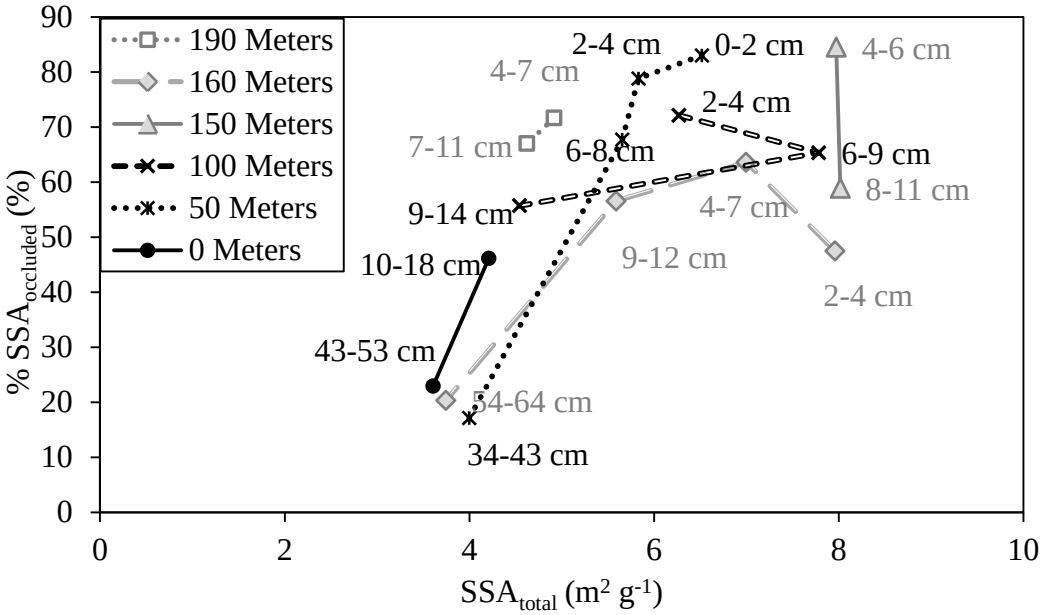

(d)

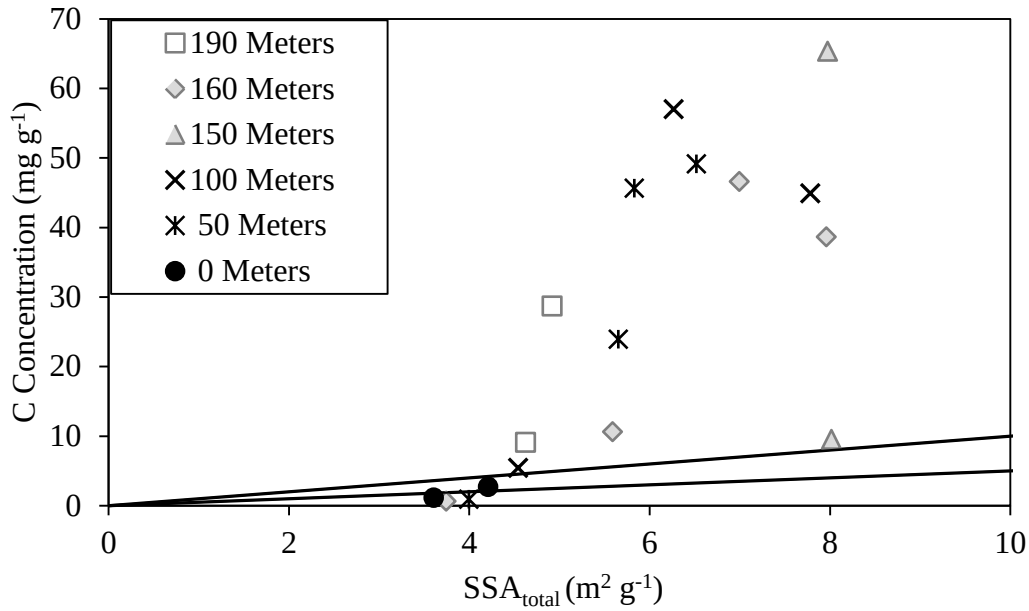

Fig. 1-18. Continued: Mineral surface area and its OM coverage in the heavy fractions. (a) Mass equivalent depth profiles of total mineral surface area, (b) Mass equivalent depth profiles of OC loading with a range indicating mono-layer equivalent, (c) Relationship between SSA_{total} and $\%SSA_{occluded}$, and (d) C contents of heavy fraction vs. measured SSA_{total} of the heavy fraction materials. Solid lines represent the monolayer equivalent.

Chapter 2.

Carbon-mineral interactions along an earthworm invasion gradient at a sugar maple forest in Northern Minnesota

This chapter was published in *Applied Geochemistry* in 2011.

Full citation information is:

Lyttle A, Yoo K, Hale CM, Aufdenkampe A, Sebestyen. 2011. Carbon–mineral interactions along an earthworm invasion gradient at a Sugar Maple Forest in Northern Minnesota. Applied Geochemistry 26: S85-S88.

Chapter Summary

The interactions of organic matter and minerals contribute to the capacity of soils to store carbon. Such interactions may be controlled by the processes that determine the availability of organic matter and minerals, and their physical contacts. One of these processes is bioturbation, and earthworms are the best known organisms that physically mix soils. Earthworms are not native species to areas previously glaciated, and the introduction of earthworms to these regions has been associated with often dramatic changes in soil structure and geochemical cycles. We are studying carbon mineral interaction along an approximately 200 meter long earthworm invasion transect in a hardwood forest in northern Minnesota. This transect extends from the soils where earthworms are absent to soils that have been invaded by earthworms for nearly 30-40 years. Pre-invaded soils have approximately five cm thick litter layer, thin (~5cm) A horizon, silt rich E horizon, and clay-rich Bt horizons. The A and E horizons formed from aeolian deposits, while the clay-rich Bt horizons probably developed from underlying glacial till. With the advent of earthworm invasion, the litter layer disappears and the A horizons thicken at the expense of the O and E horizons. In addition, organic carbon contents in the A horizons significantly increase with the arrival of earthworms. Simultaneously, measured mineral specific surface areas suggest that minerals' capacities to complex the organic matter appear to be greater in soils with active earthworm populations. Based on the data from two end member soils along the transect, mineral specific surface area in the A and E horizons are larger in the earthworm invaded soil than in the pre-invasion soil. Additionally, within < 5 years of earthworm invasions, A

horizon materials are turned from single grain to strong medium granular structure. While A horizon organic matter content and organic C-mineral complexation increase after earthworm invasion, they are also more vigorously mixed. This growing data set, when ultimately combined with ongoing measurements of (1) the population dynamics of earthworms along the invasion transect, (2) carbon-mineral association (via surface adsorption and physical collusion in mineral aggregates) and (3) dissolved organic carbon, will show how and how much soils capacity to store carbon are affected by burrowing organisms, who are often the keystone species of given ecosystems.

1. Introduction

Earthworms are not native to glaciated regions of North American; however, human activities, such as dumping of unused fishing bait and movement of soils containing earthworms or earthworm cocoons, have introduced exotic earthworm species to areas previously free of earthworms. Most notably, redistribution of leaf litter deep into the soils, which involves the reduction of O horizons while increasing A horizon thicknesses, has been associated with the invasion of exotic earthworms. Earthworms, based on their mixing behavior, are classified into several functional groups. Epigeic earthworm species live and feed in the litter layer and are typically found in surface litter. Endogeic and anecic earthworm species both feed at the surface, ingesting the litter layer and organically rich soils, but dwell within the mineral soil. Endogeic species live and burrow in the topsoil and anecic species live and burrow in deep soils (up to 2 meters depth), creating permanent burrows. It is the burrowing of endogeic and anecic species that mix organic and mineral soil, thus relocating organic carbon.

In the absence of vertical mixing, leaf litter remains on the soil surface. Bioturbators, such as earthworms, may however translocate organic matter into deeper soil zones where the organic matter can interact with minerals. Likewise, physical vertical mixing may translocate clay minerals from the B horizons and allow contact with organic matter. When complexed onto minerals, organic carbon is better stabilized (Oades, 1988). Therefore, we hypothesize that the advent of earthworm vertical soil mixing may lead to greater carbon mineral complexation and thus slower mineralization of organic matter.

Hardwood forests in the Great Lakes Region, when perturbed by exotic earthworms, have been shown to experience changes in soil structure and the storage and availability of nutrients. However, changes in carbon storage following earthworm invasions are not well understood. Earthworms' ability to remove litter may result in a decline of total soil carbon. On the other hand, the expansion of the A horizon and formation of A/E horizon may compensate for the loss of carbon in the O horizon (Hale et al., 2005; Bohlen et al., 2004). Therefore, examining the effect of earthworms on the amount of carbon in litter layers and A horizons, the rate and depth of soil mixing, and the rate of C mineralization, will elucidate the overall rate of carbon loss/gain due to earthworm invasion in hardwood forests.

Taking advantage of a well-studied earthworm invasion chronosequence that stretches approximately 200 meters (where the distance is measured from a heavily invaded location near a paved road) (Hale, 2004), we are exploring the relationship between earthworms, carbon storage in leaf litter and mineral soils, mineral specific surface area, and soil mixing rates.

2. Results

2.1. Earthworm Biomass along the Transect

The earthworm invasion forefront advanced significantly from the year 2009 to year 2010. In 2010, epigeic earthworms were found at 160 and 180 meters, where no earthworms had been found in 2009. In 2009 anecic species' forefront was found at the distance of 60 meters while endogeic species' forefront was at 100 meters. Both

forefronts have migrated to 120 and 150 meters, respectively. Earthworm biomass varies significantly but abruptly decreases at 130 meters (Fig. 2-1).

2.2. Earthworm Species Compositions along the Transect in the Years 2009 and 2010

In 2009, the largest fraction of the total biomass was explained by anecic species (40 %), followed closely by epi-anecic (23 %) and epigeic (19 %). Epi-endogeic species were responsible for only 6% of the total biomass. Such species composition largely persisted in the 2010 survey, with the exception of epi-anecic and endogeic which showed increase in their biomass (Fig. 2-2).

2.3. Litter Layer Biomass

Litter biomass, although slightly varying in the first 130 meters, abruptly increases at 130 and 160 meters (Fig. 2-1). Earthworm survey showed that the endogeic species invasion front was at 100 and 150 meters in 2009 and 2010, respectively, suggesting that this group plays the most important role in reducing the litter layer.

2.4. Soil Organic Carbon Contents and Storage

Where high litter biomass is present, soil organic carbon content rapidly decreases with increasing depth (Fig. 2-3). In earthworm invaded soils, organic carbon contents decrease less dramatically with increasing depth than in the pre-invaded soils. Earthworm-invaded areas with higher organic content throughout the A horizon are associated with little or no litter biomass (Fig. 2-1 and 2-3). Lastly, carbon storage in the A horizon increases with the introduction of earthworms (Fig. 2-4).

2.5. Mineral Specific Surface Areas

Mineral specific surface areas in the A horizons are greater in the earthworm invaded soil (0 meter distance) than in the non-invaded soils (at 190 meters) (Fig. 2-5), which is also true in the upper E horizon.

3. Discussion

Soils that have been heavily invaded by anecic and endogeic species have significantly lower litter biomass, but higher organic matter contents to depths of 12 cm where the A horizon thickens, and mixed zone of A and E horizons (A/E) appear. These data support the findings from other studies that earthworm invasions into pristine soils result in the incorporation of surface organic matter into the A horizon (Alban and Berry, 1994; Bohlen et al., 2004).

Earthworm activities increase mineral specific surface area in the organic matter rich A horizons. First, as earthworms travel between the A and Bt horizons, they may bring up clay minerals from the Bt horizon. Our preliminary analysis of ^{210}Pb activities in the soil, however, suggests that earthworm burrowing activities in the Bt horizon may be minimal. Secondly, when minerals pass through earthworm intestines, they may be ground up and thus new mineral surface area is produced (Suzuki et al., 2003). Third, we found that earthworm-worked soil materials have a greater amount of crystalline pedogenic iron oxides (dithionite citrate extracted), which is known to have higher specific surface area.

Regardless of the mechanisms involved in mineral surface generation, the increase of mineral specific surface area in invaded soils may have increased organic matter complexation onto mineral surfaces. Our next step is to understand (1) how earthworms affect mineral specific surface area and (2) how much of the increased organic matter in the earthworm affected A horizon are complexed with mineral surfaces.

4. Conclusion

While our data set continues to grow, early findings suggest that earthworms have great impacts on soil carbon storage in ecosystems that have developed free of native earthworms. The earthworm invasion in northern hardwood forests has led to changes in the location of organic carbon and mineral specific surface area within the soils, which may influence soils' capacity to store carbon. Further investigation of organic carbon contents and surface area measurement from nine different soil pits along the invasion chronosequence will allow us to determine the overall effects of earthworms on carbon-mineral complexation. We will also investigate changes in the manner and intensity of mineral contact with organic matter along the invasion chronosequence, which will elucidate the long term ability of soils to store carbon.

5. References

Alban, D.H., Berry, E.C., 1994. Effects of earthworm invasion on morphology, carbon and nitrogen of a forest soil. Appl Soil Ecol 1:243-9.

Bohlen, P.J., Scheu S., Hale, C.M., McLean, M.A., Migge, S., Groffman, P.M., Parkinson, D., 2004. Non-native invasive earthworms as agents of change in northern temperate forests. Front Ecol Environ 2(8): 427-435.

Hale, C.M., 2004. Ecological consequences of exotic invaders: interactions involving European earthworms and native plant communities in hardwood forests. PhD dissertation. University of Minnesota, Dept of Forest Resources, St. Paul, MN.

Hale, C.M., Frelich, L.E., Reich, P.B., Pastor, J., 2005. Effect of European earthworm invasion on soil characteristics in northern hardwood forests of Minnesota, USA. Ecosystems 8:911-927.

Oades, J.M., 1988. The retention of organic matter in soils. Biogeochemistry 5:35-70.

Suzuki, Y., Matsubara, T., Hoshino, M., 2003. Breakdown of mineral grains by earthworms and beetle larvae. Geoderma 112 (1-2): 131-142.

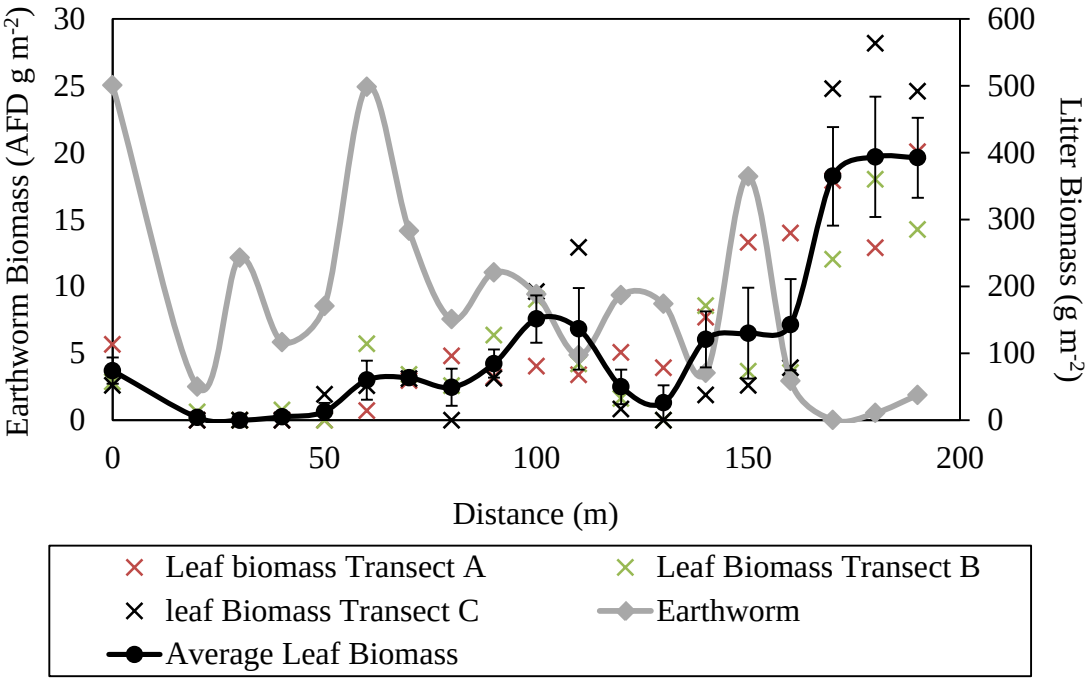

Fig. 2-1. Ash free dry (AFD) biomass of earthworms and leaf litter biomass along an earthworm invasion transect. At 0 meters soil is heavily invaded by earthworms and at 200 meters earthworm populations are minimal. Litter samples were taken from three different invasion transects, while earthworms from transect B were identified. Significant increase of litter biomass at 160 meters is associated with a decrease in earthworm biomass.

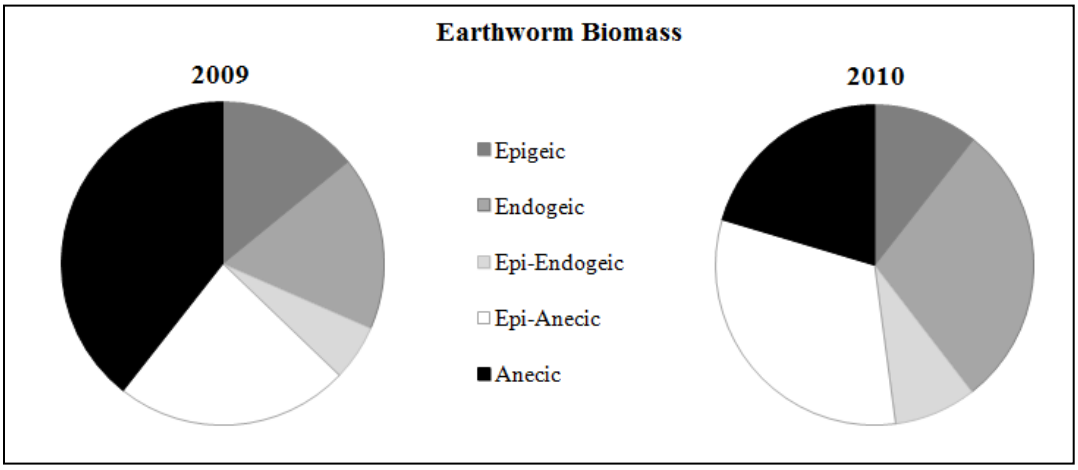

Fig. 2-2. Earthworm biomass by functional groups in the years 2009 and 2010.

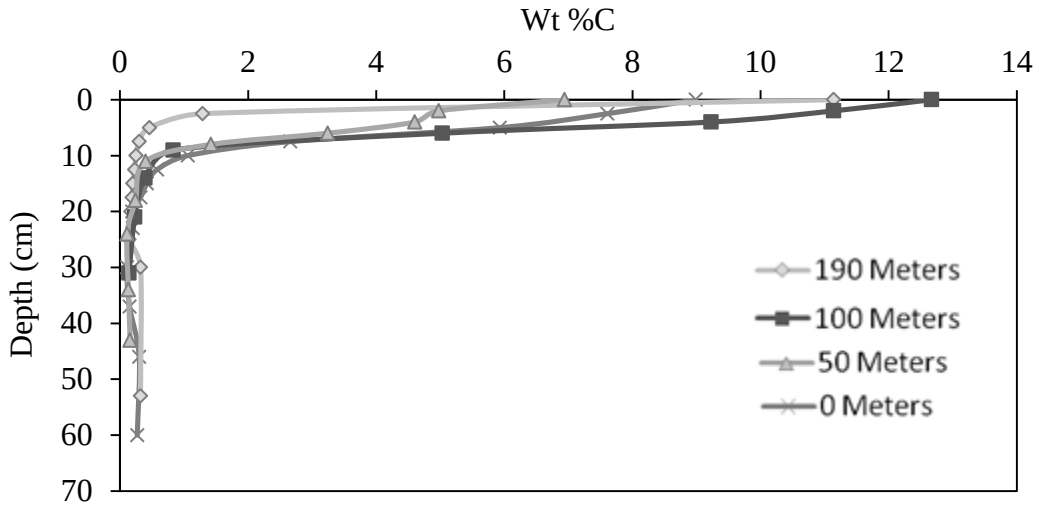

Fig. 2-3. Weight % Carbon versus depth at four different pits along an earthworm invasion transect. At 0 meters, the soil is heavily invaded by earthworms, while the earthworm population is minimal at 190 meters. Soils with low earthworm biomass and high litter biomass are associated with a rapid decrease in % carbon with soil depth.

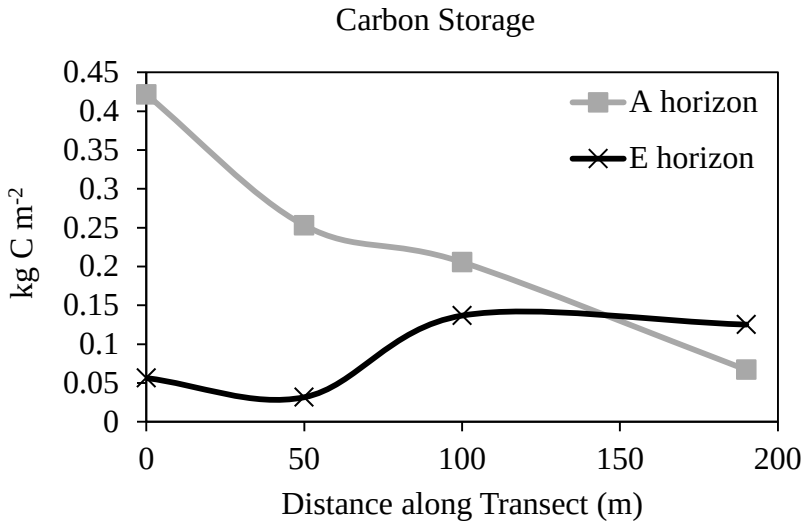

Fig. 2-4. Carbon Storage along an earthworm invasion transect. The longer the soil has been invaded by earthworms, the greater the carbon storage in the A horizon, which is partly compensated by the reduction of C storage in the E horizons.

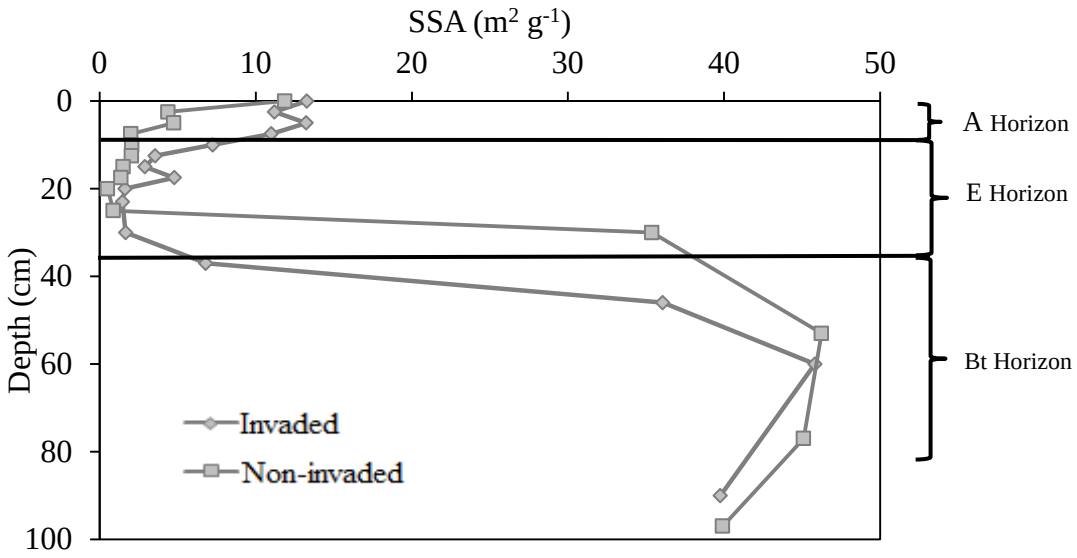

Fig. 2-5. Soil specific surface area versus depth along an earthworm invasion transect.

BIBLIOGRAPHY

Adams MB, Loughry LH, Plaugher LP. 2004. Experimental Forests and Ranges of the USDA Forest Service. U.S. Department of Agriculture. Newtown Square PA, USA.

Ahsan T. 1992. The surface properties of pure and modified precipitated calcium carbonate by adsorption of nitrogen and water vapor. Colloids and Surfaces 64:167-176.

Alban DH, Berry EC. 1994. Effects of earthworm invasion on morphology, carbon and nitrogen of a forest soil. Applied Soil Ecology 1:243-249.

Arnarson TS, Keil RG. 2001. Organic – mineral interactions in marine sediments studied using density fractionation and X-ray photoelectron spectroscopy. Organic Geochemistry 32:1401-1415.

Aufdenkampe AK, Hedges JI, Richey JE. 2001. Sorptive fractionation of dissolved organic nitrogen and amino acids onto fine sediments within the Amazon Basin. Limnology and Oceanography 46(8):1921-1935.

Aufdenkampe AK, Mayorga E, Hedges JI, Llerena C, Quay PD, Gudeman J, Krusche AV, Richey JE. 2007. Organic matter in the Peruvian headwaters of the Amazon: compositional evolution from the Andes to the lowland Amazon mainstem. Organic Geochemistry 38:337-364.

Baldock JA, Skjemstad JO. 2000. Role of the soil matrix and minerals in protecting natural organic materials against biological attack. Organic Geochemsitry 31(7): 697-710.

Balesdent J, Besnard E, Arrouays D, Chenu C. 1998. The dynamics of carbon in particle-size fractions of soil in a forest-cultivation sequence. Plant and Soil 201:49-57.

Bernoux M, Cerri CC, Neill C, de Moraes JFL. 1998. The use of stable carbon isotopes for estimating soil organic matter turnover rates. Geoderma 82:43-58.

Blair JM, Crossley DA, Jr. 1988. Litter decomposition, nitrogen dynamics and litter microarthropods in a southern Appalachian hardwood forest 8 years following clearcutting. Journal of Applied Ecology. 25: 683-698.

Bohlen PJ, Pelletier D, Groffman PM, Fahey TJ, Fist MC. 2004a. Ecosystem consequences of exotic earthworm invasion of north temperate forests. Ecosystems 7:1-12.

Bohlen PJ, Pelletier DM, Groffman PM, Fahey, TJ, Fisk MC. 2004b. Influence of earthworm invasion on redistribution and retention of soil carbon and nitrogen in northern temperate forests. Ecosystems 7:13-27.

Bohlen PJ, Scheu S, Hale CM, McLean MA, Migge S, Groffman PM, Parkinson D. 2004c. Non-native invasive earthworms as agents of change in northern temperate forests. Frontiers in Ecology and the Environment 2(8):427-435.

Borggaard OK. 1982. The influence of iron oxides on the surface area of soil. Journal of Soil Science 33: 443-449.

Boström B, Comstedt D, Ekblad A. 2007. Isotope fractionation and 13C enrichment in soil profiles during the decomposition of soil organic matter. Ecosystem Ecology 153:89-98.

Burtelow AE, Bohlen PJ, Groffman PM. 1998. Influence of exotic earthworm invasion on soil organic matter, microbial biomass and denitrification potential in forest soils of the northeastern United States. Applied Soil Ecology 9:197-202.

Chenu S, Stotzky G. 2002. Intereactions between microorganisms and soil particles. An overview. Huang PM, Bollag JM, Senesi N, editors. Interactions between soil particles and microorganisms Weinheim Wiley-VCH p. 3–39.

Chiou CT. 1990. The surface area of soil organic matter. Environmental Science Technology 24:1164-1166

Coderre D, Mauffette Y, Gagnon D, Tousignant S, Besette G. 1995. Earthworm populations in healthy and declining sugar maple forests. Pedobiologia 39:86-96.

Cornell, RM, Schwertmann U. 2003. The iron oxides: structure, properties, reactions, occurrences and uses. Weinheim (DE): Wiley-VCH. p. 664.

Crow SE, Filley TR, McCormick M, Szlavecz K, Stott DE, Gamblin D, Conyers G. 2009. Earthworms, stand age, and species composition interact to influence particulate organic matter chemistry during forest succession. Biogeochemistry 92:61-82.

de Jonge H, Mittelmeijer-Hazeleger MC. 1996. Adsorption of CO2 and N2 on soil organic matter: nature of porosity, surface area, and diffusion mechanism. Environmental Science Technology 30:408-413.

Degryze S, Six J, Paustin K, Morris SJ, Paul EA, Merckx R. 2004. Soil organic carbon pool changes following land-use conversions. Global Change Biology 10: 1120-1132.

Drake HL, Schramm, Horn MA. 2006. Earthworm gut microbial biomes: their importance to soil microorganisms, denitrification, and the terrestrial production of the greenhouse gas N2O. Soil Biology 6:65-87.

Eberl, DD. 2003. User's guide to Rockjock – a program for determining quantitative mineralogy from powder X-ray diffraction data. U.S. Geological Survey Open-File Report: 03-78. p. 46.

Eusterhues K, Rumpel C, Kleber M, Kögel-Knabner I. 2003. Stabilisation of soil organic matter by interactions with minerals as revealed by mineral dissolution and oxidative degradation. Organic Geochemistry 34:1591-1600.

Eusterhues K, Rumpel C, Kögel-Knabner I. 2005. Organo-mineral associations in sandy acid forest soils: importance of specific surface area, iron oxides and micropores. European Journal of Soil Science 56:753-763.

Filley TR, McCormick MK, Crow ME, Szlavecz K, Whigham DF, Johnston CT, van den Huevel RN. 2008. Comparison of the chemical alteration trajectory of *Liriodendron tulipifera L*. leaf litter among forests with different earthworm abundance. Journal of Geophysical Research: Biogeosciences (2005-2012) 113:G1.

Frelich LE, Hale CM, Scheu S, Holdsworth AR, Henegham L, Bohlen PJ, Reich PB. 2006. Earthworm invasion into previously earthworm-free temperate and boreal forests. Biological Invasions 8:1235-1245.

Gates GE. 1982. Farewell to North American megadriles. Megadrilogica 4:12-77.

Gundale MJ. 2002. The influence of exotic earthworms on soil organic horizon and the rare fern Botrychium mormo. Conservation Biology 16:1555-73.

Hale CM. 2004. Ecological consequences of exotic invaders: interactions involving European earthworms on native plan communities in hardwood forests. Ph.D. Dissertation, University of Minnesota, Department of Forest Resources, St. Paul, Minnesota.

Hale CM, Frelich LE, Reich PB. 2004. Allometric equations for estimation of ash-free dry mass from length measurements for selected European earthworm species (Lumbricidae) in the western Great Lakes region. American Midland Naturalist Journal 151(1): 179-185.

Hale CM, Frelich LE, Reich PB, Pastor J. 2005a. Effects of European earthworm invasion on soil characteristics in northern hardwood forests of Minnesota, USA. Ecosystems 8:911-927.

Hale CM, Frelich LE, Reich, PB. 2005b. Exotic European earthworm invasion dynamics in northern hardwood forests of Minnesota, USA. Ecological Applications 15: 848-860.

Hale CM, Frelich LE, Reich PB. 2006. Changes in cold-temperate hardwood forest understory plant communities in response to invasion by European earthworms. Ecology 87:1637-1649.

Hale CM. 2007. Earthworms of the Great Lakes. Duluth (MN): Kollath and Stensaas Publishing. p.36.

Hale CM. 2008a. Evidence for human-mediated dispersal of exotic earthworms: support for exploring strategies to limit further spread. Molecular Ecology 17:1165-1169.

Hale CM, Frelich LE, Reich PB, Pastor P. 2008b. Exotic earthworm effects on hardwood forest floor, nutrient availability and native plants: a mesocosm study. Oecologia 155:509-518.

Hassink J. 1997. The capacity of soils to preserve organic C and N by their association with clay and silt particles. Plant and Soil 191:77-87.

Hendrix PF, Bohlen PJ. 2002. Exotic earthworm invasions in North American: ecological and policy implications. BioScience 52(9): 801-811.

Hendrix PF, Callaham MA,Jr, Drake JA, Huang CY, James SW, Snyder BA, Zhang W. 2008. Pandora's box contained bait: the global problem of introduced earthworms. Annual Review of Ecology, Evolution, and Systematics 39:593-613.

Holdsworth AR, Frelich LE, Reich PB. 2008. Litter decomposition in earthworm-invaded northern hardwood forests: role of invasion degree and litter chemistry. Ecoscience 15(4):536-544.

Holmgren GGS. 1967. A rapid citrate-dithionate extractable iron procedure. Soil Science Society of America Proceedings 31: 210–211

Horn MA, Schramm A, Drake HL. 2003. The earthworm gut: an ideal habitat for ingested N_2O – producing microorganisms. Applied and Environmental Microbiology 69(3):1662-1669.

Jackson ML, Lim CH, Zelazny LW. 1986. Oxides, hydroxides, and aluminosilicates. Klute A, editor. Methods of soil analysis, Part I. Physical and mineralogical methods. Madison: Soil Science Society of America. p.101-150.

Kaiser K, Guggenberger G. 2000. The role of DOM sorption to mineral surfaces in the preservation of organic matter in soils. Organic Geochemistry 31:711-725.

Kaiser K, Guggenberger G. 2003. Mineral surfaces and soil organic matter. European Journal of Soil Science 54:219-236.

Kaiser K, Guggenberger G. 2007. Sorptive stabilization of organic matter by microporous goethite: sorption into small pores vs. surface complexation. European Journal of Soil Science 58:45-59.

Keil RG, Hedges JI. 1993. Sorption of organic matter to mineral surfaces and the preservation of organic matter in coastal marine sediments. Chemical Geology 107:385-388.

Keil RG, Montlucon DB, Prahl FG, Hedges JI. 1994. Sorptive preservation of labile organic matter in marine sediments. Nature 370:549-552.

Keil RG, Mayer LM, Quay PD, Richey JE, Hedges JI. 1997. Loss of organic matter from riverine particles in deltas. Geochimica et Cosmochimica Acta 61:1507-1511.

Kleber M, Sollins P, Sutton R. 2007. A conceptual model of organo-mineral interactions in soils: self-assembly of organic molecular fragments into zonal structures on mineral surfaces. Biogeochemsitry 85: 9-24.

Langmaid KK. 1964. Some effects of earthworm invasion in virgin podzols. Canadian Journal of Soil Science 44:34-7

Lawrence AP, Bowers MA. 2002. A test of the 'hot' mustard extraction method of sampling earthworms. Soil Biology and Biochemistry 34:549-52

Lehmann MF, Bernasconi SM, Barbieri A, McKenzie JA. 2002. Preservation of organic matter and alteration of its carbon and nitrogen isotope composition during simulated and in situ early sedimentary diagenesis. Geochemica et Cosmochimica

Acta 66(20):3573-3584.

Ludwig B, John B, Ellerbrock R, Kaiser M, Flessa H. 2003. Stabilization of carbon from maize in a sandy soil in a long-term experiment. European Journal of Soil Science 54: 117-126.

Luyssaert S, Schulze ED, Börner A, Knohl A, Hessenmöller D, Law BE, Ciais P, Grace J. 2008. Old-growth forests as global carbon sinks. Nature 455:213-215.

Masiello CA, Chadwich OA, Southon J, Torn MS, Harden JW. 2004. Weathering controls on mechanisms of carbon storage in grassland soils. Global Biogeochemical Cycles 18(4): GB4023

Mayer LM. 1994. Relationship between mineral surfaces and organic carbon concentrations in soils and sediments. Chemical Geology 114:347-363.

Mayer LM. 1999. Extent of coverage of internal surfaces by organic matter in marine sediments. Geochimica et Cosmochimica Acta 63(2): 207-215.

Mayer LM, Xing B. 2001. Organic matter-surface area relationships in acid soils. Soil Science Society of America Journal 65: 250-258.

McKeague JA, Day JH. 1966. Dithionite and oxalate-extractable Fe and Al as aids in differentiating various classes of soils. Canadian Journal of Soil Science 46:13-22.

McKeague JA, Brydon JE, Miles NM. 1971. Differentiation of forms of extractable iron and aluminum in soils. Soil Science Society of America Proceedings 35:33-38.

McLean MA, Migg-Kleian S, Parkinson D. 2006. Earthworm invasion of ecosystems devoid of earthworms: effects on soil microbes. Biological Invasions 8:1257-1273.

Melillo JM, Aber JD, Linkins AE, Ricca A, Fry B, Nadelhoffer KJ. 1989. Carbon and nitrogen dynamics along the decay continuum: plant litter to soil organic matter. Plant and Soil 115:189-198.

Mikutta R, Kleber M, Kaiser K, Jahn R. 2005. Review: organic matter removal from soils using hydrogen peroxide, sodium hypochlorite, and disodium peroxodisulfate. Soil Science Society of America Journal 69:120-135.

Minnesota State Climatology Office. 2003. Minnesota climatology working group website http://climate.umn.edu, Minnesota Department of Natural Resources and the University of Minnesota, Department of Soil, Water and Climate, St. Paul , MN 55108.

Oades JM. 1988. The retention of organic matter in soils. Biogeochemistry 5:35-70.

Oyedele DJ, Schjønning P, Amunsan AA. 2006. Physiochemical properties of earthworm casts and uningested parent soil from selected sites in southwestern Nigeria. Ecological Engineering 28:106-113.

Pennell KD, Boyd SA, Abriola LM. 1995. Surface area of soil organic matter reexamined. Soil Science Society of America Journal 59:1012-1018.

Pronk GJ, Heister K, Kögel-Knabner I. 2011. Iron oxides as major available interface component in loamy arable topsoils. Soil Science Society of America Journal 75:2158-2168.

Ransom B, Kim D, Kastner M, Wainwright S. 1998. Organic matter preservation on continental slopes: importance of mineralogy and surface area. Geochimica et Cosmochimica Acta 62:1329-1345.

Reynolds JW. 1977. The earthworms (Lumbricidae and Sparganophilidae) of Ontario. Royal Ontario Museum Miscellaneous Publication, Toronto, Ontario.

Resner KE, Yoo K, Hale C, Aufdenkampe A, Blum A, Sebestyen S. 2011. Elemental and mineralogical changes in soil due to bioturbation along an earthworm invasion chronosequence in northern Minnesota. Applied Geochemistry 26: S127-S131.

SAS Institute Inc. 2010. JMP, version 9.0.2. SAS Institute Inc. 100 SAS Campus Drive, Cary NC 27513-2414 USA.

Savage NM. 1988. The use of sodium polytungstate for conodont separations. Journal of Micropalaeontology 7(1):39-40.

Scheu S, Parkinson D. 1994a. Effects of earthworms on nutrient dynamics, carbon turnover and microorganisms in soil from cool temperate forests of the Canadian Rocky Mountains – laboratory studies. Applied Soil Ecology 1:113-25.

Scheu S, Parkinson D. 1994b. Effects of invasion of an aspen forest (Canada) by Dendrobaena octaedra (Lumbricidae) on plant growth. Ecology 75:2348-2361.

Schmidt MWI, Torn MS, Abiven S, Dittmar T, Guggenberger G, Janssesn IA, Kleber M, Kögel-Knabner I, Lehmann J, Manning DAC, Nannipieri P, Rasse DP, Weiner S, Trumbore SE. 2011. Persistence of soil organic matter as an ecosystem property. Nature 478: 49-56.

Schwert, DP. 1990. Oligochaeta: Lumbricidae. Dindal DL, editor. Soil biology guide. New York: John Wiley and Sons. p.341-356.

Sequi P, Aringhieri R. 1977. Destruction of organic matter by hydrogen peroxide in the presence of pyrophosphate and its effect on soil specific surface area. Soil Science Society of America Journal 41(2): 340-342

Six J, Conant RT, Paul EA, Paustian K. 2002a. Stabilization mechanisms of soil organic matter: implications for C-saturation of soils. Plant and Soil 241:155-176.

Six J, Feller C, Denef K, Ogle S, deMoraes Sa JC, Albrecht. 2002b. Soil organic matter, biota and aggregation in temperate and tropical soils – Effects of no-tillage. Agronomie – Sciences des Productions Vegetales et de l'Environment 22:755-775.

Soil-Survey. 1997. Soil survey of Cass County, Minnesota, United States Department of Agriculture, p.300.

Sollins P, Homann P, Caldwell BA. 1996. Stabilization and destabilization of soil organic matter: mechanisms and controls. Geoderma 74(1):65-105.

Sollins P, Swantston C, Kleber M, Filley T, Kramer M, Crow S, Caldwell B, Lajtha K, Bowden R. 2006. Organic C and N stabilization in a forest soil: evidence from sequential density fractionation. Soil Biology and Biochemistry 38: 3313-3324.

Sollins P, Swanston C, Kramer M. 2007. Stabilization and destabilization of soil organic matter – a new focus. Biogeochemistry 85:1-7.

Sollins P, Kramer M, Swantson C, Lajtha K, Filley T, Aufdenkampe A, Wagai R, Bowden R. 2009. Sequential density fractionation across soils of contrasting mineralogy: evidence for both microbial- and mineral-controlled soil organic matter stabilization. Biogeochemistry 96:209-231

Sørensen LH. 1975. The influence of clay on the rate of decay of amino acid metabolites synthesized in soils during decomposition of cellulose. Soil Biology and Biochemistry 7:171-177.

Rumpel C, Kögel-Knabner I. 2011. Deep soil organic matter – a key but poorly understood component of terrestrial C cycle. Plant Soil 338:143-158.

Torn MS, Trumbore SE, Chadwich OA, Vitousek PM, Hendricks MD. 1997. Mineral control of soil organic carbon storage and turnover. Nature 389:170-173.

Torresan M. 1987. The use of sodium polytungstate in heavy mineral separations. U.S. Geological Survey Open-File Report. p.87-590.

Townsend AR, Vitousek PM, Desmarais DJ, Tharpe A. 1997. Soil carbon pool structure and temperature sensitivity inferred using CO2 and 13CO2 incubation fluxes from five Hawaiian soils. Biogeochemistry 38:1-17.

Trumbore S. 2009. Radiocarbon and soil carbon dynamics. Annual Review of Earth and Planetary Sciences 37:47-66.

von Lutzow M, Kögel-Knabner I, Ekschmitt K, Matzner E, Guggenberger G, Marschner B, Flessa H. 2006. Stabilization of organic matter in temperate soils: mechanisms and their relevance under different soil conditions – a review. European Journal of Soil Science 57:426-445.

von Lutzow M, Kögel-Knabner I, Ekschmitt K, Flessa H, Guggenberger G, Matzner E, Marschner B. 2007. SOM fractionation methods: relevance to functional pools and to stabilization mechanisms. Soil Biology and Biochemistry 39:2187-2207.

von Lutzow M, Kögel-Knabner I, Ludwig B, Matzner E, Flessa H, Ekschmitt K, Guggenberger G, Marschner B, Kalbitz K. 2008. Stabilization mechanisms of organic matter in four temperate soils: development and application of a conceptual model. Journal of Plant Nutrition and Soil Science 171: 111-124.

Wagai R, Mayer LM. 2007. Sportive stabilization of organic matter in soils by hydrous iron oxides. Geochimica et Cosmochimica Acta 71:25-35.

Wagai R. Lawrence MM, Kitayama K, Knicker H. 2008. Climate and parent material controls on organic matter storage in surface soils: a three-pool, density-seperation approach. Geoderma 147:23-33.

Wagai R, Mayer LM, Kitayama K. 2009. Extent and nature of organic coverage of soil mineral surfaces assessed by a gas sorption approach. Geoderma 149:152-160.

Wagner TL, Mattson WJ, Witter JA. 1977. A survey of soil invertebrates in two Aspen forests in northern Minnesota. St. Paul (MN): North Central Forest Experiment Station, Forest Service, General Technical Report NC-40:1-23.

Webb PA, Orr C. 1997. Analytical methods in fine particle technology. Micromeritics Instrument Corp, Norcross. p.301.

Wedin DA, Tieszen LL, Dewey B, Pastor J. 1995. Carbon isotope dynamics during grass decomposition and soil organic matter formation. Ecology 76:1383-1392.

Weilder PG, Stanjek H. 1998. The effect of dry heating of synthetic 2-line and 6-line ferrihydrite: II. surface area, porosity and fractal dimension. Clay Mineralogy 33:277-384.

Wironen M, Moore TR. 2006. Exotic earthworm invasion increases soil carbon and nitrogen in an old-growth forest in southern Quebec. Canadian Journal of Forest Research 36: 845-854.

Yoo K, Ji J, Aufdenkampe A, Klaminder J. 2011. Rates of soil mixing and associated carbon fluxes in a forest versus tilled agricultural field: implications for modeling the soil carbon cycle. Journal of Geophysical Research: Biogeosciences (2005-2012) 166:G1

APPENDIX

Appendix A.

The expected SSA was calculated as follows:

$$SSA_{expected} = \frac{(SSA_{total190} \times M_{190}) + (SSA_{totalE} \times M_{E\rightarrow A})}{M_x}$$

Where $SSA_{total190}$ is the weighted average of the measured SSA_{total} over the A horizon at 190 m (190 m is considered least invaded by exotic earthworms); M_{190} is equal to the mineral mass at 190 meters (integrated product of bulk density and thickness); SSA_{totalE} is the weighted average of the measured SSA_{total} of the A horizon at 190 meters. $M_{E\rightarrow A}$ is the calculated mineral mass of the E horizon mixed into the A horizon at distance x, and M_x is the mineral mass at distance x along the earthworm invasion gradient. M_x was determined using a fitted trend line from the A horizon mineral mass data points in 2009 and 2011.

The $M_{E\rightarrow A}$ was calculated as follows:

$$M_{E\rightarrow A} = M_x - M_{190}$$

Where M_x is the mineral mass of the A horizon at distance x, and M_{190} is the mineral mass of the A horizon at 190 meters.

Appendix B.

The measured SSA_{total} was the weighted average of SSA_{total} from the mass equivalent depths of 0-1.9 g cm^{-2} (Fig. 1-14). The measured SSA_{total} was calculation by:

$$\text{Measured } SSA_{total} = \frac{\sum_{i=1}^{N}(SSA_{totali} \times BD_i \times \Delta z_i)}{\text{Mass Equivalent Depth}_i}$$

where SSA_{total} is the specific surface area after the sample had been muffled and OM was removed (m^2 g^{-1}), BD is the bulk density (g cm^{-3}), Δz is the thickness of the sampled layer (cm), i indicates the i-th layer sampled, and N is the total number of sampled layers above the depth of interest – in this case the mass equivalent depth of 1.9 g cm^{-2}.

Appendix C. – Earthworm and Litter Biomass

Method

Earthworms were collected from a 0.3 m^2 plot using a liquid mustard extraction. One gallon of water was mixed with 1/3 cup of powdered mustard. The mixture was poured over the bare soil inside the 0.3 m^2 plots; when a litter layer was present the litter was stripped away until the bare soil was visible and the mixture was poured over the bare soil. Earthworms were collected and placed in 70 % isopropyl. Earthworms were collected until ~5 minutes after the entire mixture was poured. Earthworms were identified to species and stored in 10 % formalin.

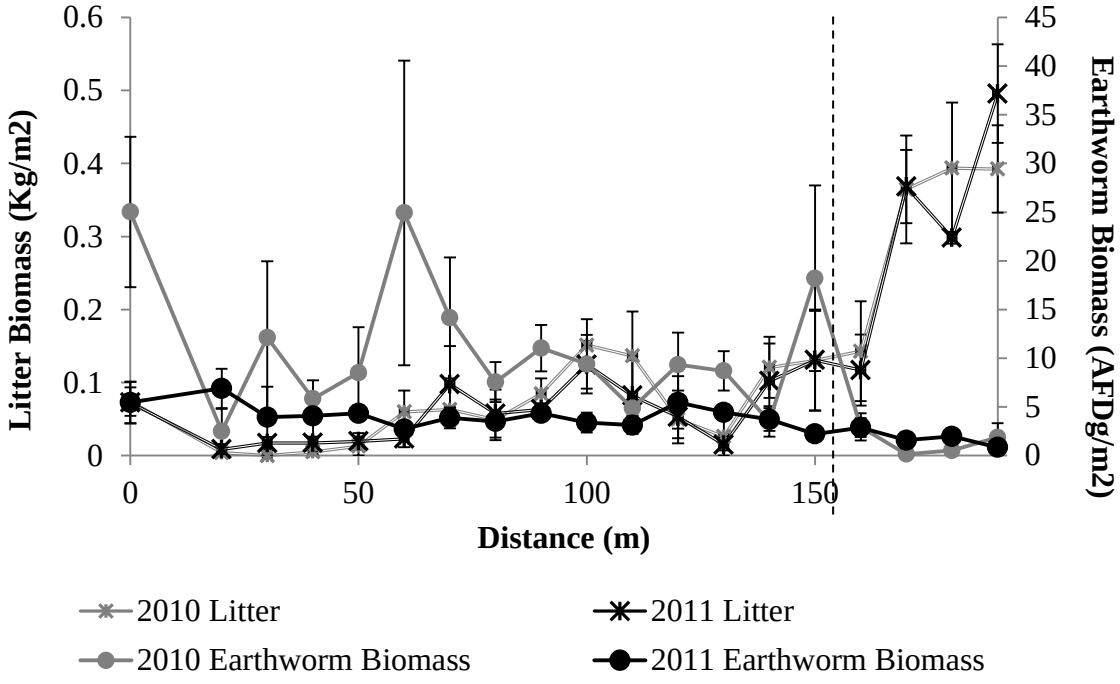

Fig. AC-1. Mean and standard errors of earthworm and leaf litter biomasses along the earthworm invasion chronosequence. The distance is measured from the soil pit nearest to the road. Dotted vertical line indicates transition from thick forest floor (150-190 m) to bare mineral soil (0-150 m).

Table AC-1. Biomasses of earthworm species (AFD g m^{-2}) collected from transect B in 2009.

Distance (m)	***Apporectodea***	***Dendrobaena***	***Octolasion***	***L.* juvenile**	***L. rubellus***	***L. terrestris***
190	0.000	0.473	0.000	0.146	0.000	0.000
180	0.000	0.000	0.000	0.000	0.000	0.000
170	0.000	0.286	0.000	0.150	0.000	0.000
160	0.000	0.000	0.000	0.000	0.000	0.000
150	0.000	0.624	0.000	0.572	0.244	0.000
140	0.000	0.081	0.000	1.288	0.000	0.000
130	0.072	0.303	0.000	1.372	0.000	0.000
120	0.028	0.662	0.000	1.486	1.785	0.000
110	0.090	0.384	0.000	0.000	0.000	0.000
100	1.406	1.168	0.000	1.364	0.345	0.000
90	0.413	0.206	0.000	0.265	0.000	0.000
80	0.421	0.171	0.000	0.692	0.000	0.000
70	1.615	0.629	0.000	0.340	0.000	0.000
60	1.216	0.651	0.000	1.098	0.000	2.342
50	0.663	0.479	0.000	0.732	0.276	4.538
40	2.567	0.226	0.000	0.767	0.000	9.567
30	0.000	0.039	0.000	0.665	0.309	0.000
20	0.216	0.352	0.209	0.837	0.000	4.376
0	0.297	0.736	0.000	0.639	0.000	0.000

Table AC-2. Biomasses of leaf litter layer and total earthworms in 2009, 2010, and 2011. Total earthworm collection was not replicated and no leaf litter layer was collected in 2009.

	2009	2010				2011			
Distance (m)	**Total Earthworm Biomass (AFD g m^{-2})**	**Litter Biomass (kg m^{-2})**	**Standard Error n=3**	**Total Earthworm Biomass (AFD g m^{-2})**	**Standard Error n=3**	**Litter Biomass (kg m^{-2})**	**Standard Error n=3**	**Total Earthworm Biomass (AFD g m^{-2})**	**Standard Error n=3**
190	0.620	0.392	0.060	1.880	1.448	0.496	0.067	0.850	0.558
180	0.000	0.394	0.090	0.530	0.150	0.298	0.008	1.975	0.304
170	0.437	0.365	0.074	0.160	0.081	0.368	0.050	1.581	0.602
160	0.000	0.143	0.068	2.942	1.399	0.117	0.049	2.884	0.971
150	1.441	0.130	0.068	18.208	9.528	0.131	0.069	2.226	0.465
140	1.369	0.121	0.042	3.522	1.556	0.102	0.052	3.711	1.176
130	1.747	0.026	0.026	8.701	2.031	0.015	0.008	4.439	0.656
120	3.962	0.050	0.026	9.342	3.296	0.053	0.036	5.467	2.691
110	0.474	0.137	0.061	4.860	0.787	0.082	0.048	3.128	0.913
100	4.283	0.151	0.035	9.410	3.006	0.125	0.033	3.384	1.021
90	0.885	0.085	0.021	11.050	2.385	0.063	0.008	4.350	0.381
80	1.285	0.049	0.028	7.551	2.067	0.058	0.033	3.512	0.394
70	2.584	0.063	0.003	14.144	6.201	0.098	0.052	3.878	1.056
60	5.307	0.060	0.029	24.924	15.633	0.023	0.012	2.740	0.641
50	6.688	0.013	0.013	8.522	4.662	0.019	0.011	4.347	0.683
40	13.127	0.005	0.005	5.836	1.893	0.017	0.009	4.072	2.266
30	1.013	0.000	0.000	12.132	7.819	0.017	0.009	3.942	3.130
20	5.990	0.004	0.006	2.501	2.309	0.009	0.007	6.899	2.032
0	1.672	0.074	0.020	25.024	7.713	0.072	0.029	5.464	2.129

Table AC-3. Earthworm biomass by species (AFD g m^{-2}) in 2010.

Distance (m)	***Apporectodea***	SE n=3	***Dendrobaena***	SE n=3	***Octolasion***	SE n=3	***L.* juvenile**	SE n=3	***L. rubellus***	SE n=3	***L. terrestris***	SE n=3
190	0.000	0.00	0.378	0.18	0.000	0.00	0.279	0.16	0.282	0.28	0.000	0.00
180	0.003	0.00	0.396	0.21	0.000	0.00	0.101	0.06	0.000	0.00	0.000	0.00
170	0.000	0.00	0.160	0.08	0.000	0.00	0.000	0.00	0.000	0.00	0.000	0.00
160	0.291	0.16	0.657	0.16	0.000	0.00	0.313	0.16	0.221	0.22	0.000	0.00
150	2.359	0.80	1.103	0.36	0.000	0.00	1.459	0.53	0.346	0.17	1.296	1.30
140	0.459	0.35	0.732	0.28	0.000	0.00	0.887	0.12	0.081	0.08	0.000	0.00
130	1.144	0.50	0.882	0.29	0.000	0.00	1.925	0.27	0.341	0.34	1.459	1.46
120	1.035	0.73	0.653	0.07	0.000	0.00	1.135	0.48	0.506	0.29	1.400	1.01
110	0.926	0.09	0.625	0.08	0.000	0.00	1.636	1.09	0.000	0.00	0.000	0.00
100	2.262	1.17	0.442	0.13	0.000	0.00	2.057	0.51	0.984	0.98	0.000	0.00
90	2.019	1.13	0.647	0.11	0.000	0.00	3.378	0.81	0.463	0.31	0.714	0.71
80	0.947	0.07	0.785	0.40	0.000	0.00	2.176	0.48	0.637	0.33	0.000	0.00
70	3.961	1.67	0.673	0.05	0.000	0.00	1.169	0.28	0.492	0.49	0.000	0.00
60	3.497	1.76	0.527	0.23	0.259	0.26	1.812	0.92	0.291	0.29	5.164	2.69
50	1.644	1.40	0.148	0.08	0.520	0.52	3.027	0.63	1.010	0.84	1.532	1.53
40	0.288	0.07	0.129	0.13	0.552	0.45	1.956	0.59	0.280	0.15	1.658	1.66
30	1.303	0.67	0.182	0.06	0.281	0.28	2.098	1.09	0.642	0.32	1.296	1.30
20	0.275	0.17*	0.119	0.10*	0.029	0.03*	1.727	1.53*	0.221	0.22*	0.000	0.00*
0	1.952	0.70	0.379	0.08	0.252	0.15	2.098	0.82	0.811	0.68	3.901	2.08

SE = Standard Error
*Standard error n=2

Table AC-4. Earthworm biomass by species (AFD g m^{-2}) in 2011.

Distance (m)	***Apporectodea***	SE n=3	***Dendrobaena***	SE n=3	***Octolasion***	SE n=3	***L.* juvenile**	SE n=3	***L. rubellus***	SE n=3	***L. terrestris***	SE n=3
190	0.000	0.00	0.451	0.16	0.000	0.00	0.088	0.09	0.311	0.31	0.000	0.00
180	0.005	0.01	1.352	0.20	0.000	0.00	0.250	0.13	0.367	0.37	0.000	0.00
170	0.069	0.07	0.343	0.17	0.000	0.00	0.609	0.25	0.560	0.34	0.000	0.00
160	0.457	0.35	1.062	0.33	0.000	0.00	1.031	0.42	0.333	0.17	0.000	0.00
150	0.298	0.09	0.587	0.25	0.027	0.03	0.803	0.36	0.511	0.51	0.000	0.00
140	1.537	1.20	0.428	0.11	0.000	0.00	1.230	0.34	0.516	0.01	0.000	0.00
130	0.719	0.33	0.370	0.12	0.000	0.00	2.177	0.26	0.193	0.19	0.981	0.98
120	0.636	0.25	0.454	0.15	0.000	0.00	1.584	0.47	0.645	0.37	2.148	1.42
110	0.775	0.27	0.560	0.24	0.000	0.00	1.341	0.53	0.452	0.25	0.000	0.00
100	1.172	0.30	0.224	0.05	0.000	0.00	1.617	0.68	0.370	0.22	0.000	0.00
90	0.554	0.11	0.433	0.18	0.000	0.00	2.947	0.61	0.416	0.22	0.000	0.00
80	0.564	0.14	0.379	0.13	0.000	0.00	2.270	0.14	0.299	0.30	0.000	0.00
70	0.745	0.27	0.394	0.09	0.009	0.01	1.543	0.85	0.000	0.00	1.186	1.19
60	0.872	0.16	0.125	0.10	0.077	0.08	1.666	0.53	0.000	0.00	0.000	0.00
50	1.036	0.16	0.187	0.19	0.135	0.12	2.008	0.70	0.000	0.00	0.981	0.98
40	0.961	0.19	0.031	0.02	0.447	0.44	0.671	0.33	0.000	0.00	1.963	1.96
30	0.000	0.00*	0.023	0.02*	0.004	0.00*	0.664	0.10*	0.000	0.00*	3.251	3.25*
20	0.349	0.22*	0.052	0.05*	0.557	0.14*	1.054	0.04*	0.000	0.00*	3.416	3.24*
0	0.609	0.29	0.068	0.04	0.126	0.07	2.383	0.37	0.000	0.00	2.277	1.45

SE = Standard Error
*Standard error n=2

Appendix D – Soil Properties

Method

Six soil pits were excavated across the invasion gradient in 2009. Soil samples were collected in 2.5 cm intervals in the A horizon, 5 cm intervals in the E horizon, and 10 cm intervals in the B horizon. Archived samples are located at the University of Minnesota. Samples were initially wet sieved with a 2 mm sieve, and the soil samples <2 mm were used for analysis. Bulk densities were determined for each horizon using a sliding hammer corer followed by drying and weighing of the core samples.

Samples <2 mm were analyzed for elemental C and N contents by VarioMax CN Elemental Analyzer. Oven dried soil samples were treated with HCl to remove carbonate prior to analysis. Duplicate samples of 0.5 g were used to analyze C and N contents in the sample. Approximately 250 mg of the standard material glutamic acid were run every 20 samples.

In 2011, soil cores with 3.175 cm diameter and 30 cm length were collected adjacent to all plots along transect B to detail the thicknesses of A and E horizons along the transect. Samples were sieved at 2 mm. Bulk densities were measured for the A horizon (0-6 cm and >6 cm) and E horizon (A-E horizon boundary to 30cm).

Table AD-1. Soil properties collected from excavated soil pit 3 at 190 m in 2009.

Distance (m)	Horizon	Depth (cm)	Bulk Density (g/cm^3)	Weight % Carbon (%)
190	A	0-2	0.27	19.91
190	A	2-4	0.27	22.44
190	A	4-7	0.86	4.75
190	E	7-11	0.81	1.07
190	E	11-15	0.81	0.76
190	E	15-25	1.13	0.42
190	E	25-35	1.13	0.31
190	E	35-45	1.2	0.17
190	E	45-56	1.2	0.13
190	1B	56-71	1.22	0.18
190	2B	71-83	1.13	0.26
190	2C	83-110	1.21	0.64
190	2C	110-144	1.21	0.70
190	2C	144-156	1.21	1.44

Table AD-2. Soil properties collected from excavated soil pit 4 at 160 m in 2009.

Distance (m)	Horizon	Depth (cm)	Bulk Density (g/cm^3)	Weight % Carbon (%)
160	A	0-2	0.24	24.15
160	A	2-4	0.24	21.30
160	A	4-7	0.24	12.31
160	A	7-9	0.61	2.84
160	A	9-12	0.61	1.31
160	AE	12-17	1	0.68
160	E	17-25	1.2	0.31
160	E	25-35	1.2	0.18
160	E	35-44	1.31	0.18
160	1B	44-54	1.31	0.24
160	1B	54-64	1.31	0.14
160	1C	64-74	1.31	0.14
160	1C	74-84	1.31	0.16
160	1C	84-94	1.31	0.14
160	1C	94-104	1.31	0.14
160	1C	104-114	1.31	0.15
160	2C	114-126	1.37	1.07
160	C2	126-140	1.37	1.23
160	C2	140-167		

Table AD-3. Soil properties collected from excavated soil pit 5 at distance 150 m in 2009.

Distance (m)	Horizon	Depth (cm)	Bulk Density (g/cm^3)	Weight % Carbon (%)
150	A	0-2	0.33	26.51
150	A	2-4	0.33	21.90
150	A	4-6	0.33	12.82
150	A	6-8	0.5	3.23
150	A	8-11	0.5	1.26
150	AE	11-17	0.9	0.48
150	E	17-27	1.24	0.28
150	E	27-37	1.24	0.19
150	1B	37-44	1.19	0.31
150	1B	44-54	1.14	0.21
150	1B	54-64	1.14	0.24
150	1B	64-74	1.14	0.24
150	1B	74-90	1.17	0.20
150	2B	90-100	1.17	0.25
150	2B	100-113	1.54	0.56
150	2C	113-130	1.54	0.41
150	2C	130-160	1.54	1.02

Table AD-4. Soil properties collected from excavated soil pit 6 at 100 m in 2009.

Distance (m)	Horizon	Depth (cm)	Bulk Density (g/cm^3)	Weight % Carbon (%)
100	1A	0-2	0.24	11.36
100	1A	2-4	0.24	9.68
100	1A	4-6	0.24	9.29
100	1A	6-9	0.24	5.05
100	1EA	9-14	0.56	0.84
100	1E	14-21	1.3	0.40
100	1E	21-31	1.3	0.24
100	1E	31-41	1.3	0.15
100	1EB	41-53	1.3	0.14
100	2Bt1	53-58	1.35	0.22
100	2Bt1	58-68	1.35	0.12
100	2Bt2	68-77	1.28	0.15
100	2Bt2	77-87	1.28	0.15
100	2Bt3	87-97	1.28	0.17
100	2Bt3	97-107	1.28	0.20
100	2Bt3	107-123	1.28	0.33
100	2C	123-130	1.28	1.00

Table AD-5. Soil properties collected from excavated soil pit 7 at 50 m in 2009.

Distance (m)	Horizon	Depth (cm)	Bulk Density (g/cm^3)	Weight % Carbon (%)
50	A	0-2	0.55	7.26
50	A	2-4	0.55	5.90
50	A	4-6	0.55	4.78
50	A	6-8	0.55	3.27
50	A	8-11	0.55	1.56
50	E/A	11-18	1.09	0.43
50	E	18-24	1.32	0.26
50	E	24-34	1.32	0.12
50	1B	34-43	1.16	0.14
50	1B	43-53	1.16	0.16
50	2B	53-63	1.16	0.16
50	2B	63-73	1.16	0.22
50	2B	73-83	1.16	0.23
50	2B	83-93	1.16	0.23
50	2B	93-103	1.16	0.24
50	2B	103-113	1.16	0.28
50	2B	113-123	1.16	0.45
50	2B	123-133	1.41	0.97
50	2B	133-150	1.41	1.29
50	2C	150-180	1.41	1.45

Table AD-6. Soil properties collected from excavated soil pit 8 at 0 m (point of invasion) in 2009.

Distance (m)	Horizon	Depth (cm)	Bulk Density (g/cm^3)	Weight % Carbon (%)
0	A	0-2	0.67	7.44
0	A	2-4	0.67	6.35
0	A	4-6	0.67	5.34
0	A	6-8	0.67	4.82
0	A	8-10	0.67	3.53
0	E/A	10-18	1.14	0.50
0	E	18-28	1.1	0.22
0	E	28-43	1.1	0.18
0	B	43-53	1.28	0.26
0	B	53-63	1.28	0.19
0	B	63-73	1.28	0.24
0	B	73-83	1.28	0.16
0	B	83-94	1.28	0.42
0	B	94-100	1.32	1.71
0	1C	100-107	1.25	2.60

Table AD-7. Carbon inventory for mass equivalent depth of 1.9 g cm^{-2} and 18.2 g cm^{-2}, as well as the C inventory for the light (< 2.0 g cm^{-3}) and heavy (> 2.0 g cm^{-3}) fraction within 1.9 g cm^{-2} from data collected in 2009.

Distance (m)	Carbon Inventory		Carbon Inventory 1.9 g cm^{-2}	
	1.9 Mass Equivalent Depth (g cm^{-2})	18.2 Mass Equivalent Depth (g cm^{-2})	Light Fraction (< 2.0 g cm^{-3})	Heavy Fraction (> 2.0 g cm^{-3})
190	3.57	4.58	3.08	0.49
160	3.79	4.34	3.36	0.43
150	4.66	5.08	3.73	0.93
100	1.87	2.47	1.16	0.72
50	2.50	2.88	0.53	1.97
0	3.54	4.11	2.92	0.62

Table AD-8. Depths to the A-E horizon boundary determined in 2009 and 2011. The changing depth to A-E horizon boundary was used to predict A horizon SSA_{total} due to enhanced physical mixing (Fig. 1-14).

Year	Transect	Distance (m)	Depth A-E Horizon Boundary (cm)
2011	B	190	6.00
2009	B	190	7.00
2011	B	180	8.89
2011	B	170	7.82
2011	B	160	7.48
2009	B	160	17.00
2011	B	150	11.87
2009	B	150	17.00
2011	B	140	7.70
2011	B	130	15.26
2011	B	120	9.39
2011	B	110	10.45
2011	B	100	9.94
2009	B	100	9.00
2011	B	90	10.20
2011	B	80	13.34
2011	B	70	13.32
2011	B	60	10.86
2011	B	50	14.65
2009	B	50	11.00
2011	B	40	11.98
2011	B	30	15.81
2011	B	20	19.97
2009	A	0	10.00
2011	B	0	10.00

Table AD-9. Soil properties for the depth interval of 0-6 cm. Samples were collected by hammer cores with 3.175 cm diameter and 30 cm length in 2011.

Distance (m)	Depth (cm)	Bulk Density		Weight Percent Carbon	
		($g\ m^{-3}$)	Standard Error n=2	(%)	Standard Error n=2
190	0-6	0.29	0.03	13.33	1.46
180	0-6	0.25	0.15	9.95	1.03
170	0-6	0.27	0.14	13.67	1.66
160	0-6	0.55	0.03	7.90	0.38
150	0-6	0.29	0.09	16.47	2.34
140	0-6	0.42	0.04	5.66	0.00
130	0-6	0.22	0.02	14.20	2.05
120	0-6	0.46	0.13	4.93	0.08
110	0-6	0.29	0.10	10.99	0.82
100	0-6	0.49	0.03	5.30	0.44
90	0-6	0.35	0.00	12.84	1.87
80	0-6	0.39	0.02	5.04	0.10
70	0-6	0.38	0.08	6.86	0.43
60	0-6	0.53	0.06	4.94	0.04
50	0-6	0.36	0.06	6.80	0.03
40	0-6	0.43	0.02	5.86	0.09
30	0-6	0.62	0.09	6.38	0.04
20	0-6	0.23	0.02	8.99	0.63
0	0-6	0.54		3.87	0.03

Table AD-10. Soil properties for the depth intervals > 6 cm in the A horizon, collected by hammer cores with 3.175 cm diameter and 30 cm length in 2011.

Distance (m)	Depth (cm)	Bulk Density		Weight Percent Carbon
		($g\ m^{-3}$)	Standard Error n=2	(%)
190		N/A	N/A	N/A
180	6-10	0.43	**	7.32
170	6-10	0.40	**	9.07
160	6-9	0.58	**	1.79
150	6-12	0.47	0.16	10.47
140	6-10	0.62	**	4.93
130	6-15	0.49	0.00	7.67
120	6-11	0.60	**	3.89
110	6-11	0.74	0.06	6.76
100	6-11	0.51	**	4.07
90	6-10	0.65	0.07	6.88
80	6-13	0.44	0.06	4.18
70	6-13	0.59	0.21	5.06
60	6-11	0.93	0.21	3.76
50	6-15	0.55	0.07	5.41
40	6-12	0.61	0.16	4.04
30	6-16	0.57	0.30	5.29
20	6-20	0.45	0.05	5.91
0	6-10	0.54	**	3.87

**Samples with blank Standard Error did not have any replicate samples analyzed

Appendix E. – Specific Surface Area

Method

Soils in the <2 mm size fraction were analyzed for specific surface area (SSA) with a Micromeritics TriStar 3020 Surface Area and Porosity Analyzer at the University of Minnesota. From each depth interval, 1.0-1.5 g of soil sample was dried at 60 ℃, and degassed for 4-6 hours or until no water was left on the side of tube. Degassing consisted of heating samples to 150 ℃ and purging N_2 gas. After degassing, the sample mass was recorded and secured on the TriStar 3020 for analysis. The Brunauer-Emmett-Teller (BET) theory was applied to the isotherm data which were collected at 11 different pressure points at 77 K using N_2 as adsorbent gas.

To remove OM from soil samples, samples were muffled at 350 ℃ for 12 hours: initial ramp rate of 0.9 ℃ min^{-1} was used until a temperature of 350 ℃ was reached and soaked for 12 hours. After 12 hours, a ramp rate of 1.2 ° C min^{-1} was used to reach a temperature of 50 ℃ and soaked at 50 ℃ for four hours. Samples were then weighed and the above procedure for SSA was used to determine the SSA of soil sample without OM.

Table AE-1. Specific surface areas of soils collected from soil pit 3 at 190 m in 2009.

Pit	Distance (m)	Depth (cm)	Mass Equivalent Depth (g cm^{-2})	$SSA_{untreated}$		SSA_{total}		$SSA_{Occluded}$	
				(m^2 g^{-1})	Standard Error n=2	(m^2 g^{-1})	Standard Error n=2	(m^2 g^{-1})	% Occluded
3	190	0-2	0.54	1.39	0.08*	23.61	2.41	22.22	94.12
3	190	2-4	1.08	1.41	0.11*	20.05	0.85	18.65	92.99
3	190	4-7	3.66	2.21	0.12*	7.00	0.16	4.79	68.41
3	190	7-11	6.9	1.97	0.19	4.32	0.60	2.35	54.42
3	190	11-15	10.14	2.17	0.07	4.06	0.19	1.89	46.63
3	190	15-25	21.44	2.06	0.19	3.07	0.15	1.01	33.00
3	190	25-35	32.74	1.83	0.18	3.07	0.00	1.24	40.53
3	190	35-45	44.74	2.03	0.00	3.34	0.04	1.31	39.18
3	190	45-56	57.94	2.08	0.38	3.37	0.08	1.30	38.40
3	190	56-71	76.24	6.76	0.37	8.82	0.23	2.06	23.35
3	190	83-110	89.8	14.87	**	16.56	**	1.69	10.21
3	190	110-114	116.42	6.66	**	7.83	**	1.17	14.94

*Standard error n=4

**Samples with blank Standard Error did not have any replicate samples analyzed.

Table AE-2. Specific surface areas of soils collected from soil pit 4 at 160 m in 2009.

Pit	Distance (m)	Depth (cm)	Mass Equivalent Depth (g cm^{-2})	$SSA_{untreated}$		SSA_{total}		$SSA_{Occluded}$	
				(m^2 g^{-1})	Standard Error n=2	(m^2 g^{-1})	Standard Error n=2	(m^2 g^{-1})	% Occluded
4	160	0-2	0.48	1.36	0.02*	33.95	1.64	32.59	96.01
4	160	2-4	0.96	2.22	0.10*	22.80	2.85	20.57	90.24
4	160	4-7	1.68	2.94	0.03*	16.34	2.03	13.40	82.01
4	160	7-9	2.9	3.40	0.16*	10.14	1.39	6.74	66.50
4	160	9-12	4.73	3.60	0.40	7.18	0.80	3.58	49.84
4	160	12-17	9.73	3.34	0.34	5.93	0.73	2.59	43.71
4	160	17-25	19.33	5.85	3.10	3.77	0.02	0.00	0.00
4	160	25-35	44.22	3.02	0.01	4.00	0.37	0.98	24.45
4	160	35-44	44.22	9.01	0.05	10.56	0.12	1.55	14.70
4	160	44-54	57.32	11.07	0.00	12.86	0.00	1.80	13.96
4	160	54-64	70.42	5.46	**	5.83	**	0.37	6.31
4	160	64-74	83.52	6.63	**	7.38	**	0.75	10.18
4	160	74-84	96.62	6.53	**	8.55	**	2.02	23.64
4	160	84-94	109.72	5.76	**	6.10	**	0.34	5.55
4	160	94-104	122.82	7.09	**	7.96	**	0.88	11.03
4	160	114-126	135.92	9.92	**	10.66	**	0.75	6.99

*Standard error n=4

**Samples with blank Standard Error did not have any replicate samples analyzed.

Table AE-3. Specific surface areas of soils collected from soil pit 5 at 150 m in 2009.

Pit	Distance (m)	Depth (cm)	Mass Equivalent Depth (g cm^{-2})	$SSA_{untreated}$		SSA_{total}		$SSA_{Occluded}$	
				(m^2 g^{-1})	Standard Error n=2	(m^2 g^{-1})	Standard Error n=2	(m^2 g^{-1})	% Occluded
5	150	0-2	0.66	0.62	0.00	13.76	2.82	13.14	95.47
5	150	2-4	1.32	1.20	0.02	14.71	0.00	13.51	91.85
5	150	4-6	1.98	2.24	0.25	12.74	4.44	10.50	82.39
5	150	6-8	2.98	2.34	0.08	6.56	1.73	4.23	64.42
5	150	8-11	4.48	2.79	0.07	5.63	0.03	2.85	50.52
5	150	1-17	9.88	2.13	0.29	3.27	0.70	1.14	34.88
5	150	17-27	22.28	2.18	0.47	3.58	0.06	1.40	39.06
5	150	27-37	34.68	3.16	0.01	3.91	0.08	0.74	19.06
5	150	37-44	43.01	10.47	0.36	11.73	0.98	1.27	10.79
5	150	44-54	54.41	7.22	**	8.60	**	1.38	16.07
5	150	54-64	65.81	9.13	**	10.08	**	0.95	9.43
5	150	64-74	77.21	13.31	**	13.35	**	0.04	0.33
5	150	74-90	95.93	10.51	**	10.86	**	0.35	3.22
5	150	90-100	107.63	13.10	**	13.47	**	0.37	2.74
5	150	100-113	127.65	13.20	**	12.69	**	0.00	0.00

**Samples with blank Standard Error did not have any replicate samples analyzed.

Table AE-4. Specific surface areas of soils collected from soil pit 6 at 100 m in 2009.

Pit	Distance (m)	Depth (cm)	Mass Equivalent Depth (g cm^{-2})	$SSA_{untreated}$		SSA_{total}		$SSA_{Occluded}$	
				(m^2 g^{-1})	Standard Error n=2	(m^2 g^{-1})	Standard Error n=2	(m^2 g^{-1})	% Occluded
6	100	0-2	0.48	2.12	0.25	11.92	1.80	9.80	82.22
6	100	2-4	0.96	2.41	0.26	11.35	1.37	8.94	78.78
6	100	4-6	1.44	2.47	0.37	10.54	0.16	8.07	76.55
6	100	6-9	2.16	3.43	0.16	9.53	1.06	6.10	63.97
6	100	9-14	4.96	2.92	0.21	4.78	0.55	1.86	38.89
6	100	14-21	14.06	2.61	0.02	4.04	0.39	1.43	35.46
6	100	21-31	27.06	2.01	0.12	3.26	0.28	1.24	38.22
6	100	31-41	40.06	2.39	0.06	3.23	0.08	0.84	25.99
6	100	41-53	55.66	3.66	0.17	5.21	0.34	1.55	29.79
6	100	53-58	62.41	10.36	1.35	12.85	0.05	2.49	19.37
6	100	58-68	75.91	4.35	**	5.73	**	1.38	24.02
6	100	87-97	100.23	17.80	**	19.13	**	1.32	6.92
6	100	97-107	113.03	16.15	**				

**Samples with blank Standard Error did not have any replicate samples analyzed.

Table AE-5. Specific surface areas of soils collected from soil pit 7 at 50 m in 2009.

Pit	Distance (m)	Depth (cm)	Mass Equivalent Depth (g cm-2)	$SSA_{untreated}$		SSA_{total}		$SSA_{Occluded}$	
				(m^2 g^{-1})	Standard Error n=2	(m^2 g^{-1})	Standard Error n=2	(m^2 g^{-1})	% Occluded
7	50	0-2	1.1	1.80	0.14	9.66	0.33	7.87	81.41
7	50	2-4	2.2	2.04	0.09	10.70	0.32	8.67	80.97
7	50	4-6	3.3	2.53	0.32	9.80	0.06	7.27	74.16
7	50	6-8	4.4	3.56	0.04	8.81	0.28	5.25	59.56
7	50	8-11	6.05	4.12	0.20	7.19	0.24	3.08	42.76
7	50	11-18	13.68	2.95	0.01	4.47	0.18	1.52	34.01
7	50	18-24	21.6	2.76	0.00	3.71	0.01	0.95	25.52
7	50	24-34	34.8	2.12	0.00	3.09	0.02	0.98	31.65
7	50	34-43	45.24	5.10	0.45	7.00	0.40	1.90	27.20
7	50	43-53	56.84	14.43	**	14.37	**	0.00	0.00
7	50	53-63	68.44	20.85	**	22.85	**	2.00	8.77
7	50	63-73	80.04	42.35	**	42.83	**	0.48	1.12
7	50	73-83	91.64	45.16	**	46.93	**	1.77	3.77
7	50	83-93	103.24	44.95	**	47.46	**	2.51	5.30
7	50	93-103	114.84	44.05	**	44.34	**	0.29	0.65
7	50	103-113	126.44	26.91	**	45.83	**	18.92	41.28
7	50	113-123	138.04	26.66	**	42.94	**	16.28	37.91

**Samples with blank Standard Error did not have any replicate samples analyzed.

Table AE-6. Specific surface areas of soils collected from soil pit 8 at 0 m in 2009.

Pit	Distance (m)	Depth (cm)	Mass Equivalent Depth (g cm-2)	$SSA_{untreated}$		SSA_{total}		$SSA_{Occluded}$	
				(m^2 g^{-1})	Standard Error n=2	(m^2 g^{-1})	Standard Error n=2	(m^2 g^{-1})	% Occluded
8	0	0-2	1.34	2.84	0.26	9.77	1.40	6.93	70.96
8	0	2-4	2.68	2.97	0.14	11.31	0.78	8.34	73.76
8	0	4-6	4.02	3.44	0.18	10.14	0.74	6.70	66.07
8	0	6-8	5.36	3.66	0.62	9.26	1.29	5.61	60.52
8	0	8-10	6.7	4.29	0.59	7.98	1.28	3.70	46.30
8	0	10-18	15.82	2.26	0.27	3.66	0.17	1.39	38.06
8	0	18-28	26.82	1.81	0.15	2.80	0.04	0.99	35.32
8	0	28-43	43.32	1.87	0.54	3.40	0.00	1.52	44.87
8	0	43-53	56.12	8.71	1.58	11.46	0.42	2.74	23.96
8	0	53-63	68.92	9.74	0.26	11.92	0.36	2.17	18.23
8	0	63-73	81.72	8.7094	**	14.6282	**	5.92	40.46
8	0	73-83	94.52	12.048	**	13.8545	**	1.81	13.04
8	0	83-94	108.6						
8	0	94-100	116.52	5.2593	**	5.1329	**	0.00	0.00
8	0	100-107	125.27	31.6908	**	31.985	**	0.29	0.92

**Samples with blank Standard Error did not have any replicate samples analyzed.

Table AE-7. Inventories of SSA_{total} and $SSA_{occluded}$ from soils collected in 2009. Inventories are reported for mass equivalent depths of 1.9 g cm^{-2} (consistent A horizon mass equivalent depth) and 18.2 g cm^{-2} (A+E horizon).

Pit	Distance (m)	SSA_{total} Inventory		$SSA_{Occluded}$ Inventory	
		1.9 Mass Equivalent Depth (g cm^{-2})	18.2 Mass Equivalent Depth (g cm^{-2})	1.9 Mass Equivalent Depth (g cm^{-2})	18.2 Mass Equivalent Depth (g cm^{-2})
3	190	293016.04	935463.99	259854.67	563465.35
4	160	412252.94	1261137.88	366445.86	628927.04
5	150	261939.37	896160.95	236876.36	507921.13
6	100	206214.34	867090.06	156796.46	406498.65
7	50	191679.02	1056218.50	155668.98	529112.04
8	0	194544.16	1049281.07	139825.70	569457.31

Table AE-8. Calculated *C*- constants via BET equation for soils collected from pit 3 excavated in 2009.

Pit	Distance (m)	Depth	Mass Equivalent Depth (g m^{-2})	*C*- Constant
3	190	0-2	0.54	45.71
3	190	2-4	1.08	43.97
3	190	4-7	3.66	61.15
3	190	7-11	6.9	89.84
3	190	1-15	10.14	71.15
3	190	15-25	21.44	89.71
3	190	25-35	32.74	70.16
3	190	35-45	44.74	68.88
3	190	45-55	57.94	195.24

Table AE-9. Calculated *C*- constants via BET equation for soils collected from pit 4 excavated in 2009.

Pit	Distance (m)	Depth	Mass Equivalent Depth (g m^{-2})	*C*- Constant
4	160	0-2	0.48	48.52
4	160	2-4	0.96	48.82
4	160	4-7	1.68	60.18
4	160	7-9	2.9	82.01
4	160	9-12	4.73	80.36
4	160	12-17	9.73	108.71
4	160	17-25	19.33	112.78
4	160	25-35	44.22	79.04

Table AE-10. Calculated *C*- constants via BET equation for soils collected from pit 5 excavated in 2009.

Pit	Distance (m)	Depth	Mass Equivalent Depth (g m^{-2})	*C*- Constant
5	150	0-2	0.66	56.40
5	150	2-4	1.32	37.82
5	150	4-6	1.98	49.77
5	150	6-8	2.98	86.34
5	150	8-11	4.48	80.64
5	150	11-17	9.88	103.40
5	150	17-27	22.28	111.62
5	150	27-37	34.68	105.40

Table AE-11. Calculated *C*- constants via BET equation for soils collected from pit 6 excavated in 2009.

Pit	Distance (m)	Depth	Mass Equivalent Depth (g m^{-2})	*C*- Constant
6	100	0-2	0.48	102.98
6	100	2-4	0.96	50.16
6	100	4-6	1.44	120.33
6	100	6-9	2.16	77.55
6	100	9-14	4.96	105.84
6	100	14-21	14.06	111.55
6	100	21-31	27.06	223.46
6	100	31-41	40.06	191.48
6	100	41-53	55.66	98.19
6	100	53-58	62.41	111.91
6	100	68-77	87.43	171.70
6	100	77-87	100.23	161.23
6	100	87-97	113.03	119.00

Table AE-12. Calculated *C*- constants via BET equation for soils collected from pit 7 excavated in 2009.

Pit	Distance (m)	Depth	Mass Equivalent Depth (g m^{-2})	*C*- Constant
7	50	0-2	1.1	71.72
7	50	2-4	2.2	65.04
7	50	4-6	3.3	79.80
7	50	6-8	4.4	96.54
7	50	8-11	6.05	147.15
7	50	11-18	13.68	152.03
7	50	18-24	21.6	180.40
7	50	24-34	34.8	82.56
7	50	34-43	45.24	129.56

Table AE-13. Calculated *C*- constants via BET equation for soils collected from pit 8 excavated in 2009.

Pit	Distance (m)	Depth	Mass Equivalent Depth (g m^{-2})	*C*- Constant
8	0	0-2	1.34	66.14
8	0	4-6	4.02	83.54
8	0	6-8	5.36	95.71
8	0	8-10	6.7	96.84
8	0	10-18	15.82	109.68
8	0	18-28	26.82	99.43
8	0	28-43	43.32	185.32
8	0	43-53	56.12	156.13

Appendix F. – Density Fractionation

Method

Approximately 10 g of a fine soil sample (<2 mm) was used for density fractionation. Samples were lightly ground using a rolling pin for 3 minutes. Samples were then sieved at 250 μm to rid any fine roots. Both >250 μm and <250 μm were weighed for mass balance calculations. Density fractionation was only performed on samples <250 μm; all soil <250 μm was placed in a 50 ml falcon tube with 25 ml of sodium polytungstate (SPT) at density 2 g cm^{-3}. (Approximately 50 mg of SPT was mixed with 35 ml Nano pure water and adjusted accordingly to reach a density of 2 g cm^{-3}.) Falcon tubes with both the samples of <250 μm and SPT were placed on the shaker for 2-3 hours. The falcon tubes were then centrifuged at 2600 rpm for 20-30 minutes and the light and heavy fraction were extracted from the tubes. Each sample was rinsed ~5 times to conductivity of 50 μS cm^{-1}, to rid of SPT. The rinsed heavy and light fractions were then oven dried at 60 °C and weighed separately for mass balance calculations.

Elemental C and N analysis and SSA analysis were performed for the density fractionated samples as described above (Appendix D and E).

Heavy and light fractions of soils (<250 μm) were also analyzed for values of $\delta^{13}C$ and $\delta^{15}N$. Samples were analyzed by Thermo-Finnigan Delta Plus XP Isotope Ratio Mass Spectrometer. Soil sample size was determined by the predicted amount of C and N in the sample via C:N ratio; a sample size of 1.5 mg was used for A horizon soils, 15 mg for E horizon soils, and 30 mg for B horizon soils. Prior to analysis, samples were placed in desiccators containing beakers of HCl for 18 hours to remove any carbonate present. Analytical error for the instrument was ± 0.47% for $\delta^{13}C$ and ± 0.08% for $\delta^{15}N$. IU Acetanilide was used as the standard material.

Table AF-1. Soil properties from the heavy fraction (>2.0 g cm^{-3}) of soil <250 μm. The soil samples were collected from the excavated soil pits across the invasion chronosequence in 2009.

Pit	Distance (m)	Depth (m)	Mass Equivalent Depth (g m^{-2})	Mass % with regards to bulk soil (%)	Weight Percent Carbon (%)	Weight Percent Nitrogen (%)	$\delta^{13}C$ (‰)	$\delta^{15}N$ (‰)
3	190	2-4	1.08	17.48	4.56	0.41	-27.15	5.22
3	190	4-7	3.66	94.04	2.87	0.28	-25.52	6.76
3	190	7-11	6.9	99.66	0.91	0.10	-26.80	6.84
4	160	2-4	0.96	17.80	3.86	0.32	-26.42	7.09
4	160	4-7	1.68	69.60	4.66	0.36	-27.23	8.10
4	160	9-12	4.73	99.40	1.06	0.12	-24.83	6.63
4	160	54-64	50.42	99.59	0.06	0.01	-24.85	1.69
5	150	4-6	1.98	61.73	6.53	0.53	-29.37	6.07
5	150	8-11	4.48	99.33	0.95	0.11	-25.63	4.68
6	100	2-4	0.96	57.43	5.70	0.43	-28.88	4.61
6	100	6-9	2.16	94.73	4.49	0.35	-27.48	5.43
6	100	9-14	4.96	98.41	0.54	0.06	-25.25	6.88
7	50	0-2	1.1	93.70	4.91	0.38	-28.72	3.79
7	50	2-4	2.2	97.42	4.56	0.36	-28.42	4.33
7	50	6-8	4.4	98.42	2.39	0.21	-25.98	5.07
7	50	34-43	45.24	98.28	0.09	0.02	-25.21	3.11
8	0	10-18	15.82	99.63	0.27	0.03	-25.06	6.37
8	0	43-53	56.12	99.71	0.11	0.02	-25.03	5.45

Table AF-2. Soil properties from the light fraction (<2.0 g cm^{-3}) of soil <250 μm. The soil samples were collected from the excavated soil pits across the invasion chronosequence in 2009.

Pit	Distance (m)	Depth (m)	Mass Equivalent Depth (g m^{-2})	Mass % with regards to bulk soil (%)	Weight Percent Carbon (%)	Weight Percent Nitrogen (%)	$\delta^{13}C$ (‰)	$\delta^{15}N$ (‰)
3	190	2-4	1.08	17.48	27.57	1.91	-26.39	3.60
3	190	4-7	3.66	94.04	27.52	1.79	-26.19	4.46
3	190	7-11	6.9	99.66	28.94	1.46	-26.66	4.06
4	160	2-4	0.96	17.80	23.11	1.67	-25.67	4.19
4	160	4-7	1.68	69.60	24.07	1.52	-25.84	4.74
4	160	9-12	4.73	99.40	29.20	1.24	-27.46	1.81
5	150	2-4	1.32	11.44	28.98	1.95	-26.29	2.97
5	150	4-6	1.98	61.73	24.59	1.56	-26.03	3.53
5	150	8-11	4.48	99.33	29.00	1.71	-26.66	3.64
6	100	2-4	0.96	57.43	17.11	1.19	-25.48	3.73
6	100	9-14	4.96	98.41	6.08	0.39	-26.28	
7	50	0-2	1.1	93.70	25.22	1.31	-27.04	1.09
7	50	2-4	2.2	97.42	23.81	1.26	-26.99	1.64
7	50	6-8	4.4	98.42	17.01	0.85	-26.51	0.87
8	0	10-18	15.82	99.63	19.83	0.93	-25.66	1.91

Table AF-3. Specific surface areas for the heavy fraction (>2.0 g cm^{-3}) of soil <250 μm. The soil samples were collected from the excavated soil pits across the invasion chronosequence in 2009.

Pit	Distance (m)	Depth (m)	Mass Equivalent Depth (g m^{-2})	$SSA_{Untreated}$		SSA_{Total}		OC Loading (mg m^{-2})
				(m^2 g^{-1})	Standard Error n=2	(m^2 g^{-1})	Standard Error n=2	
3	190	4-7	3.66	1.39	0.02	4.92	0.72	5.84
3	190	7-11	6.9	1.52	0.12	4.62	0.53	1.97
4	160	2-4	0.96	4.18	0.00	7.96	0.05	4.85
4	160	4-7	1.68	2.55	0.03	7.00	0.75	6.66
4	160	9-12	4.73	2.43	0.13	5.59	0.00	1.90
4	160	54-64	50.42	2.99	0.51	3.75	0.07	0.16
5	150	4-6	1.98	1.24	0.13	7.97	0.19	8.19
5	150	8-11	4.48	3.30	0.41	8.02	1.44	1.18
6	100	2-4	0.96	1.75	0.28	6.27	0.13	9.09
6	100	6-9	2.16	2.70	0.07	7.78	0.18	5.77
6	100	9-14	4.96	2.01	0.30	4.54	0.37	1.19
7	50	0-2	1.1	1.11	0.08	6.52	0.00	7.53
7	50	2-4	2.2	1.23	0.08	5.83	0.02	7.82
7	50	6-8	4.4	1.83	0.11	5.66	0.30	4.23
7	50	34-43	45.24	3.31	0.37	4.00	0.36	0.23
8	0	10-18	15.82	2.27	0.03	4.21	0.15	0.64
8	0	43-53	56.12	2.78	0.24	3.61	0.22	0.30

Table AF-4. Carbon contributions to total C in the light (<2.0 g cm^{-3}) and heavy (>2.0 g cm^{-3}) fractions of soil <250 μm.

Pit	Distance (m)	Depth (cm)	Mass Equivalent Depth (g cm^{-2})	Contributions to Total Carbon	
				Light (%)	Heavy (%)
8	0	10-18	15.82	21.65	78.35
7	50	0-2	1.1	25.67	74.33
7	50	2-4	2.2	12.15	87.85
7	50	6-8	4.4	10.28	89.72
6	100	2-4	0.96	68.99	31.01
6	100	9-14	4.96	15.37	84.63
5	150	4-6	1.98	70.01	29.99
5	150	8-11	4.48	17.10	82.90
4	160	2-4	0.96	96.51	3.49
4	160	4-7	1.68	69.29	30.71
4	160	9-12	4.73	14.30	85.70
3	190	2-4	1.08	96.61	3.39
3	190	4-7	3.66	37.79	62.21
3	190	7-11	6.9	9.82	90.18

Appendix G. – Quantitative XRD

Methods

Samples weighing ~ 1.0 g were ground with a ZnO internal standard in a McCrone mill for 5 minutes. Using a Siemens D500 XRD producing Cu and Kα radiation, the samples were scanned from 5 to 65 degrees with scanning rate of 2θ at 0.02° step and 2 second count time. The RockJock program was used to determine mineral concentrations, where the observed sample spectra were fitted with the measured stands.

Table AG-1. Concentrations of illite/smectite and kaolinite. Samples were from soil pit 3. Mineralogical compositions were determined with quantitative XRD techniques.

Pit	Distance (m)	Depth (cm)	Mass Equivalent Depth (g cm^{-2})	Kaolinite (wt%)	Illite + Smectite (wt%)
3	190	0-2	0.54	4.9	22
3	190	2-4	1.08	0.9	10.8
3	190	4-7	3.66	0.4	1
3	190	7-11	6.9	0	5.8
3	190	11-15	10.14	0	4.9
3	190	15-25	21.44	0	3.7
3	190	25-35	32.74	0	3.8
3	190	45-55	57.94	0.1	3.6

Table AG-2. Concentrations of illite/smectite and kaolinite. Samples were from soil pit 6. Mineralogical compositions were determined with quantitative XRD techniques.

Pit	Distance (m)	Depth (cm)	Mass Equivalent Depth (g cm^{-2})	Kaolinite (wt%)	Illite + Smectite (wt%)
6	100	0-2	0.48	1.9	8
6	100	4-6	1.44	0.7	6.9
6	100	6-9	2.16	0.4	7.5
6	100	9-14	4.96	0	5.8
6	100	14-21	14.06	0.1	4.3
6	100	31-41	40.06	0	3.5

Table AG-3. Concentrations of illite/smectite and kaolinite. Samples were collected from soil pit 8. Mineralogical compositions were determined with quantitative XRD techniques.

Pit	Distance (m)	Depth (cm)	Mass Equivalent Depth (g cm^{-2})	Kaolinite (wt%)	Illite + Smectite (wt%)
8	0	0-2	1.34	0.3	7.9
8	0	2-4	2.68	0.7	9.3
8	0	4-6	4.02	0.6	7.4
8	0	6-8	5.36	0	9.3
8	0	8-10	6.7	0.4	8.7
8	0	10-18	15.82	0	3.7
8	0	18-28	26.82	0	3
8	0	28-43	43.32	0	4

Appendix H. – Extractable Fe Oxides

Methods

Crystalline Fe oxides were extracted via citrate-bicarbonate-dithionite. Soil samples weighing 5-10 g were placed in a 250 ml bottle, and 20 g Na-citrate, 2 g $Na_2S_2O_4$, and 125 ml DI water were then added into the bottle. The bottles were placed on a shaker over night for approximately 15 hours. Then, the bottles were centrifuged at 2,000 rpm for 15 minutes. An extract of solution was transferred to sample bottle and the sample was processed for ICP-AES analysis at the University of Minnesota.

Non-crystalline Fe oxides were extracted via ammonium oxalate. Initially, 28.4 g of ammonium oxalate was placed into a 1 L flask and DI was filled until the 1 L mark. In a separate 1 L flask, 25.2 g of oxalate acid were added and DI was filled until the 1 L mark. The pH of the ammonium oxalate was measured and adjusted to pH 3by adding oxalate acid. After pH 3 was reached, 50 ml were added into a 75 mL centrifuge tube that had been covered with aluminum foil so no light could penetrate inside. Then, 0.5g of soil was added and centrifuge tubes were placed on a shaker for 4 hours. After sitting overnight, tubes were centrifuged at 400 rpm for 15minutes. An extract of solution was transferred to sample bottle and samples were processed for ICP-AES analysis at the University of Minnesota.

Table AH-1. Amorphous Fe oxides as determined as ammonium oxalate extractable Fe and pedogenic crystalline Fe oxides as determined as citrate-bicarbonate-dithionite extractable Fe. The samples were from soil pit 3 excavated in 2009.

Pit	Distance (m)	Depth (cm)	Mass Equivalent Depth (g cm^{-2})	Fe %	
				Ammonium Oxalate Extractable (%)	Dithionite Citrate Extractable (%)
3	190	0-2	0.54	0.24	0.05
3	190	2-4	1.08	0.24	0.07
3	190	4-7	3.66	0.17	0.07
3	190	7-11	6.9	0.20	0.1
3	190	11-15	10.14	0.22	0.12
3	190	15-25	21.44	0.26	0.14
3	190	25-35	32.74	0.25	0.13
3	190	35-45	44.74	0.25	
3	190	45-55	57.94		0.12

Table AH-2. Amorphous Fe oxides as determined as ammonium oxalate extractable Fe and pedogenic crystalline Fe oxides as determined as citrate-bicarbonate-dithionite extractable Fe. The samples were from the soil pit 3 excavated in 2009.

Pit	Distance (m)	Depth (cm)	Mass Equivalent Depth (g cm^{-2})	Fe %	
				Ammonium Oxalate Extractable (%)	Dithionite Citrate Extractable (%)
4	160	0-2	0.48	0.24	0.03
4	160	2-4	0.96	0.30	0.11
4	160	4-7	1.68	0.30	0.07
4	160	7-9	2.9	0.34	0.15
4	160	9-12	4.73	0.36	0.17
4	160	12-17	9.73	0.32	0.12
4	160	17-25	19.33	0.30	0.12
4	160	25-35	44.22	0.25	0.12
4	160	35-45	44.22		0.27

Table AH-3. Amorphous Fe oxides as determined as ammonium oxalate extractable Fe and pedogenic crystalline Fe oxides as determined as citrate-bicarbonate-dithionite extractable Fe. The samples were from the soil pit 5 excavated in 2009.

Pit	Distance (m)	Depth (cm)	Mass Equivalent Depth (g cm^{-2})	Fe %	
				Ammonium Oxalate Extractable (%)	Dithionite Citrate Extractable (%)
5	150	0-2	0.66	0.14	0.04
5	150	2-4	1.32	0.20	0.07
5	150	4-6	1.98	0.19	0.07
5	150	6-8	2.98	0.23	0.12
5	150	8-11	4.48	0.25	0.09
5	150	11-17	9.88	0.24	0.13
5	150	17-27	22.28	0.28	0.14
5	150	27-37		34.68	0.13

Table AH-4. Amorphous Fe oxides as determined as ammonium oxalate extractable Fe and pedogenic crystalline Fe oxides as determined as citrate-bicarbonate-dithionite extractable Fe. The samples were from the soil pit 6 excavated in 2009.

Pit	Distance (m)	Depth (cm)	Mass Equivalent Depth (g cm^{-2})	Fe %	
				Ammonium Oxalate Extractable (%)	Dithionite Citrate Extractable (%)
6	100	0-2	0.48	0.28	0.09
6	100	2-4	0.96	0.24	0.11
6	100	4-6	1.44	0.32	0.11
6	100	6-9	2.16	0.30	0.14
6	100	9-14	4.96	0.31	0.17
6	100	14-21	14.06	0.37	0.14
6	100	21-31	27.06	0.24	
6	100	31-41	40.06		0.15

Table AH-5. Amorphous Fe oxides as determined as ammonium oxalate extractable Fe and pedogenic crystalline Fe oxides as determined as citrate-bicarbonate-dithionite extractable Fe. The samples were from the soil pit 7 excavated in 2009.

Pit	Distance (m)	Depth (cm)	Mass Equivalent Depth (g cm^{-2})	Fe %	
				Ammonium Oxalate Extractable (%)	Dithionite Citrate Extractable (%)
7	50	0-2	1.1	0.28	0.12
7	50	2-4	2.2	0.29	0.01
7	50	4-6	3.3	0.29	0.13
7	50	6-8	4.4	0.35	0.16
7	50	8-11	6.05	0.27	0.14
7	50	11-18	13.68	0.28	0.16
7	50	18-24	21.6	0.21	0.15
7	50	24-34	34.8		0.15

Table AH-6. Amorphous Fe oxides as determined as ammonium oxalate extractable Fe and pedogenic crystalline Fe oxides as determined as citrate-bicarbonate-dithionite extractable Fe. The samples were from the soil pit 8 excavated in 2009.

Pit	Distance (m)	Depth (cm)	Mass Equivalent Depth (g cm^{-2})	Fe %	
				Ammonium Oxalate Extractable (%)	Dithionite Citrate Extractable (%)
8	0	0-2	1.34	0.30	0.15
8	0	2-4	2.68	0.37	0.16
8	0	4-6	4.02	0.35	0.16
8	0	6-8	5.36	0.33	0.17
8	0	8-10	6.7	0.00	0.18
8	0	10-18	15.82	0.24	0.14
8	0	18-28	26.82	0.17	0.12
8	0	28-43	43.32		0.13

Appendix I. - Total Elemental Concentration

Method

Soil samples <2 mm were fine ground in a SPEX Shatter Box with a tungsten carbide ring. The ground samples were subjected to lithium metaborate fusion and further analyzed with Inductively Coupled Plasma Mass Spectrometry (ICP-MS) at the ALS Chemex.

Table AI-1. Trace elemental concentration (ppm) in fine fraction (<2 mm). The samples were from soil pit 3.

Pit	Distance (m)	Horizon	Depth (cm)	Co (ppm)	Cr (ppm)	Cs (ppm)	Cu (ppm)	Ni (ppm)	Pb (ppm)	Zr (ppm)	LOI (%)	Total (%)
3	190	A	0-2	25.6	20	0.73	24	7	40	97	59.9	98.6
3	190	A	2-4	24.4	30	1.04	22	15	31	136	53.5	99.4
3	190	A	4-7	19.7	40	1.41	10	<5	12	343	11.2	98.9
3	190	E	7-11	22.9	40	1.48	7	<5	7	360	3.64	97.6
3	190	E	11-15	27.5	70	1.32	6	16	8	368	2.84	97.8
3	190	E	15-25	29	40	1.15	5	8	11	370	1.72	94.6
3	190	E	25-35	26.3	50	0.98	5	11	12	354	1.17	94.7
3	190	E	35-45	21.4	40	1	<5	<5	12	322	1.06	98.2
3	190	E	45-56	18.5	40	0.86	<5	5	18	319	1.38	92.5
3	190	1B	56-71	15.8	40	1.24	5	11	8	346	1.85	99
3	190	2B	71-83	18.5	90	2	12	46	8	305	3.91	98.9
3	190	2C	83-110	13.5	40	1.67	10	13	8	225	4.61	101
3	190	2C	105-130	21.4	40	1.13	8	12	8	238	3.4	99.5
3	190	2C	144-156	16.2	30	1.57	10	16	7	99	7.26	100

Table AI-2. Trace elemental concentration (ppm) in fine fraction (<2 mm). The samples were from soil pit 4.

Pit	Distance (m)	Horizon	Depth (cm)	Co (ppm)	Cr (ppm)	Cs (ppm)	Cu (ppm)	Ni (ppm)	Pb (ppm)	Zr (ppm)	LOI (%)	Total (%)
4	160	A	0-2	2.9	10	1.12	13	11	15	78	65.6	100
4	160	A	2-4	4.5	30	1.48	19	33	20	123	54.1	97.9
4	160	A	4-7	36.2	30	1.78	21	19	12	256	30.2	97.6
4	160	A	7-9	18	50	1.81	9	14	13	374	8.29	97.7
4	160	A	9-12	15.2	40	1.65	11	8	12	397	5.03	95.9
4	160	AE	12-17	14.6	40	1.46	8	6	12	421	3.3	96.6
4	160	E	17-25	15.1	40	1.21	<5	7	7	414	1.92	99.3
4	160	E	25-35	19	40	1.15	5	7	7	428	1.7	98.5
4	160	E	35-44	NSS	NSS	NSS	NSS	NSS	NSS	NSS	2.3	95.1
4	160	1B	44-54	14	50	1.52	7	15	12	348	3.04	98.8
4	160	1B	54-64	14.9	40	0.97	5	<5	11	277	1.73	98
4	160	1C	64-74	15.7	40	1.17	7	5	13	307	2.11	97.7
4	160	1C	74-84	14.2	40	1.14	7	<5	12	324	2.19	99.9
4	160	1C	84-94	16.1	40	1	6	6	11	303	1.82	99.6
4	160	1C	94-104	14.6	40	1.17	9	13	11	375	1.48	97.7
4	160	1C	104-114	16	50	1.33	10	13	7	432	2.36	98
4	160	2C	114-126	15.6	60	1.05	11	9	7	319	5.75	101
4	160	C2	126-140	12.3	50	1	10	7	9	158	6.09	101
4	160	C2	140-167	NSS	NSS	NSS	NSS	NSS	NSS	NSS	7.07	100.5

NSS = Not sufficient sample

Table AI-3. Trace elemental concentration (ppm) in fine fraction (<2 mm). The samples were from soil pit 5.

Pit	Distance (m)	Horizon	Depth (cm)	Co (ppm)	Cr (ppm)	Cs (ppm)	Cu (ppm)	Ni (ppm)	Pb (ppm)	Zr (ppm)	LOI (%)	Total (%)
5	150	A	0-2	22	10	0.76	14	<5	19	85	66.9	98.2
5	150	A	2-4	18.9	20	1.11	15	<5	26	129	55.3	98.1
5	150	A	4-6	42.9	30	1.61	11	<5	22	226	32.6	98.4
5	150	A	6-8	29	40	1.79	7	9	14	418	8.66	99.2
5	150	A	8-11	29.5	50	1.69	6	10	13	458	4.3	99.3
5	150	AE	11-17	33.2	50	1.29	<5	7	12	462	2.33	97.9
5	150	E	17-27	51.5	50	1.06	<5	7	11	454	1.38	98.2
5	150	E	27-37	45.5	50	1.08	<5	9	12	472	1.76	100.5
5	150	1B	37-44	25.5	60	1.53	6	14	13	416	3.4	98.3
5	150	1B	44-54	28.4	50	1.21	5	15	13	406	2.19	99.2
5	150	1B	54-64	22	50	1.32	6	15	12	401	2.87	99
5	150	1B	64-74	21.1	60	1.44	8	17	13	406	3.34	100
5	150	1B	74-90	23.7	50	1.29	7	15	12	336	2.76	99.9
5	150	2B	90-100	17.6	60	1.55	10	19	13	400	2.94	99.5
5	150	2B	100-113	23.1	60	1.46	11	24	13	361	4.31	99.7
5	150	2C	113-130	15.9	40	1.96	10	24	12	171	4.33	100.5
5	150	2C	130-160	17.5	30	1.37	7	12	10	185	5.7	98.2

Table AI-4. Trace elemental concentration (ppm) in fine fraction (<2 mm). The samples were from soil pit 6.

Pit	Distance (m)	Horizon	Depth (cm)	Co (ppm)	Cr (ppm)	Cs (ppm)	Cu (ppm)	Ni (ppm)	Pb (ppm)	Zr (ppm)	LOI (%)	Total (%)
6	100	A	0-2	3.7	50	1.52	13	16	13	309	32.4	100.5
6	100	A	2-4	10.1	40	1.7	13	13	17	319	26.4	101
6	100	A	4-6	24.1	40	1.77	12	12	17	346	22	99.4
6	100	A	6-9	85	40	1.79	10	12	16	410	13.2	99
6	100	1EA	9-14	49.4	50	1.51	5	8	14	455	3.33	99.6
6	100	1E	14-21	26.8	50	1.33	<5	9	13	477	2.06	99.3
6	100	1E	21-31	25.6	50	1.15	<5	9	11	476	1.7	100.5
6	100	1E	31-41	21.2	50	1.03	<5	11	12	482	1.35	98.4
6	100	1EB	41-53	18.4	50	1.04	<5	11	12	399	1.75	98.5
6	100	2Bt1	53-58	18.8	60	1.49	6	17	13	383	3.22	99.4
6	100	2Bt2	58-68	17.1	50	1.02	<5	11	11	375	2.16	100
6	100	2Bt2	68-77	22	60	1.78	6	23	14	295	3.11	100
6	100	2Bt2	77-87	20.4	60	1.7	8	18	12	291	2.93	99.7
6	100	2Bt3	87-97	16.4	60	1.97	9	19	12	323	3.58	99.8
6	100	2Bt3	97-107	16.1	50	2.24	12	17	12	211	4.75	100.5
6	100	2Bt3	107-123	25.3	50	2.33	14	27	13	219	4.79	100.5
6	100	2C	123	17.5	50	2.59	19	28	12	190	7.55	100.5

Table AI-5. Trace elemental concentration (ppm) in fine fraction (<2 mm). The samples were from soil pit 7.

Pit	Distance (m)	Horizon	Depth (cm)	Co (ppm)	Cr (ppm)	Cs (ppm)	Cu (ppm)	Ni (ppm)	Pb (ppm)	Zr (ppm)	LOI (%)	Total(%)
7	50	A	0-2	4.2	50	1.53	7	16	16	334	18.35	98.8
7	50	A	2-4	3.9	50	1.57	7	21	16	326	14.8	98
7	50	A	4-6	13.6	50	1.63	7	16	17	373	12.4	99.4
7	50	A	6-8	13.1	40	1.65	6	15	16	389	9.47	99.6
7	50	A	8-11	14.3	40	1.51	5	8	13	393	4.3	98.7
7	50	E/A	11-18	17.7	50	1.29	<5	11	11	399	2.18	99.2
7	50	E	18-24	14.7	40	1.06	<5	8	11	392	1.56	98.2
7	50	E	24-34	14.2	40	0.95	<5	6	11	390	0.78	98.3
7	50	1B	34-43	14.4	40	1.23	<5	10	11	350	1.57	98.5
7	50	1B	43-53	14.8	50	1.9	7	15	12	276	3.23	98.1
7	50	2B	53-63	15.6	40	2.3	9	15	12	243	4.54	100
7	50	2B	63-73	19.4	50	3.38	14	19	13	171	6.64	97.8
7	50	2B	73-83	18.4	50	3.59	21	18	13	153	7.37	99.9
7	50	2B	83-93	20.4	50	3.52	17	23	13	149	7.66	100
7	50	2B	93-103	19.4	50	3.42	17	39	12	146	7.14	99.3
7	50	2B	103-113	18.8	50	3.31	16	43	13	150	7.09	99.2
7	50	2B	113-123	23.3	50	3.27	16	26	13	135	7.23	98.2
7	50	2B	123-133	17.6	50	3.12	16	26	12	153	8.81	99.3
7	50	2B	133-150	15.4	40	3.16	16	27	12	143	9.76	99.9
7	50	2C	150-180	18.8	50	3.38	18	34	12	148	10.95	100.5

Table AI-6. Trace elemental concentration (ppm) in fine fraction (<2 mm). The samples were from soil pit 8.

Pit	Distance (m)	Horizon	Depth (cm)	Co (ppm)	Cr (ppm)	Cs (ppm)	Cu (ppm)	Ni (ppm)	Pb (ppm)	Zr (ppm)	LOI (%)	Total (%)
8	0	A	0-2	6.2	50	1.75	12	26	16	213	18.35	94.5
8	0	A	2-4	8.8	50	1.79	12	25	17	225	15.85	94.2
8	0	A	4-6	31.7	30	1.8	11	16	17	254	13.95	99.5
8	0	A	6-8	26.1	50	1.85	12	23	18	245	12.55	99.9
8	0	A	8-10	21.3	30	1.78	10	18	16	252	9.84	97.5
8	0	E/A	10-18	21.8	40	1.2	<5	15	11	370	2.4	101
8	0	E	18-28	23.6	50	1.03	<5	17	11	364	1.49	101
8	0	E	28-43	24.6	110	1.06	<5	40	11	393	1.1	101
8	0	B	43-53	11.3	50	1.46	6	22	12	310	3.39	99.9
8	0	B	53-63	15.9	50	1.42	6	25	12	319	2.58	98.5
8	0	B	63-73	36.8	60	1.47	8	29	11	305	2.97	101
8	0	B	73-83	9.5	50	1.39	7	22	12	339	2.09	97.9
8	0	B	83-94	9.6	50	1.19	8	27	11	342	2.83	99.1
8	0	B	94-100	9.4	40	0.86	5	14	9	300	7.03	100
8	0	1C	100-107	9.9	40	2.64	15	20	10	143	13.4	98.4

Table AI-7. Major elemental concentration (%) in fine fraction (<2 mm). The samples were from soil pit 3.

Pit	Distance (m)	Horizon	Depth (cm)	SiO_2 (%)	Al_2O_3 (%)	Fe_2O_3 (%)	CaO (%)	MgO (%)	Na_2O (%)	K_2O (%)	LOI (%)	Total (%)
3	190	A	0-2	28.4	3.27	0.89	3.68	0.44	0.55	0.73	59.9	98.6
3	190	A	2-4	34.5	4.18	1.14	3.23	0.45	0.68	0.9	53.5	99.4
3	190	A	4-7	71.6	8.09	1.44	1.77	0.45	1.7	1.72	11.2	98.9
3	190	E	7-11	77.4	8.84	1.47	1.4	0.42	1.87	1.82	3.64	97.6
3	190	E	11-15	78.2	8.92	1.51	1.41	0.42	1.91	1.84	2.84	97.8
3	190	E	15-25	76.1	8.65	1.63	1.47	0.44	2.02	1.85	1.72	94.6
3	190	E	25-35	76.6	8.71	1.62	1.54	0.44	2.08	1.87	1.17	94.7
3	190	E	35-45	79.5	9.32	1.69	1.64	0.45	2.07	1.82	1.06	98.2
3	190	E	45-56	74.4	8.61	1.66	1.61	0.45	2.08	1.72	1.38	92.5
3	190	1B	56-71	78.1	9.89	2.37	1.72	0.59	2.03	1.74	1.85	99
3	190	2B	71-83	73.1	10.85	4.14	1.74	0.96	1.81	1.64	3.91	98.9
3	190	2C	83-110	76	9.39	2.81	2.8	1.39	1.72	1.54	4.61	101
3	190	2C	105-130	77.4	8.78	1.96	3	0.95	1.89	1.55	3.4	99.5
3	190	2C	144-156	71.6	8.3	2.12	5.54	1.75	1.53	1.4	7.26	100

Table AI-7. Continued: Major elemental concentration (%) in fine fraction (<2 mm). Samples were from soil pit 3.

Pit	Distance (m)	Horizon	Depth (cm)	Cr_2O_3 (%)	TiO_2 (%)	MnO (%)	P_2O_5 (%)	SrO (%)	BaO (%)	LOI (%)	Total (%)
3	190	A	0-2	<0.01	0.18	0.23	0.24	0.01	0.05	59.9	98.6
3	190	A	2-4	<0.01	0.22	0.3	0.25	0.01	0.06	53.5	99.4
3	190	A	4-7	0.01	0.43	0.23	0.12	0.02	0.08	11.2	98.9
3	190	E	7-11	0.01	0.45	0.11	0.11	0.03	0.07	3.64	97.6
3	190	E	11-15	<0.01	0.44	0.08	0.1	0.03	0.06	2.84	97.8
3	190	E	15-25	0.01	0.43	0.04	0.15	0.03	0.06	1.72	94.6
3	190	E	25-35	0.01	0.4	0.04	0.11	0.03	0.06	1.17	94.7
3	190	E	35-45	0.01	0.35	0.05	0.15	0.03	0.06	1.06	98.2
3	190	E	45-56	0.01	0.33	0.04	0.14	0.03	0.06	1.38	92.5
3	190	1B	56-71	0.01	0.37	0.05	0.15	0.03	0.06	1.85	99
3	190	2B	71-83	0.01	0.43	0.09	0.18	0.03	0.05	3.91	98.9
3	190	2C	83-110	0.01	0.34	0.09	0.12	0.03	0.05	4.61	101
3	190	2C	105-130	<0.01	0.28	0.08	0.09	0.03	0.05	3.4	99.5
3	190	2C	144-156	<0.01	0.22	0.12	0.08	0.02	0.05	7.26	100

Table AI-8. Major elemental concentration (%) in fine fraction (<2 mm). Samples were from soil pit 4.

Pit	Distance (m)	Horizon	Depth (cm)	SiO_2 (%)	Al_2O_3 (%)	Fe_2O_3 (%)	CaO (%)	MgO (%)	Na_2O (%)	K_2O (%)	LOI (%)	Total (%)
4	160	A	0-2	24.2	3.27	1.05	3.68	0.43	0.34	0.65	65.6	100
4	160	A	2-4	31.8	4.35	1.31	3.21	0.43	0.52	0.87	54.1	97.9
4	160	A	4-7	52.2	6.71	1.62	2.48	0.46	1.07	1.35	30.2	97.6
4	160	A	7-9	72.3	8.82	1.83	1.57	0.49	1.61	1.75	8.29	97.7
4	160	A	9-12	73.6	8.77	1.81	1.5	0.48	1.77	1.86	5.03	95.9
4	160	AE	12-17	76.1	8.84	1.73	1.44	0.48	1.88	1.92	3.3	96.6
4	160	E	17-25	79.6	9.23	1.87	1.5	0.47	1.96	1.92	1.92	99.3
4	160	E	25-35	79.3	9.18	1.74	1.54	0.48	1.95	1.91	1.7	98.5
4	160	E	35-44	74.5	9.3	2.47	1.5	0.57	1.8	1.88	2.3	95.1
4	160	1B	44-54	76.3	10.1	2.76	1.59	0.62	1.87	1.82	3.04	98.8
4	160	1B	54-64	78.1	9.6	1.94	1.7	0.51	2.06	1.71	1.73	98
4	160	1C	64-74	76.8	9.62	2.14	1.77	0.57	2.16	1.82	2.11	97.7
4	160	1C	74-84	78.3	10.1	2.41	1.8	0.6	2.07	1.76	2.19	99.9
4	160	1C	84-94	79.3	9.6	2.07	1.76	0.55	2.08	1.73	1.82	99.6
4	160	1C	94-104	77.7	9.58	2.24	1.72	0.59	2.02	1.69	1.48	97.7
4	160	1C	104-114	76.8	9.57	2.63	1.72	0.64	1.94	1.68	2.36	98
4	160	2C	114-126	72.2	8.8	3.59	4.3	2.03	1.93	1.48	5.75	101
4	160	C2	126-140	73.3	8.6	2.32	4.59	2.05	1.9	1.48	6.09	101
4	160	C2	140-167	74.3	8.37	2.25	3.33	1.71	1.33	1.53	7.07	100.5

Table AI-8. Continued: Major elemental concentration (%) in fine fraction (<2 mm). Samples were from soil pit 4.

Pit	Distance (m)	Horizon	Depth (cm)	Cr_2O_3 (%)	TiO_2 (%)	MnO (%)	P_2O_5 (%)	SrO (%)	BaO (%)	LOI (%)	Total (%)
4	160	A	0-2	<0.01	0.18	0.39	0.33	0.01	0.06	65.6	100
4	160	A	2-4	0.01	0.24	0.66	0.32	0.01	0.09	54.1	97.9
4	160	A	4-7	0.01	0.38	0.78	0.21	0.02	0.11	30.2	97.6
4	160	A	7-9	0.01	0.48	0.32	0.16	0.02	0.07	8.29	97.7
4	160	A	9-12	0.01	0.5	0.27	0.15	0.03	0.07	5.03	95.9
4	160	AE	12-17	0.01	0.51	0.17	0.13	0.02	0.07	3.3	96.6
4	160	E	17-25	0.01	0.55	0.07	0.12	0.03	0.06	1.92	99.3
4	160	E	25-35	0.01	0.47	0.06	0.11	0.03	0.06	1.7	98.5
4	160	E	35-44	0.01	0.45	0.05	0.14	0.03	0.06	2.3	95.1
4	160	1B	44-54	0.01	0.42	0.05	0.16	0.03	0.06	3.04	98.8
4	160	1B	54-64	0.01	0.32	0.05	0.13	0.03	0.06	1.73	98
4	160	1C	64-74	0.01	0.36	0.05	0.15	0.03	0.06	2.11	97.7
4	160	1C	74-84	0.01	0.38	0.06	0.14	0.03	0.06	2.19	99.9
4	160	1C	84-94	0.01	0.34	0.06	0.16	0.03	0.06	1.82	99.6
4	160	1C	94-104	0.01	0.37	0.06	0.13	0.03	0.06	1.48	97.7
4	160	1C	104-114	0.01	0.39	0.07	0.11	0.02	0.05	2.36	98
4	160	2C	114-126	0.01	0.37	0.12	0.12	0.03	0.05	5.75	101
4	160	C2	126-140	0.01	0.25	0.13	0.09	0.03	0.05	6.09	101
4	160	C2	140-167	0.01	0.29	0.15	0.12	0.02	0.06	7.07	100.5

Table AI-9. Major elemental concentration (%) in fine fraction (<2 mm). Samples were from soil pit 5.

Pit	Distance (m)	Horizon	Depth (cm)	SiO_2 (%)	Al_2O_3 (%)	Fe_2O_3 (%)	CaO (%)	MgO (%)	Na_2O (%)	K_2O (%)	LOI (%)	Total (%)
5	150	A	0-2	21.5	2.7	0.76	4.21	0.47	0.34	0.6	66.9	98.2
5	150	A	2-4	31.6	3.96	1.07	3.51	0.5	0.55	0.84	55.3	98.1
5	150	A	4-6	51.8	6.29	1.45	2.44	0.49	1.04	1.31	32.6	98.4
5	150	A	6-8	73.8	8.64	1.71	1.44	0.46	1.7	1.78	8.66	99.2
5	150	A	8-11	78	8.92	1.63	1.37	0.44	1.85	1.88	4.3	99.3
5	150	AE	11-17	78.6	8.93	1.6	1.4	0.44	1.96	1.9	2.33	97.9
5	150	E	17-27	79.9	8.85	1.71	1.42	0.42	1.9	1.91	1.38	98.2
5	150	E	27-37	80.7	9.38	1.83	1.58	0.48	2.1	1.93	1.76	100.5
5	150	1B	37-44	75.2	10.2	2.85	1.56	0.63	1.89	1.83	3.4	98.3
5	150	1B	44-54	77.8	9.89	2.41	1.68	0.58	2.1	1.82	2.19	99.2
5	150	1B	54-64	76.8	10	2.61	1.62	0.61	2.03	1.8	2.87	99
5	150	1B	64-74	76.3	10.4	3.02	1.68	0.67	2.04	1.81	3.34	100
5	150	1B	74-90	78.1	9.84	2.57	1.62	0.62	2.06	1.72	2.76	99.9
5	150	2B	90-100	76.5	10.25	2.92	1.64	0.72	1.98	1.79	2.94	99.5
5	150	2B	100-113	74.6	9.72	2.86	2.57	1.26	1.97	1.72	4.31	99.7
5	150	2C	113-130	77.8	9.08	2.33	2.06	1.12	1.61	1.6	4.33	100.5
5	150	2C	130-160	74.2	7.67	1.76	4	1.52	1.56	1.34	5.7	98.2

Table AI-9. Continued: Major elemental concentration (%) in fine fraction (<2 mm). Samples were from soil pit 5.

Pit	Distance (m)	Horizon	Depth (cm)	Cr_2O_3 (%)	TiO_2 (%)	MnO (%)	P_2O_5 (%)	SrO (%)	BaO (%)	LOI (%)	Total (%)
5	150	A	0-2	<0.01	0.14	0.18	0.32	0.01	0.04	66.9	98.2
5	150	A	2-4	<0.01	0.21	0.24	0.25	0.01	0.05	55.3	98.1
5	150	A	4-6	<0.01	0.34	0.31	0.2	0.02	0.06	32.6	98.4
5	150	A	6-8	0.01	0.52	0.27	0.14	0.02	0.07	8.66	99.2
5	150	A	8-11	0.01	0.53	0.14	0.1	0.03	0.07	4.3	99.3
5	150	AE	11-17	0.01	0.5	0.07	0.09	0.03	0.06	2.33	97.9
5	150	E	17-27	0.01	0.47	0.06	0.08	0.03	0.06	1.38	98.2
5	150	E	27-37	0.01	0.46	0.06	0.1	0.03	0.06	1.76	100.5
5	150	1B	37-44	0.01	0.43	0.05	0.14	0.03	0.06	3.4	98.3
5	150	1B	44-54	0.01	0.4	0.05	0.14	0.03	0.06	2.19	99.2
5	150	1B	54-64	0.01	0.4	0.05	0.14	0.03	0.06	2.87	99
5	150	1B	64-74	0.01	0.43	0.05	0.15	0.03	0.06	3.34	100
5	150	1B	74-90	0.01	0.37	0.05	0.13	0.03	0.06	2.76	99.9
5	150	2B	90-100	0.01	0.44	0.06	0.14	0.03	0.06	2.94	99.5
5	150	2B	100-113	0.01	0.41	0.07	0.13	0.03	0.06	4.31	99.7
5	150	2C	113-130	0.01	0.3	0.1	0.1	0.02	0.06	4.33	100.5
5	150	2C	130-160	<0.01	0.21	0.12	0.07	0.02	0.05	5.7	98.2

Table AI-10. Major elemental concentration (%) in fine fraction (<2 mm). Samples were from soil pit 6.

Pit	Distance (m)	Horizon	Depth (cm)	SiO_2 (%)	Al_2O_3 (%)	Fe_2O_3 (%)	CaO (%)	MgO (%)	Na_2O (%)	K_2O (%)	LOI (%)	Total (%)
6	100	A	0-2	53.8	6.47	1.42	2.31	0.44	1.2	1.34	32.4	100.5
6	100	A	2-4	59.3	7.07	1.55	2.18	0.45	1.34	1.46	26.4	101
6	100	A	4-6	61.3	7.52	1.7	2.05	0.46	1.38	1.55	22	99.4
6	100	A	6-9	68.8	8.26	1.82	1.71	0.47	1.59	1.73	13.2	99
6	100	1EA	9-14	79	9.01	1.7	1.42	0.45	1.92	1.92	3.33	99.6
6	100	1E	14-21	79.7	9.16	1.76	1.46	0.47	2	1.93	2.06	99.3
6	100	1E	21-31	80.9	9.27	1.78	1.54	0.48	2.08	1.94	1.7	100.5
6	100	1E	31-41	79.4	9.13	1.78	1.56	0.47	2.09	1.89	1.35	98.4
6	100	1EB	41-53	78.5	9.4	2.04	1.62	0.5	2.12	1.84	1.75	98.5
6	100	2Bt1	53-58	76.4	10.2	2.86	1.59	0.62	1.97	1.82	3.22	99.4
6	100	2Bt2	58-68	79.6	9.45	2.14	1.67	0.53	2.16	1.8	2.16	100
6	100	2Bt2	68-77	74.5	11.65	3.01	1.92	0.81	2.62	1.74	3.11	100
6	100	2Bt2	77-87	76.8	10.05	3.16	1.62	0.78	1.97	1.67	2.93	99.7
6	100	2Bt3	87-97	76.9	9.75	3.23	1.45	0.78	1.73	1.64	3.58	99.8
6	100	2Bt3	97-107	76.3	10.1	3.22	1.42	0.86	1.61	1.63	4.75	100.5
6	100	2Bt3	107-123	75.4	10.4	3.25	1.54	0.96	1.68	1.67	4.79	100.5
6	100	2C	123	71.2	9.4	3.12	3.45	2.04	1.4	1.6	7.55	100.5

Table AI-10. Continued: Major elemental concentration (%) in fine fraction (<2 mm). Samples were from soil pit 6.

Pit	Distance (m)	Horizon	Depth (cm)	Cr_2O_3 (%)	TiO_2 (%)	MnO (%)	P_2O_5 (%)	SrO (%)	BaO (%)	LOI (%)	Total (%)
6	100	A	0-2	0.01	0.39	0.48	0.19	0.02	0.08	32.4	100.5
6	100	A	2-4	0.01	0.42	0.52	0.18	0.02	0.09	26.4	101
6	100	A	4-6	0.01	0.45	0.65	0.2	0.02	0.1	22	99.4
6	100	A	6-9	0.01	0.51	0.61	0.16	0.02	0.1	13.2	99
6	100	1EA	9-14	0.01	0.53	0.12	0.09	0.03	0.07	3.33	99.6
6	100	1E	14-21	0.01	0.51	0.08	0.1	0.03	0.06	2.06	99.3
6	100	1E	21-31	0.01	0.5	0.06	0.11	0.03	0.06	1.7	100.5
6	100	1E	31-41	0.01	0.46	0.05	0.11	0.03	0.06	1.35	98.4
6	100	1EB	41-53	0.01	0.4	0.05	0.13	0.03	0.06	1.75	98.5
6	100	2Bt1	53-58	0.01	0.4	0.05	0.16	0.03	0.06	3.22	99.4
6	100	2Bt2	58-68	0.01	0.39	0.06	0.13	0.03	0.06	2.16	100
6	100	2Bt2	68-77	0.01	0.41	0.08	0.14	0.04	0.06	3.11	100
6	100	2Bt2	77-87	0.01	0.4	0.09	0.12	0.03	0.05	2.93	99.7
6	100	2Bt3	87-97	0.01	0.38	0.13	0.1	0.03	0.06	3.58	99.8
6	100	2Bt3	97-107	0.01	0.36	0.11	0.11	0.02	0.06	4.75	100.5
6	100	2Bt3	107-123	0.01	0.38	0.1	0.12	0.02	0.06	4.79	100.5
6	100	2C	123	0.01	0.33	0.17	0.12	0.02	0.06	7.55	100.5

Table AI-11. Major elemental concentration (%) in fine fraction (<2 mm). Samples were from soil pit 7.

Pit	Distance (m)	Horizon	Depth (cm)	SiO_2 (%)	Al_2O_3 (%)	Fe_2O_3 (%)	CaO (%)	MgO (%)	Na_2O (%)	K_2O (%)	LOI (%)	Total (%)
7	50	A	0-2	64.9	7.65	1.56	1.82	0.48	1.51	1.58	18.35	98.8
7	50	A	2-4	67.5	8.01	1.57	1.63	0.4	1.6	1.62	14.8	98
7	50	A	4-6	70.4	8.35	1.7	1.64	0.48	1.68	1.71	12.4	99.4
7	50	A	6-8	73.1	8.6	1.74	1.55	0.47	1.75	1.78	9.47	99.6
7	50	A	8-11	77	8.96	1.74	1.46	0.47	1.92	1.89	4.3	98.7
7	50	E/A	11-18	79.5	9.07	1.72	1.48	0.46	2.06	1.93	2.18	99.2
7	50	E	18-24	79.5	8.89	1.7	1.5	0.46	2	1.91	1.56	98.2
7	50	E	24-34	79.9	9.05	1.76	1.62	0.45	2.17	1.9	0.78	98.3
7	50	1B	34-43	78.3	9.52	2.23	1.62	0.54	2.13	1.85	1.57	98.5
7	50	1B	43-53	75.5	10.05	2.8	1.48	0.68	1.9	1.79	3.23	98.1
7	50	2B	53-63	76.1	10.15	2.99	1.32	0.77	1.66	1.78	4.54	100
7	50	2B	63-73	71.7	10.3	3.57	1.02	0.97	1.19	1.69	6.64	97.8
7	50	2B	73-83	72.6	10.55	3.71	1.04	1.04	1.14	1.7	7.37	99.9
7	50	2B	83-93	72.7	10.5	3.69	1.04	1.06	1.07	1.68	7.66	100
7	50	2B	93-103	72.4	10.35	3.55	1.18	1.06	1.18	1.69	7.14	99.3
7	50	2B	103-113	72.6	10.1	3.45	1.28	1.1	1.15	1.68	7.09	99.2
7	50	2B	113-123	71.1	9.89	3.33	1.78	1.37	1.16	1.64	7.23	98.2
7	50	2B	123-133	69.2	9.56	3.11	3.09	2.06	1.15	1.6	8.81	99.3
7	50	2B	133-150	68.7	9.06	3.03	4.06	2.15	0.95	1.52	9.76	99.9
7	50	2C	150-180	66.8	9.28	3.16	4.63	2.44	0.97	1.51	10.95	100.5

Table AI-11. Continued: Major elemental concentration (%) in fine fraction (<2 mm). Samples were from soil pit 7.

Pit	Distance (m)	Horizon	Depth (cm)	Cr_2O_3 (%)	TiO_2 (%)	MnO (%)	P_2O_5 (%)	SrO (%)	BaO (%)	LOI (%)	Total (%)
7	50	A	0-2	0.01	0.43	0.26	0.16	0.02	0.06	18.35	98.8
7	50	A	2-4	0.01	0.4	0.25	0.16	0.02	0.06	14.8	98
7	50	A	4-6	0.01	0.47	0.36	0.15	0.02	0.07	12.4	99.4
7	50	A	6-8	0.01	0.48	0.39	0.13	0.02	0.07	9.47	99.6
7	50	A	8-11	0.01	0.49	0.26	0.1	0.03	0.07	4.3	98.7
7	50	E/A	11-18	0.01	0.47	0.09	0.11	0.03	0.07	2.18	99.2
7	50	E	18-24	0.01	0.44	0.05	0.09	0.03	0.06	1.56	98.2
7	50	E	24-34	0.01	0.43	0.06	0.12	0.03	0.06	0.78	98.3
7	50	1B	34-43	0.01	0.41	0.06	0.13	0.03	0.06	1.57	98.5
7	50	1B	43-53	0.01	0.39	0.08	0.12	0.03	0.06	3.23	98.1
7	50	2B	53-63	0.01	0.37	0.1	0.11	0.02	0.06	4.54	100
7	50	2B	63-73	0.01	0.38	0.11	0.1	0.02	0.06	6.64	97.8
7	50	2B	73-83	0.01	0.39	0.13	0.1	0.02	0.06	7.37	99.9
7	50	2B	83-93	0.01	0.4	0.14	0.09	0.02	0.06	7.66	100
7	50	2B	93-103	0.01	0.39	0.13	0.09	0.02	0.06	7.14	99.3
7	50	2B	103-113	0.01	0.38	0.14	0.1	0.02	0.06	7.09	99.2
7	50	2B	113-123	0.01	0.37	0.14	0.1	0.02	0.06	7.23	98.2
7	50	2B	123-133	0.01	0.36	0.13	0.09	0.02	0.06	8.81	99.3
7	50	2B	133-150	0.01	0.34	0.15	0.09	0.02	0.06	9.76	99.9
7	50	2C	150-180	0.01	0.37	0.19	0.1	0.02	0.06	10.95	100.5

Table AI-12. Major elemental concentration (%) in fine fraction (<2 mm). Samples were from soil pit 8.

Pit	Distance (m)	Horizon	Depth (cm)	SiO_2 (%)	Al_2O_3 (%)	Fe_2O_3 (%)	CaO (%)	MgO (%)	Na_2O (%)	K_2O (%)	LOI (%)	Total (%)
8	0	A	0-2	62.6	6.62	1.52	1.48	0.35	1.17	1.41	18.35	94.5
8	0	A	2-4	64.1	7.03	1.64	1.49	0.38	1.2	1.48	15.85	94.2
8	0	A	4-6	69.7	7.92	1.72	1.54	0.43	1.52	1.64	13.95	99.5
8	0	A	6-8	71.1	8.13	1.76	1.52	0.43	1.58	1.71	12.55	99.9
8	0	A	8-10	71.4	8.15	1.77	1.4	0.42	1.61	1.7	9.84	97.5
8	0	E/A	10-18	81.6	8.92	1.53	1.46	0.4	2.18	1.9	2.4	101
8	0	E	18-28	82.4	9.03	1.56	1.51	0.41	2.24	1.94	1.49	101
8	0	E	28-43	82.3	9.17	1.71	1.54	0.44	2.24	1.97	1.1	101
8	0	B	43-53	77.5	9.85	2.56	1.5	0.59	2.03	1.88	3.39	99.9
8	0	B	53-63	77.7	9.49	2.43	1.48	0.52	1.91	1.74	2.58	98.5
8	0	B	63-73	78.1	10.15	2.75	1.58	0.63	2.15	1.84	2.97	101
8	0	B	73-83	76.1	10.05	2.76	1.66	0.66	2.12	1.78	2.09	97.9
8	0	B	83-94	76.4	9.56	2.37	2.35	1.01	2.18	1.78	2.83	99.1
8	0	B	94-100	70.5	8.31	1.8	5.6	2.82	2.01	1.6	7.03	100
8	0	1C	100-107	60.2	7.83	2.44	9.41	2.25	1.03	1.31	13.4	98.4

Table AI-12. Continued: Major elemental concentration (%) in fine fraction (<2 mm). Samples were from soil pit 8.

Pit	Distance (m)	Horizon	Depth (cm)	Cr_2O_3 (%)	TiO_2 (%)	MnO (%)	P_2O_5 (%)	SrO (%)	BaO (%)	LOI (%)	Total(%)
8	0	A	0-2	0.01	0.35	0.37	0.14	0.02	0.07	18.35	94.5
8	0	A	2-4	0.01	0.4	0.37	0.16	0.02	0.08	15.85	94.2
8	0	A	4-6	0.01	0.43	0.42	0.13	0.02	0.09	13.95	99.5
8	0	A	6-8	0.01	0.43	0.48	0.12	0.02	0.09	12.55	99.9
8	0	A	8-10	0.01	0.44	0.49	0.12	0.02	0.09	9.84	97.5
8	0	E/A	10-18	0.01	0.4	0.1	0.07	0.03	0.07	2.4	101
8	0	E	18-28	0.01	0.39	0.05	0.08	0.03	0.06	1.49	101
8	0	E	28-43	0.02	0.4	0.06	0.09	0.03	0.06	1.1	101
8	0	B	43-53	0.01	0.37	0.04	0.11	0.02	0.06	3.39	99.9
8	0	B	53-63	0.01	0.36	0.04	0.13	0.03	0.06	2.58	98.5
8	0	B	63-73	0.01	0.35	0.05	0.11	0.03	0.06	2.97	101
8	0	B	73-83	0.01	0.37	0.05	0.12	0.03	0.06	2.09	97.9
8	0	B	83-94	0.01	0.37	0.06	0.13	0.03	0.06	2.83	99.1
8	0	B	94-100	0.01	0.31	0.05	0.11	0.03	0.05	7.03	100
8	0	1C	100-107	0.01	0.3	0.1	0.08	0.02	0.05	13.4	98.4